University of South Florida

DIGITAL COMMONS
@ UNIVERSITY OF SOUTH FLORIDA

Digital Commons @ University of South Florida

USF Tampa Graduate Theses and Dissertations

USF Graduate Theses and Dissertations

10-23-2014

Assessments of surface-pelagic drift communities and behavior of early juvenile sea turtles in the northern Gulf of Mexico

Robert F. Hardy
University of South Florida, rfhardy@mail.usf.edu

Follow this and additional works at: https://digitalcommons.usf.edu/etd

 Part of the Marine Biology Commons, and the Oceanography Commons

Scholar Commons Citation

Hardy, Robert F., "Assessments of surface-pelagic drift communities and behavior of early juvenile sea turtles in the northern Gulf of Mexico" (2014). *USF Tampa Graduate Theses and Dissertations.*
https://digitalcommons.usf.edu/etd/5367

This Thesis is brought to you for free and open access by the USF Graduate Theses and Dissertations at Digital Commons @ University of South Florida. It has been accepted for inclusion in USF Tampa Graduate Theses and Dissertations by an authorized administrator of Digital Commons @ University of South Florida. For more information, please contact digitalcommons@usf.edu.

Assessments of Surface-Pelagic Drift Communities and Behavior of Early Juvenile Sea Turtles in the Northern Gulf of Mexico

by

Robert F. Hardy

A thesis submitted in partial fulfillment
of the requirements for the degree of
Master of Science
College of Marine Science
University of South Florida

Major Professor: Chuanmin Hu, Ph.D.
Brian Lapointe, Ph.D.
Anne Meylan, Ph.D.
Ernst Peebles, Ph.D.
Blair Witherington, Ph.D.

Date of Approval:
23 October 2014

Keywords: developmental habitat, critical habitat, remote sensing, Landsat, *Sargassum*, satellite telemetry

Copyright © 2014, Robert F. Hardy

DEDICATION

This work is dedicated to my family, especially Stacie, who supported and encouraged me in this pursuit.

ACKNOWLEDGMENTS

This work would not have been possible without the expert guidance of Dr. Chuanmin Hu. I am grateful for everything you contributed to this effort. Thank you for accepting me into your lab and for agreeing to tackle these questions regarding *Sargassum.* From pioneering floating algae detection methods used herein to providing a lab environment where students can succeed, thank you for sharing your accomplishments to benefit your students' scientific pursuits. I am especially grateful for the guidance and encouragement provided by committee members: Dr. Brian Lapointe, Dr. Anne Meylan, Dr. Ernst Peebles, and Dr. Blair Witherington. Thank you for sharing your knowledge and for providing thorough critiques of this work. This could not have been completed without you all. I have had the good fortune to study sea turtles with a many accomplished biologists and dedicated conservationists. To Blair Witherington and Shigetomo Hirama, I am grateful to have the opportunity to contribute to the work you have led for so many years. Most knowledge regarding the details of the "lost years" comes from your research. Thank you for allowing me to participate in this research with you. Anne Meylan has been an influential mentor for many years. Thank you, Anne, for sharing your wealth of sea turtle knowledge and for sharing with me an opportunity to add to that knowledge as part of your research. Thank you for providing encouragement and for always having an open door. Thank you to my colleagues within FWC's Sea Turtle Research and Conservation program; it is a pleasure to work with such passionate sea turtle biologists. This work also benefited from the contributions of Rhonda Bailey, Simona Ceriani, Brittany Combs, Allen Foley, Robin Giove, and (especially) Leo Meirose of FWC. I am grateful for the support of my friends and colleagues within the USF Optical Oceanography Laboratory.

Thank you to Brian Barnes, Jen Cannizzaro, and David English for sharing your knowledge of optics and remote sensing. Brock Murch maintained the computing environment within which most of this work was conducted. Without Brock's tireless efforts, much of the great work conducted by the USF Optical Oceanography Laboratory would not be possible. I am extremely grateful for the encouragement provided by my undergraduate academic adviser, Dr. Jeanne Jones of Mississippi State University. "Doc's" infectious passion for conservation has inspired many students and I am very fortunate to have been one of them. To my family, thank you for your love and support during this pursuit; thanks for letting me go my own way and for encouraging me when I needed it. And to Stacie: Thank you for your patience, love, and support during this endeavor. Thanks for providing technical guidance on databases and code. Thanks for entertaining seemingly endless discussions on sea turtles and (also endless) iterations of manuscripts.

The free access to Landsat imagery was fundamental to this study. Those data were provided by the National Satellite Land Remote Sensing Data Archive at the United States Geological Survey's Earth Resources Observation and Science Center and the Landsat missions of the National Aeronautics and Space Administration. This research was principally funded by NOAA Fisheries through a Species Recovery Grant (NA10NMF4720031). Other financial support came from a NASA ROSES grant and revenues generated by sales of Florida's Sea Turtle License Plate.

TABLE OF CONTENTS

List of Tables iii

List of Figures iv

Abstract vii

Chapter One: Characterizing a Sea Turtle Developmental Habitat Using Landsat Observations of Surface-Pelagic Drift Communities within the Eastern Gulf of Mexico 1
1. Abstract 1
2. Introduction 2
2.1. Sea Turtle Life History and the "Lost Year" 2
2.2. *Sargassum*-Dominated Surface-Pelagic Drift Communities 4
2.3. Attempts to Quantify Pelagic *Sargassum* 6
2.4. Objectives of the Present Study 8
3. Methods 9
3.1. Study Area 9
3.2. Surface-Pelagic Sea Turtles 10
3.3. Remote Sensing 10
4. Results 12
4.1. Summary of SPDC within the Eastern Gulf of Mexico 12
4.2. Density of Surface-Pelagic Sea Turtles within the Eastern Gulf of Mexico 13
4.3. Wind Velocity and SPDC Abundance 14
5. Discussion 14
5.1. SPDC within the Eastern Gulf of Mexico 14
5.2. Low Abundance of SPDC During 2010 16
5.3. The Eastern Gulf of Mexico — A Critical Developmental Habitat for Sea Turtles in the Northwestern Atlantic 17
5.4. Threats to SPDC and Conservation Efforts 18
5.5. Conclusions 22
Literature Cited 24
Tables 29
Figures 31

Chapter Two: Movements and Habitat Associations of Surface-Pelagic Juvenile Kemp's Ridleys (*Lepidochelys kempii*) within the Northern Gulf of Mexico 46
1. Abstract 46
2. Introduction 47
3. Methods 50
3.1. Satellite Transmitter Deployments 50
3.2. Transmitter Temperature and Battery Voltage 51

3.3. Argos Positional Data Treatment 51
3.4. Positional Interpolation and State-Space Modeling 52
3.5. Remotely-Sensed Habitat Information 53
3.6. Statistical Methods 54
4. Results 55
4.1. Movement Characteristics and Behavior 55
4.2. Apparent Departure from the Surface-Pelagic Environment 56
4.3. Sea Surface Habitat 57
5. Discussion 60
5.1. Behavior 62
5.2. Evidence for Recruitment 65
5.3. Distribution and Habitat Association 66
5.4. Conclusions 68
Literature Cited 69
Tables 74
Figures 78

Chapter Three: Assessment of Surface-Pelagic Drift Communities within the Northern Gulf of Mexico Using Landsat Observations Collected from 2009–2011 93
1. Abstract 93
2. Introduction 94
3. Methods 96
4. Results 98
5. Discussion 100
5.1 Conclusions 103
Literature Cited 105
Tables 107
Figures 109

LIST OF TABLES

Table 1.1: Summary of eastern Gulf of Mexico Landsat scenes examined for the presence of surface-pelagic drift communities (SPDC) 29

Table 1.2: Area of surface-pelagic drift communities (SPDC) observed within Landsat images from the eastern Gulf of Mexico 30

Table 2.1: Satellite transmitter deployment characteristics for 10 surface-pelagic juvenile Kemp's ridleys tracked from capture locations in the northern and eastern Gulf of Mexico 74

Table 2.2: Summary of duration, behavior, and movements observed from satellite transmitter deployments on 10 surface-pelagic Kemp's ridleys 75

Table 2.3: Summary of travel path direction, surface circulation direction, and surface circulation velocity for 10 satellite-tracked surface-pelagic Kemp's ridleys 76

Table 2.4: Summary of depths (m) occupied by satellite-tracked surface-pelagic Kemp's ridleys 76

Table 2.5: The occurrence of surface-pelagic drift communities (SPDC) within eastern Gulf of Mexico Landsat scenes corresponding to satellite tracks from 10 surface-pelagic juvenile Kemp's ridleys 77

Table 3.1: The occurrence and coverage of surface-pelagic drift communities (SPDC) within the northern Gulf of Mexico from 2009–2011 107

Table 3.2: Area of surface-pelagic drift communities (SPDC) detected within northern Gulf of Mexico Landsat images collected from 2009–2011 108

LIST OF FIGURES

Figure 1.1: The extents of Landsat 5 and 7 scenes within the eastern Gulf of Mexico, paths 16–20 and rows 39–42 31

Figure 1.2: Landsat 5 image of path 19 row 40 collected on 1 August 2005 over waters southwest of Apalachicola, Florida 32

Figure 1.3: Landsat 7 image of path 17 row 41 collected on 15 September 2006, showing waters within the Tampa Bay region of west-central Florida 33

Figure 1.4: Landsat 5 image of path 19 row 40 collected on 1 August 2005 over waters southwest of Apalachicola, Florida 34

Figure 1.5: The extents of Landsat 5 and 7 scenes within the eastern Gulf of Mexico area of interest of the present study, paths 16–20 and rows 39–42 35

Figure 1.6: Annual mean area (km^2) of surface-pelagic drift communities (SPDC) observed within the eastern Gulf of Mexico 36

Figure 1.7: Monthly mean area (km^2) of surface-pelagic drift communities (SPDC) observed within the eastern Gulf of Mexico 37

Figure 1.8: Monthly mean area (km^2) of surface-pelagic drift communities (SPDC) observed per Landsat path within the eastern Gulf of Mexico 38

Figure 1.9: Density of surface-pelagic drift communities (SPDC) observed within Landsat path 20, rows 39 and 40 from 2003–2011 39

Figure 1.10: Density of surface-pelagic drift communities (SPDC) observed within Landsat paths 18 and 19, rows 39 and 40 from 2003–2011 40

Figure 1.11: Density of surface-pelagic drift communities (SPDC) observed within Landsat path 17, row 41 from 2003–2011 41

Figure 1.12: Density of surface-pelagic drift communities (SPDC) observed within Landsat path 16, row 42 from 2003–2011 42

Figure 1.13: Density of surface-pelagic drift communities (SPDC) observed within Landsat path 16, row 43 from 2005–2011 43

Figure 1.14: Density of surface-pelagic drift communities (SPDC) observed within the eastern Gulf of Mexico from 2003–2011 44

Figure 1.15: Wind velocity and the frequency of occurrence of surface-pelagic drift communities (SPDC) within eastern Gulf of Mexico Landsat images 45

Figure 2.1: The locations where satellite-tracked surface-pelagic juvenile Kemp's ridley turtles were released within the northern and eastern Gulf of Mexico during 2011 78

Figure 2.2: A surface-pelagic juvenile Kemp's ridley bearing a 9.5 g solar-powered satellite transmitter attached with silicone adhesive 79

Figure 2.3: Estimated travel rates (km hr^{-1}) among mean daily Argos positions collected for each satellite-tracked Kemp's ridley 80

Figure 2.4: The quality of Argos locations received from satellite transmitters deployed on 10 surface-pelagic juvenile Kemp's ridleys 81

Figure 2.5: Transmitter battery voltage reported by satellite transmitters attached to 10 surface-pelagic juvenile Kemp's ridleys 82

Figure 2.6: Interpolated travel paths of 10 surface-pelagic juvenile Kemp's ridley turtles that were satellite-tracked during 2011 83

Figure 2.7: Interpolated positions and travel path for the surface-pelagic juvenile Kemp's ridley, turtle 105466 84

Figure 2.8: Daily mean number of Argos messages received from the transmitter affixed to turtle 105466 85

Figure 2.9: Sea surface temperature (SST) values corresponding to satellite-tracked surface-pelagic juvenile Kemp's ridleys 86

Figure 2.10: Interpolated travel paths for 10 surface-pelagic juvenile Kemp's ridleys 87

Figure 2.11: Interpolated positions and travel path for the surface-pelagic juvenile Kemp's ridley, turtle 105465 88

Figure 2.12: Interpolated positions and travel path for the surface-pelagic juvenile Kemp's ridley, turtle 105464 89

Figure 2.13: Interpolated positions and travel path for the surface-pelagic juvenile Kemp's ridley, turtle 105468 90

Figure 2.14: Interpolated positions and travel path for the surface-pelagic juvenile Kemp's ridley, turtle 105469 91

Figure 2.15: Interpolated positions and travel path for the surface-pelagic juvenile Kemp's ridley, turtle 105470 92

Figure 3.1: The northern Gulf of Mexico study area as defined by the extents of Landsat scenes that were available during 2009–2011 109

Figure 3.2: The mean area (km^2) of surface-pelagic drift communities (SPDC) observed (by month) within the northern Gulf of Mexico, 2009–2011 110

Figure 3.3: The mean area (km^2) of surface-pelagic drift communities (SPDC) per month observed within the eastern Gulf of Mexico, 2009–2011 111

Figure 3.4: The mean area (km^2) of surface-pelagic drift communities (SPDC) per month observed within the western Gulf of Mexico, 2009–2011 112

Figure 3.5: Generalized patterns of spring and summer peaks in abundance of surface-pelagic drift communities (SPDC) across the northern and eastern Gulf of Mexico 113

Figure 3.6: The density of surface-pelagic drift communities (SPDC) within the northern and eastern Gulf of Mexico, 2009–2011 114

Figure 3.7: The mean monthly area (km^2) of surface-pelagic drift communities (SPDC) within the western (A) and eastern (B) Gulf of Mexico, 2009–2011. 115

Figure 3.8: Wind velocity and the frequency of occurrence of surface-pelagic drift communities (SPDC) within northern Gulf of Mexico Landsat images 116

Figure 3.9: The extent of the surface oil from the Deepwater Horizon oil spill (April–August 2010) and the density of surface-pelagic drift communities (SPDC) within the northern and eastern Gulf of Mexico (2009–2011) 117

Figure 3.10: Scatterplot of wind velocity (1 m s^{-1}) and the area (km^2) of surface-pelagic drift communities (SPDC) observed within northern Gulf of Mexico Landsat images 118

ABSTRACT

Knowledge of species distribution and habitat associations are essential for conservation measures. Such information is lacking for many marine species due to their occupancy of broad and ephemeral habitats that are difficult to access for study. Sea turtles, specifically the surface-pelagic juvenile stage of some species, are a group for which significant knowledge gaps remain surrounding their distribution and habitat use. Recent research has confirmed the long-standing hypothesis that the surface-pelagic juvenile stage occurs within surface-pelagic drift communities (SPDC). Within the North Atlantic and surrounding basins, the holopelagic macroalgae *Sargassum* spp. dominates SPDC and serves as a remotely-detectable indicator of SPDC. The present study focuses on surface-pelagic habitats of four sea turtle species and addresses knowledge gaps using two approaches: habitat mapping and behavioral examination. Remote sensing techniques were used to identify SPDC, and satellite telemetry to examine behavior. This work was conducted in three parts and is presented in three chapters.

Imagery collected from the Landsat satellites (5 and 7) was used to quantify the area of SPDC (km^2). Approximately 1,800 Landsat images collected from 2003–2011 were examined for SPDC. The first chapter discusses the abundance, seasonality, and distribution of SPDC within the eastern Gulf of Mexico waters where surface-pelagic green, hawksbill, Kemp's ridley, and loggerhead turtles are known to occur. SPDC was found year-round within the eastern Gulf of Mexico, and the amount of habitat peaked during summer months. The amount of SPDC within the eastern Gulf of Mexico varied annually with peaks in 2005, 2009, and 2011. High concentrations of SPDC were discovered within offshore waters of the northeastern Gulf of Mexico and southern West Florida Shelf.

Within the second chapter, the behavior of 10 surface-pelagic juvenile Kemp's ridleys was examined using satellite telemetry. Using remotely-sensed imagery, the sea surface habitats used by tracked turtles were examined. Surface-pelagic juveniles are hypothesized to be principally passive drifters. The behavior of tracked turtles was examined to determine if they exhibited periods of active and passive behavior, which may indicate periods of swim and drift. The proximity of tracked turtles to remotely-detected SPDC was examined when coincident Landsat imagery was available (within one day of the turtle's position). Turtles were tracked for 36.5 days (mean) and exhibited primarily passive behavior during the tracking period. The satellite transmitters messaged frequently and reported temperatures significantly higher than sea surface temperatures. Landsat imagery was available coincident to the tracks of nine individuals. SPDC was present within 74% of images, and the mean distance between tracked turtles and SPDC was 54 km. Close associations between tracked turtles and SPDC were documented for four individuals. Results suggest that the tracked turtles spent a majority of the time drifting within SPDC.

The final chapter discusses the density of SPDC within northern and western Gulf of Mexico waters from 2009–2011. Seasonal abundance peaks occurred throughout the study area, but the timing varied. SPDC peaked earlier (late spring) within the northwestern Gulf of Mexico. Moving eastward, the timing of seasonal peaks shifted progressively later during the year. Within the western portions of the study area, SPDC was found to be significantly higher than in the eastern Gulf of Mexico.

The eastern Gulf of Mexico may provide critical developmental habitats for several North Atlantic sea turtle species. Additional study is necessary to determine if portions of the western Gulf of Mexico could serve in a similar capacity. SPDC is extremely vulnerable to anthropogenic impacts, specifically oil spills and the occurrence of persistent marine debris. Conservation of SPDC may be challenged by its ephemeral nature; however, the results presented herein could advise conservation efforts (e.g., delineation of critical habitat). The present study described spatial patterns of SPDC occurrence, regions

of high abundance, and seasonality. The description of the behavior surface-pelagic sea turtles offers refinements to the spatial distribution of this life stage. These results, coupled with information on circulation patterns and the distribution of sea turtle nesting beaches, can be used to better predict when and where sea turtles and SPDC may be found. For example, the year-round persistence of SPDC within the eastern Gulf of Mexico and the location of major nesting beaches located upstream support the area's designation as critical habitat for surface-pelagic green, hawksbill, Kemp's ridley, and loggerhead turtles.

CHAPTER ONE:

CHARACTERIZING A SEA TURTLE DEVELOPMENTAL HABITAT USING LANDSAT OBSERVATIONS OF SURFACE-PELAGIC DRIFT COMMUNITIES WITHIN THE EASTERN GULF OF MEXICO

1. Abstract

Knowledge of the surface-pelagic (oceanic) juvenile life stages remains limited compared to our understanding of most other aspects of sea turtle biology. Recent discoveries have found that North Atlantic cheloniids (the "hard-shelled" sea turtles) appear to closely associate with surface-pelagic drift communities (SPDC), which tend to be dominated by the *Sargassum* spp. macroalgae. The present study sought to quantify SPDC within the eastern Gulf of Mexico — a region that has hosts four species of cheloniids during their surface-pelagic juvenile life stages. Landsat satellite imagery was used to identify SPDC within the eastern Gulf during 2003–2011. The mean area of SPDC observed per each Landsat image was 2.78 km^2 (Landsat scene size: 180x185 km). SPDC was present year-round and varied annually, seasonally, and spatially. SPDC was most abundant during 2005, 2009, and 2011. Abundance was lowest during 2004 and 2010. The 2010 analysis, however, was affected by the Deepwater Horizon Oil spill, which occurred within the study region. Within the eastern Gulf, SPDC abundance peaked during June–August of each year. SPDC was most abundant in the western portion of the study area and within nearshore waters along western Florida. Although SPDC appears less abundant within the eastern Gulf compared to other regions of the Gulf of Mexico and North Atlantic, recent in-water research found surface-pelagic juvenile green, hawksbill, Kemp's ridley, and loggerhead turtles within

the region. Eastern Gulf of Mexico SPDC may provide important developmental habitats to four sea turtle species.

2. Introduction

Marine ecosystem conservation efforts must often consider dynamic habitats and varying patterns of occurrence of the associated organisms. Many marine species are wide-ranging and exhibit complex life-history strategies. As a result, uncertainty regarding their distribution and abundance further challenges conservation efforts (Botsford and Parma 2005; Pearce and Boyce 2006). Life histories with juvenile dispersal stages or lengthy migrations are common in marine fauna. Although wide ranging, many highly migratory species may spend a majority of the time associated with discrete habitats where conservation efforts could focus (Ban et al. 2014). Sea turtles are no exception; they transition among a variety of marine habitats during different life-history stages (Carr et al. 1978).

2.1 Sea Turtle Life History and the "Lost Year"

Sea turtles are long lived and wide-ranging marine vertebrates. Most sea turtles exhibit an early developmental phase that takes place within ocean surface waters and is a period when early juveniles may be carried far from their nesting beaches of origin by surface currents (Musick and Limpus 1997). One exception is the flatback (*Natator depressus*), which appears to remain within neritic (< 200 m) waters during the early developmental phase (Bolten 2003). Another exception is the leatherback (*Dermochelys coriacea*), which principally exists within pelagic waters worldwide. The habitats occupied by juvenile leatherbacks (< 100 cm in length) have not yet been described (Saba 2013). Five species of cheloniids (the "hard-shelled" sea turtles) occur within the North Atlantic, loggerhead (*Caretta caretta*), green (*Chelonia mydas*), hawksbill (*Eretmochelys imbricata*), Kemp's ridley (*Lepidochelys kempii*), and olive ridley (*Lepidochelys olivacea*). For all five species, the following developmental strategy generally

applies (after Bolten 2003). Hatchlings depart nesting beaches, begin a brief period of active swimming away from shore, and move to an initial developmental habitat within ocean surface waters (Musick and Limpus 1997). The time spent within this initial habitat varies across species. All eventually transition to a neritic phase for the final phases of development. The transition from primarily oceanic to primarily neritic environments represents both a shift in habitat and in diet. Additionally, ontogenetic shifts between developmental habitats may represent the longest migrations made by individuals of many species (Meylan et al. 2011). This early, oceanic developmental stage has proven difficult to access for study and, as a result, remains one of the lesser understood aspects of sea turtle biology.

Carr (1967) hypothesized that post-hatchling sea turtles (those having completed the initial active departure from the nesting beach) may associate with drifting *Sargassum*. During 1978, Carr and Meylan observed three post-hatchling green turtles within *Sargassum* off the Caribbean coast of Panama and offered a hypothesis on the oceanic habitats of early juvenile green turtles (Carr and Meylan 1980). Carr (1982) continued to compile support for this hypothesis by initiating directed surveys of *Sargassum* and by accumulating anecdotal reports of juvenile sea turtles associated with *Sargassum*. Carr's evidence included reports of beach-cast post-hatchlings associated with *Sargassum*, observations made by fishers, and notes contributed by oceanographic researchers (Carr 1987a).

Direct research on this early stage of sea turtle development has proven challenging. After Carr (1982), organized research efforts did not occur until Witherington (2002) conducted transect surveys of the oceanic habitats of post-hatchling loggerheads offshore of the major loggerhead rookeries along Florida's east coast. Witherington et al. (2012) expanded survey efforts to include eastern Gulf of Mexico waters off of Florida. Within the Gulf of Mexico, Witherington et al. (2012) found that juvenile green, hawksbill and Kemp's ridley turtles of sizes larger than post-hatchlings were closely associated with *Sargassum* habitats. Carr's hypothesis that the early developmental phase primarily occurs within *Sargassum*-dominated drift habitats is now well supported.

Carr et al. (1978) developed a life-history model for green turtles that identified the early stage of development as the "lost year." This term highlighted the uncertainty surrounding this early developmental stage as well as the importance of filling this gap in biological knowledge. The life history model of Carr et al. (1978) has been refined by various authors, and similar models have been prepared for additional species (Bolten 2003; Meylan et al. 2011). Life-history models for all cheloniids feature a discrete early life stage described as "oceanic" (Bolten 2003), "epipelagic" (Meylan et al. 2011), or "surface-pelagic" (Witherington et al. 2012). The evolution of the terminology surrounding a period that was recently described as "lost" has practical conservation implications beyond what may appear to be academic discussions among biologists (Carr 1987a). Each refinement to the life history model and terminology represents an important advancement in knowledge of sea turtle developmental biology. Research on sea turtle developmental biology defines many life-history stages in terms of level of maturation and position in the water column or habitat. Thus, these stages provide a mechanism by which cohorts can be placed at discrete points in space and time. This is particularly true for early-juveniles that are now known to have a close association with *Sargassum* (Witherington et al. 2012). Following Witherington et al. (2012), the term surface-pelagic will be used hereafter to describe the focal habitat of the present study (surface-pelagic drift communities, SPDC) and the early developmental life-history stages of sea turtles present (surface-pelagic post-hatchlings and juveniles).

2.2 *Sargassum*-Dominated Surface-Pelagic Drift Communities

Sargassum adrift within ocean surface waters forms distinct habitats that define it as a unique ecological community (Fine 1970). Within SPDC, *Sargassum* is considered a keystone taxon (Lapointe et al. 2014). Two holopelagic species of *Sargassum* dominate SPDC within the North Atlantic Ocean*, S. natans* and *S. fluitans* with the former being most abundant (Parr 1939; Thiel and Gutow 2005). Both species reproduce vegetatively and are well-adapted for the surface-pelagic environment, having

pneumatocysts for buoyancy and dense, rugose foliage (Coston-Clements et al. 1991). *Sargassum* appears to be capable of sustained growth even in oligotrophic environments such as the Sargasso Sea, a gyre within the North Atlantic Ocean (Lapointe 1986). Growth and abundance vary seasonally, annually, and spatially (Lapointe 1995; Gower et al. 2006; Gower et al. 2013). Lapointe (1995) demonstrated the nutrient-limited growth of *Sargassum,* which has implications for its spatial patterns of occurrence. *Sargassum* growth is greatest within regions of high nutrient availability, and production may also be influenced by nutrient contributions from associated biota (Lapointe 1995; Lapointe et al. 2014).

A diverse assemblage of epiphytic and motile fauna is found associated with SPDC (Weis 1968). Butler et al. (1983) described the food web of the SPDC as unique, ranging from filter feeders and omnivores to carnivores and grazers. In addition to Weis (1968), several other authors have presented detailed descriptions of the biota found within North Atlantic *Sargassum* (e.g., Dooley 1972, Butler et al. 1983, Coston-Clements et al. 1991). Several taxon-specific studies have demonstrated the association between *Sargassum* and a focal species. Haney (1986) identified several seabird species associated with *Sargassum* and found that larger seabird species (e.g., Cory's shearwater) appeared to associate with larger habitat patches while smaller seabirds (e.g., *Phalaropus* spp.) appeared to associate with smaller patches. Moser and Lee (2012) used gut contents and observational data to classify seabird species based on their associations with SPDC, with "*Sargassum* specialists" (4 species) being the most dependent on the habitat. Dooley (1972) described fish species found within SPDC off of southeast Florida and reviewed the role of SPDC in the life cycles of several species. SPDC appears to provide both foraging opportunities and shelter for many marine vertebrates.

Although the faunal associates of SPDC have been well documented, the influence of SPDC abundance on the populations of associated species is not yet known for many key inhabitants (e.g., commercially important fishes and sea turtles). Butler et al. (1983) found that associated macrofaunal

abundance increased with increasing SPDC patch size, though no change in species diversity occurred. Haney (1986) demonstrated that habitat patch size influenced seabird aggregations. Rooker et al. (2012) noted that larval sailfish abundance increased with *Sargassum* biomass; however, blue marlin, white marlin, and swordfish larval abundances decreased as *Sargassum* biomass increased. Given the complex spatial and temporal dynamics of SPDC, understanding the influences of habitat abundance on the associated species is critical to understanding the effects of habitat loss on population dynamics.

In addition to nutrient availability, physical forces are also responsible for the spatial and temporal distribution and abundance of SPDC. Major circulation features transport SPDC throughout the ocean basins (Thiel and Gutow 2005). On a more localized scale, accumulations of SPDC occur at the boundaries of water masses, fronts, and within Langmuir circulation cells (Ryther 1956). Marmorino et al. (2011) found that winds in excess of 5 m s^{-1} (10 knots) resulted in the degeneration of SPDC habitats. Within the North Atlantic, the distribution of SPDC is influenced by the North Equatorial Drift, Caribbean Current, Gulf Stream System, and Canaries Current, which surround the Sargasso Sea (Ryther 1956).

2.3 Attempts to Quantify Pelagic *Sargassum*

Reports on the occurrence of *Sargassum* within the Sargasso Sea exist in ships' logs dating back to Columbus (reviewed by Butler et al. 1983). By the late 1800s and early 1900s, several attempts were made to quantify *Sargassum* and identify the boundaries of the Sargasso Sea within the North Atlantic. Parr (1939) provided the first quantitative estimates of *Sargassum* based on net tows conducted within the Caribbean Sea, Gulf of Mexico, and northwestern Atlantic Ocean. He estimated that approximately 7 million tons of *Sargassum* existed within the North Atlantic; peaks in abundance occurred within the Sargasso Sea and, secondarily, within the Gulf of Mexico. Stoner (1983) revisited areas surveyed by Parr (1939) and found much less *Sargassum*. Aside from ship-based tows, beach-cast *Sargassum* has been assessed in an attempt to quantify the amount of *Sargassum* present within the Sargasso Sea (Butler et

al. 1983; Johnson et al. 2013). Obtaining synoptic assessments of *Sargassum* has proven difficult using such spatially and temporally discrete techniques. Spatial and seasonal variations in assessments have led to conflicting conclusions regarding *Sargassum* abundance (Butler et al. 1983; Butler and Stoner 1984).

Recent advancements in satellite remote sensing have provided opportunities to conduct broad assessments of *Sargassum*. Gower et al. (2006) developed the Maximum Chlorophyll Index (MCI) to identify *Sargassum* using data collected by the Medium Resolution Imaging Spectroradiometer (MERIS) and the Moderate Resolution Imaging Spectroradiometer (MODIS). Gower and King (2011) and Gower et al. (2013) used the MCI to demonstrate that *Sargassum* was abundant during 2011 in the northwestern Gulf of Mexico and in the eastern Caribbean. Discovery of sizable aggregations of *Sargassum* in the northwestern Gulf agrees with Parr's (1939) hypothesis that *Sargassum* adrift in the Yucatan Channel may drift north and westward with prevailing winds, accumulating within the northwestern Gulf of Mexico.

Gower and King (2011) observed seasonal shifts in *Sargassum* abundance and developed a seasonal distribution map based on those patterns of occurrence. They proposed that *Sargassum* from the northwestern Gulf becomes abundant during March and drifts eastward during late spring and early summer. *Sargassum* is then transported by the Loop Current and Gulf Stream into the northwestern Atlantic, arriving in the Sargasso Sea during fall or winter. Gower and King (2011) also discussed recent fluctuations in inter-annual *Sargassum* abundance; though, they reported very little *Sargassum* within the eastern Gulf of Mexico, an area where surface-pelagic sea turtles and habitat have been observed during May–October of an overlapping time period (Witherington et. al 2012). It is possible that *Sargassum* within the eastern Gulf did not aggregate into lines large enough to be visible within MERIS or MODIS imagery (approximately 300 m resolution).

Hu (2009) developed the Floating Algae Index (FAI) to map various species of marine algae found within ocean surface waters. The FAI captures the spike in reflectance exhibited by all plants at approximately 700 nm, by comparing the reflectance in the near-infrared (NIR) to a linear baseline interpolated between adjacent red and shortwave-infrared (SWIR) wavelengths. Reflectance values within these three regions of the electromagnetic spectrum should appear flat as water strongly absorbs light in all three wavelengths. Thus, spikes in the NIR relative to the baseline can be used to describe the presence of floating vegetation. The FAI can be applied to MODIS and Landsat Thematic Mapper (TM). The higher resolution Landsat TM data (30 m resolution) may be more appropriate for detecting relatively small SPDC features within the eastern Gulf of Mexico.

2.4 Objectives of the Present Study

In the present study, I used Landsat TM data to characterize the SPDC within the eastern Gulf of Mexico. Because *Sargassum* can be used as a remotely-identifiable tracer for SPDC and young sea turtles closely associate with SPDC, this study can be considered a habitat mapping effort (Witherington et al. 2012). The connections among *Sargassum*, SPDC, and sea turtles are based on the following findings:

- *Sargassum* is a dominant feature of surface-pelagic drift habitats within the Gulf of Mexico (Parr 1939; Thiel and Gutow 2005; Witherington et al. 2012).
- The spectral signature of *Sargassum* renders it readily identifiable within remotely-sensed imagery (Hu 2009). I used optical methods to directly observe *Sargassum* in lieu of frontal detection techniques applied to sea surface temperature or ocean color imagery. Indeed, *Sargassum* is found at fronts, convergence zones, and water mass boundaries that would be highlighted by frontal detection methods. *Sargassum* is also found in the absence of major frontal boundaries; thus, frontal detection methods alone may not adequately describe the target habitat (Witherington et al. 2012).

- Surface-pelagic life stages of four species of sea turtles are closely associated with SPDC within the Gulf of Mexico (Witherington et al. 2012).

Building on these points, the principal objective of this study was to characterize the spatial and temporal distributions of SPDC within the eastern Gulf of Mexico at a spatial scale that is complementary to ongoing research focused on surface-pelagic juvenile sea turtles.

3. Methods

3.1 Study Area

I identified a study area within the eastern Gulf of Mexico based on the availability of Landsat satellite imagery and overlap with areas where surface-pelagic juvenile sea turtles have been observed by Witherington et al. (2012; Fig. 1.1). Witherington et al. (2012) conducted transects from five ports on Florida's Gulf coast, listed from north to south: Pensacola, Apalachicola, Sarasota, Marco Island, and Key West. Their study region south of Pensacola ranged from 40–130 km offshore and encompassed waters from 30–1000 m depth. Transects conducted south of Apalachicola ranged from 20–180 km offshore and encompassed depths ranging from 20–500 m. Transects conducted west of Sarasota extended from 35–120 km offshore and encompassed depths from 20–60 m. Transects conducted west of Marco Island included waters from 40–160 km offshore and encompassed depths ranging from 20–160 m. Vessel transects originating from Key West were focused on Gulf of Mexico waters or the Straits of Florida. Key West transects ranged from 60–100 km northwest of Key West within depths of 25–35 m. Transects within the Straits of Florida were 10–40 km south of Key West and at depths of 10–500 m.

3.2 Surface-Pelagic Sea Turtles

Witherington et al. (2012) provided estimates of density (turtles per km^2 of habitat) for two size classes of turtles that they found within the eastern Gulf: surface-pelagic post-hatchling and surface-pelagic juvenile. Transect studies for surface-pelagic turtles were primarily conducted during May–October. Surface-pelagic post-hatchlings were principally found within eastern Gulf waters during July–October. Thus, the surface-pelagic turtle density estimates are scaled to habitat estimates for those two life stages and their respective time periods. Witherington et al. (2012) revised these density estimates based on additional field work that they conducted after the 2012 publication. Those revised values are used herein.

3.3 Remote Sensing

I identified SPDC using two Landsat sensors, the TM and the Enhanced Thematic Mapper Plus (ETM+) onboard Landsat 5 and Landsat 7, respectively. Both TM and ETM+ sensors collect reflectance data at 660, 825, and 1650 nm (bands 3, 4, and 5; respectively). The spatial resolution of Landsat imagery is 30 m. Landsat images were collected within scenes of fixed dimensions: 180 km (length) by 185 km (width). Landsat scenes are arranged into paths (vertical) and rows (horizontal). Individual scenes are presented based on their unique path and row position, abbreviated as p##r##. For example, p17r41 refers to the scene collected along path 17 at row 41, which includes Tampa Bay in west-central Florida (Fig. 1.1). The temporal resolution of each Landsat satellite is 16 days; combined, Landsat 5 and 7 provide 8-day temporal resolution.

Using the US Geological Survey's Global Visualization Viewer (Glovis; http://glovis.usgs.gov/), I browsed all Landsat scenes collected from 2003–2011. A minimum of 1–2 images for each month, year, and scene were selected for analysis. A specific cloud cover threshold was not used to exclude cloudy images. Images were visually inspected and those within which a majority of sea surface waters were

obstructed by thick cloud cover were not used in this study. From Glovis, I downloaded and processed raw, level 1, reflectance data from selected images.

Image processing involved several steps. First, atmospheric correction was applied to the raw reflectance data using a customized set of IDL routines (Hu et al. 2004; Exelis Visual Information Solutions, Boulder, CO). Next, I calculated the FAI using the corrected reflectance data from bands 3, 4, and 5 (Hu 2009; Fig. 1.2). I searched output FAI images, along with co-registered RGB images, for SPDC within ENVI (Exelis Visual Information Solutions, Boulder, CO). Simultaneous FAI and RGB image examination reduced the likelihood of false detection of spectrally similar features (e.g., clouds, Fig. 1.3 and 1.4). Using ENVI, I digitized SPDC and recorded the results in a Microsoft Access database. I converted the SPDC pixels to vectors (shapefiles) and recorded those as feature classes within an ArcGIS geodatabase (Esri, Redlands CA). Using ArcGIS, I calculated the density of SPDC at a spatial scale suitable for regional visualization; I calculated density within a 1 km search radius of 500 m cells.

I identified SPDC within FAI images based on physical characteristics. SPDC tends to be present in the open ocean as discrete lines, patches, or linear arrangements of patches. In some cases, SPDC could be distinguished from spectrally similar and co-occurring species (e.g., *Trichodesmium* spp.) by examining the spectral shape of the feature of interest using corresponding MODIS reflectance data. A technique to distinguish among *Sargassum* and *Trichodesmium* reflectance data was developed concurrent to the present study and was reported by Hu et al. (2010).

Most of the scenes analyzed in this study contained some land area. I standardized estimates of SPDC across scenes by calculating the extent of "searchable waters" for each Landsat image using custom Python and R routines (R Core Team 2013). The area of searchable waters was defined as the extent of the image with a clear view of surface ocean waters; i.e., land masses, vessels, thick clouds, and scan line corrector failures (present only in Landsat 7 ETM+ imagery) were excluded (Fig. 1.3). The

FAI technique was capable of detecting SPDC through thin cloud layers (Fig. 1.4). For each image, I calculated a scaled density of SPDC as follows:

SPDC coverage ‰ = (SPDC pixels / searchable water pixels) * 1000.

I extracted wind velocity values for the dates and locations corresponding to each image using the RNCEP R (Kemp et al. 2012); written for the program R, which provided wind velocity values from the global NCEP/NCAR Reanalysis 2 dataset (Kanamitsu et al. 2002). I estimated a single, geographically central location for each Landsat scene and associated zonal and meridional wind velocity values to those positions. Using ArcGIS, I excluded land from the scene footprint polygons prior to calculating the central location. Within R, I converted zonal and meridional velocity values to wind speed and direction. I examined the correlation between wind velocity and the amount of observed SPDC using Pearson's product-moment correlation test. I also compared mean wind velocities for scenes when SPDC was and was not observed using a two sample t-test.

4. Results

4.1 Summary of SPDC within the Eastern Gulf of Mexico

I examined 1,323 Landsat images collected from 2003–2011 within the eastern Gulf of Mexico study area (paths 16–20 and rows 39–42, Fig. 1.5). I found SPDC within 824 (62%) of the eastern Gulf images that I examined. I observed an average of 2.78 km^2 of SPDC per Landsat image (range: 0.0–90.84, SD: 7.77 km^2). The highest amounts of SPDC (average per scene) occurred within p20r40 (6.65 km^2) and p18r39 (5.92 km^2). The extent of SPDC was relatively low during 2004 and 2010 (0.45 and 0.92 km^2, respectively; Fig. 1.6). The average area of SPDC was highest during 2005 (4.27 km^2) and 2011 (4.20 km^2). SPDC abundance increased during May, peaked during June–August, and declined during September and October (Fig. 1.7).

I examined the monthly abundance of SPDC within each Landsat path and observed an eastward shift in the monthly peaks of SPDC abundance. SPDC abundance increased in May and peaked in June within the westernmost region of the study area (path 20, Fig. 1.8, A). SPDC abundance peaked in July within the two central regions (paths 18 and 19, Fig. 1.8, B and C). SPDC abundance peaked in August within paths 16 and 17, the easternmost portions of the Gulf of Mexico (Fig. 1.8, D).

I evaluated SPDC density across all Landsat scenes (Table 1.1) and within scenes that intersected with specific regions where vessel transects had been conducted (Fig. 1.9–1.12). The density of SPDC was lowest within rows 41 and 42 of paths 19 and 20 (Table 1.1). SPDC was distributed throughout the waters near the two northern Gulf vessel transect areas (paths 19 and 20, Fig. 1.9 and 1.10). The Landsat scenes intersecting with the northern Gulf study areas (paths 18–20, rows 39 and 40) contained high densities of SPDC, particularly within offshore waters (Table 1.1). Within the three east-central Gulf vessel transect study areas, high densities of SPDC occurred closer to shore, inshore of the 10 m bathymetric contour and along the western coastline of Florida (Fig. 1.11, 1.12 and 1.13). The density of SPDC within offshore waters of the central West Florida Shelf (WFS) was low relative to nearshore waters (Fig. 1.11). The density of SPDC increased on the southern portion of the WFS, north of Key West (Fig. 1.13). High concentrations of SPDC were found south of Key West, along the edge of the continental shelf and the Florida Current (Fig. 1.13). High densities of SPDC also occurred near the Florida coast and inshore of 10 m depth, within portions of Landsat scenes p17r40 and p18r39 that were outside of the areas where vessel transects were conducted (Fig. 1.14).

4.2 Density of Surface-Pelagic Sea Turtles within the Eastern Gulf of Mexico

I summarized SPDC density within the two time periods corresponding to those within which surface-pelagic juveniles and post-hatchlings were estimated by Witherington et al. (2012, including updates based on continued during summer and fall of 2012). I scaled estimates of turtle density based

on habitat density (Table 1.2). From May – October, the average amount of SPDC observed per scene ranged from 0.03–9.67 km^2. Witherington et al. (2012) estimated that the density of surface-pelagic juveniles during this time period was 9.73 turtles km^{-2}. Thus, the density of surface-pelagic turtles within detectable SPDC across the northern Gulf of Mexico is estimated as 0.29–94.09 turtles km^{-2}. I also calculated the area of SPDC within the time window restricted to the hatching season — July–October. The density of SPDC across the study area during the hatching season ranged from 0.05–10.94 km^2. Witherington et al. (2012) estimated that surface-pelagic post-hatchling turtle density within this period was 1.98 turtles km^{-2}. Thus, the average density of surface-pelagic post-hatchling turtles within detectable SPDC across the eastern Gulf is estimated as 0.10–21.66 turtles km^{-2}.

4.3 Wind Velocity and SPDC Abundance

Wind speeds corresponding to images when no SPDC was detected exceeded those of scenes where SPDC was detected ($t = 7.6$, $p < 0.01$, Fig. 1.15). Wind speeds corresponding to scenes within which no SPDC was found were 4.9 m s^{-1} (mean, ±2.5 SD, n = 502 images). Wind speeds corresponding to scenes within which I observed SPDC were 3.5 m s^{-1} (mean, ±2.3 SD, n = 819 images). The highest wind speed observed within an image where SPDC was detected was 11.2 m s^{-1}. Wind speeds ranged from < 1–13.7 m s^{-1} for scenes where SPDC was not detected. For all images, the area of SPDC was inversely related to wind speed ($r=-0.25$, $p < 0.001$).

5. Discussion

5.1 SPDC within the Eastern Gulf of Mexico

I found SPDC to be present within the eastern Gulf of Mexico year-round with seasonal and annual variation in abundance. Both the eastward shift in abundance peaks and the late summer peaks that

were observed across all years generally agreed with the findings of another remote sensing examination of *Sargassum* within the Gulf of Mexico (Gower and King 2011). I detected SPDC throughout eastern Gulf continental shelf waters and well away from major Gulf circulation features (the Loop Current or associated eddies). The broad continental shelf within the eastern Gulf lacks such circulation features yet SPDC and surface-pelagic juvenile sea turtles have been regularly encountered within this region (Witherington et al. 2012). The work of Yang et al. (1999) suggests that the Loop Current is not a major influence on surface drift within portions the WFS. This suggests that SPDC, and associated juvenile sea turtles, could be relatively persistent on the WFS.

Spatial resolution of the observation platform was critical in detecting SPDC within the eastern Gulf. Gower et al. (2006) found no *Sargassum* in the eastern Gulf of Mexico from September 2004–November 2005, except for the months of July–September 2005. However, the present study found that these months were periods of relatively high SPDC abundance within similar portions of the eastern Gulf. The disparity between the findings reported here and those of Gower et al. (2006) is most likely due to differing spatial resolutions of the imagery. Gower et al. (2006) used MODIS imagery summarized at 1 km resolution, while the present study used Landsat with a spatial resolution of 30 m. This illustrates an important consideration surrounding spatial resolution, research objectives and interpretation of results. Using MERIS imagery, 330 m resolution, Gower and King (2008 and 2011) were able to reconstruct broad-scale patterns of SPDC drift within the Gulf of Mexico and North Atlantic. Performing such a basin-wide analysis across multiple years would not be feasible using the higher resolution Landsat imagery and the methods outlined herein. Landsat was the appropriate platform to meet the principal objective of the present study, which was to estimate SPDC within the eastern Gulf at a scale corresponding to field observations.

Wind speed may be an important variable to consider when attempting to forecast the occurrence or predict the persistence of SPDC. Wind speeds for images when SPDC was not detected were

significantly higher than wind speeds when SPDC was detected. When wind speeds were below 5 m s^{-1}, SPDC was detected within Landsat scenes more frequently than it was not detected (Fig. 1.15). This value is consistent with the findings of Marmorino et al. (2011), which indicated that lines of SPDC may disintegrate into smaller patches when wind speeds exceed 5 m s^{-1}. This dispersal effect of wind may reduce the likelihood of SPDC detection if patches become too small to be observed within satellite imagery.

5.2 Low Abundance of SPDC During 2010

The abundance of SPDC was relatively low during 2010 and this was likely a result of multiple factors. The DWH oil spill during 2010 affected my ability to characterize SPDC within portions of our study area. Specifically, portions of path 20 (an area of high SPDC abundance) contained large amounts of surface oil during a time when *Sargassum* abundance would have peaked within the region, May–July. Oil reflects light across a broad portion of the visible range of the electromagnetic spectrum (Hu et al. 2003). Non-oiled *Sargassum* cannot be distinguished from oil or oiled *Sargassum* using the methods of the present study; therefore, I excluded oiled areas from this analysis. I used the daily MODIS oiling footprint provided by Hu et al. (2011) to identify oiled areas within Landsat scenes. This prevented some 2010 images from being fully examined and may have biased the estimate abundance of SPDC during 2010. It is also possible that large amounts of eastward drifting SPDC became entrained within the oiled area and were not available to be observed within portions of the study area that were east of the event. Results of the present study support previous findings that SPDC drifts eastward across the northern Gulf. Thus, an examination of scenes prior to and eastward of the DWH event (i.e., paths 21–25 during March–May 2010) would assist in interpreting the SPDC abundance patterns for the eastern Gulf that are presented herein (Fig. 1.14).

5.3 The Eastern Gulf of Mexico — A Critical Developmental Habitat for Sea Turtles in the Northwestern Atlantic.

The Caribbean Current, Loop Current, and Gulf Stream system influence the distribution of SPDC and surface-pelagic sea turtles within the eastern Gulf of Mexico. To date, two potential source regions for SPDC within the Gulf and Caribbean have been identified. Large blooms of *Sargassum* have recently been observed within the northwestern Gulf and the eastern Caribbean (Gower and King 2011; Gower et al. 2013; Johnson et al. 2012). Admittedly, the ability to detect such events at the scale of ocean basins is recent, due to technological advancements in satellite oceanography. It appears that surface-pelagic sea turtles in this area have evolved depending on SPDC for early developmental habitats. Thus, it is reasonable to assume that SPDC must need to form upstream of major sea turtle nesting rookeries within the region.

Witherington et al. (2012) observed four species of surface-pelagic juvenile sea turtles within SPDC in the eastern Gulf (green, hawksbill, Kemp's ridley, and loggerhead turtles). The major green turtle rookeries within the Caribbean upstream from the eastern Gulf are (listed in order of the relative magnitude of nesting activity): Tortuguero, Costa Rica; Yucatan Peninsula, Mexico; Aves Island, Venezuela (NMFS and USFWS 2007). Hawksbill turtles nest throughout the Caribbean and many rookeries may contribute surface-pelagic juvenile turtles to the Gulf of Mexico (Blumenthal et al. 2009). The loggerhead nesting beaches that could contribute surface-pelagic juveniles to the Gulf of Mexico are found in parts of the Caribbean, western Cuba, Yucatan Peninsula, and the Gulf of Mexico (Ehrhart et al. 2003; NMFS and USFWS 2008). Within the Gulf, the major loggerhead nesting beaches occur along southwestern Florida, the Dry Tortugas, and along the eastern shorelines of the Florida Panhandle (Witherington et al. 2006; FWC Statewide Nesting Beach Survey Program). On those Florida Gulf beaches, a mean of 7,772 loggerhead nests year^{-1} were documented during the 5-year period from 2009–2013 (FWC Statewide Nesting Beach Survey Program). Brost et al. (in press) estimated the mean

loggerhead clutch size to be 114 eggs and the mean emergence success to be 51.6%. Based on these values, 457,180 loggerhead hatchlings may enter eastern Gulf waters each year.

With few exceptions, Kemp's ridley turtles nest entirely along the central-western Gulf of Mexico shorelines of Mexico and Texas (NMFS, USFWS and SEMARNAT 2011). Animals emerging from those nesting beaches likely drift eastward across the northern Gulf of Mexico or encounter westward drifting eddies and remain within the western Gulf (Collard and Ogren 1990). The majority of Kemp's ridley nesting occurs at the beaches near Rancho Nuevo, Mexico. More than 20,000 Kemp's ridley nests were recorded on Rancho Nuevo and adjacent beaches during 2009, a recent high year. NMFS, USFWS and SEMARNAT (2011) presented the following Kemp's ridley reproductive parameters based on corral (hatchery): mean clutch size = 97 eggs $nest^{-1}$, hatching success = 67.8%, emergence success = 100%. Based on these values, during this recent high nesting year approximately 1,315,320 may have entered western Gulf of Mexico waters (nests * (clutch size * hatching success)).

Sea turtles originating from Gulf and Caribbean rookeries may be spending all or portions of their surface-pelagic phase within SPDC habitats of the eastern Gulf of Mexico. Research into the genetics of animals captured within the eastern Gulf, coupled with refined animal movement models, would help identify the source rookeries for Gulf sea turtles. Such knowledge is essential to understanding the role of Gulf SPDC for north Atlantic sea turtles and how impacts to this habitat will affect their populations.

5.4 Threats to SPDC and Conservation Efforts

The greatest threat to SPDC appears to be pollution, both from the constant influx of persistent marine debris and major releases of pollution, e.g., the DWH oil spill (Carr 1987b; Witherington 2002; Schuyler et al. 2014). Butler et al. (1983) noted petroleum hydrocarbons were present within *Sargassum* samples and had apparently been ingested by associated invertebrates. Witherington (2002) identified plastic pollution and tar within the mouths or gut contents of post-hatchling loggerheads

collected within the Gulf Stream, off the east coast of Florida. Other factors that could affect SPDC include direct harvest of *Sargassum* for biomedical products, although no harvesting operation appears to exist at present (SAFMC 2002).

During 2009, the government of Bermuda formed the Sargasso Sea Alliance in an effort to improve conservation and management efforts within the high seas surrounding the Bermuda Platform (Laffoley et al. 2011). In support of this effort, Laffoley et al. (2011) outlined the economic and environmental significance of the region and its namesake — *Sargassum*. As of 2014, four nations (Azores, Monaco, the United Kingdom and the United States) have joined Bermuda in recognizing the ecological value of the *Sargassum* and the Sargasso Sea (The Hamilton Declaration, March 2014). The Hamilton Declaration established a Sargasso Sea Commission that will be charged with managing the Sargasso Sea. Although the declaration is not legally binding, it represents an important acknowledgement of this marine ecosystem and an opportunity for collaborative conservation and management.

The U.S. National Marine Fisheries Service has recently identified five types of marine habitats critical to the survival of loggerheads within the Northwestern Atlantic Ocean (NMFS 2014). The *Sargassum* habitat occupied by early juveniles was one of the critical habitats identified within this ruling. The critical habitat was defined by the following physical and biological elements: (*i*) convergence zones, areas of downwelling, margins of major currents, and other locations where concentrated components of the *Sargassum* community exist (including suitable water temperatures); (*ii*) *Sargassum* in concentrations that support prey and provide cover for loggerheads; (*iii*) the presence of *Sargassum*-associated biota; and (*iv*) sufficient depth (10 m) and proximity to currents to ensure that loggerheads are transported out of the surf zone. The *Sargassum* critical habitat was defined (spatially) as a static region within the U.S. Exclusive Economic Zone including western Gulf of Mexico waters to the Mississippi River delta, extending southward to the Straits of Florida and north-northwest following the Gulf Stream Current. This designation effectively captures the western Gulf waters where

Sargassum appears most abundant (Gower and King 2011). However, most of the eastern Gulf of Mexico is excluded from this boundary, including the areas surveyed by Witherington et al. (2012) and those examined as part of the present study (Fig. 1.14). The text associated with this rule acknowledged the difficulty in identifying areas where *Sargassum* was likely to consistently accumulate, particularly within areas that are isolated from major circulation features (e.g., the Loop Current) like the eastern Gulf (NMFS 2014). Indeed, SPDC within offshore waters (> 10 m) of the eastern Gulf appeared more dispersed and less abundant than that reported from western Gulf surveys. However, SPDC did persist year-round within the eastern Gulf of Mexico waters examined herein. In addition to abundance, the availability of habitat should be considered by conservation actions. Habitat availability may be defined as proximity to sea turtle nesting rookeries in this context. Considering the findings of Witherington et al. (2012) and that eastern Gulf loggerhead rookeries are genetically distinct (Shamblin et al. 2011), the proximity to the eastern Gulf loggerhead rookeries appears relevant to the delineation of critical habitat for the species.

Regulatory actions focused on dynamic marine habitats require an understanding of habitat distribution and the spatial ecology of target species. Similar to the loggerhead critical habitat, the designation of sea ice as critical habitat for polar bears (*Ursus maritimus*) established fixed boundaries within which sea ice was known to occur (USFWS 2010). The USFWS was later ordered to vacate this rule, dissolving the established critical habitats, on the grounds that the designation was "too extensive" (Alaska Oil and Gas Association, et al. v. Salazar, et al. 2013). Considering this recent case, it was reasonable for NMFS to restrict the loggerhead-*Sargassum* critical habitat designation to waters with high concentrations of *Sargassum*. However, refinements to this ruling or establishment of surface-pelagic critical habitat for other cheloniids should consider both the presence of habitat and the availability of habitat to the surface-pelagic stage of the species of interest. Areas found downstream of *Sargassum* source regions and major sea turtle rookeries may be the best candidates for protection.

Satellite remote sensing has provided opportunities to conduct synoptic assessments of SPDC. Such research has demonstrated that SPDC exhibits high spatial, seasonal, and annual variability (Gower and King 2011; present study). The abundance of surface-pelagic juvenile sea turtles may also vary within the same dimensions. Conservation actions may benefit from focusing on the proximity of SPDC to major sea turtle rookeries. Within U.S. Gulf waters, major loggerhead nesting beaches are situated along the northwestern and west-central Florida shorelines (Florida Fish and Wildlife Conservation Commission, Statewide Sea Turtle Nesting Beach Survey Program; Fig. 1.14). Witherington et al. (2012) documented post-hatchling loggerheads within eastern Gulf waters near to these nesting beaches. The present study identified SPDC within the eastern Gulf year-round. Although SPDC may be more abundant within the western Gulf, the eastern Gulf may serve as critical developmental habitat for loggerheads within the region. Gulf SPDC habitats also support early juvenile green, hawksbill, and Kemp's ridley turtles. If critical habitats are designated for surface-pelagic life stages of these species, the following parameters should be evaluated: (*i*) the spatial distribution of nesting beaches, including density and nest productivity; (*ii*) in-water aggregations identified by direct research and/or anecdotal accounts; (*iii*) duration of the surface-pelagic stages and survivorship; (*iv*) the spatial distribution and seasonality of remotely-detected SPDC; and (*v*) the physical oceanographic parameters responsible for the distribution of SPDC and surface-pelagic juvenile turtles.

Reviewing this multidisciplinary approach highlights some information deficiencies. The spatial distribution of sea turtle nesting beaches is well-described for most regions and species; however, nest productivity (a measure of the number of turtles emerging from eggs and nests) is not well described for all rookeries. In-water research on the surface-pelagic turtles is limited based on the cost and logistical difficulties of accessing SPDC for direct sampling. Direct sampling is the only mechanism to describe the density and species occurrence of surface-pelagic juveniles within SPDC. Directed capture studies are also essential to documenting behavior, habitat associations, and genetic compositions of turtles

inhabiting SPDC. Knowledge of the duration of the surface-pelagic juvenile life stage and estimates of survivorship for each species would prove useful in evaluating the impacts of threats on populations. Remote-sensing efforts to assess the distribution and abundance of SPDC should be expanded to new regions where surface-pelagic turtles may aggregate (e.g., the southwestern Gulf of Mexico and the Sargasso Sea). Although Landsat imagery is collected at a higher resolution than MODIS or MERIS imagery previously used to map SPDC, it is possible that Landsat-derived estimates of SPDC are still underestimates. *In situ* validation of remotely-sensed SPDC is necessary to address the potential for over- or under-estimation of SPDC. For example, estimates from the present study could be refined with a validation study that couples Landsat with higher resolution imagery and field observations. Such efforts are underway for the northern Gulf of Mexico and should be integrated into any remote sensing assessment of SPDC. Finally, the distribution of surface-pelagic juvenile sea turtles and their habitats cannot be understood without considering the physical oceanographic parameters that influence their distribution. Such research, coupled with remote sensing observations, could be used to develop and test predictive models for the occurrence of SPDC. These methods could be applied to conduct near-real time assessments of SPDC to assist marine conservation management decisions.

5.5 Conclusions

The satellite remote sensing methods used in the present study were an effective mechanism for conducting an assessment SPDC within the eastern Gulf. The higher resolution imagery utilized was appropriate for making comparisons to results from vessel transect surveys of SPDC. These results demonstrate that SPDC is present within the eastern Gulf of Mexico year-round. The region is downstream of nesting beaches for green, hawksbill, Kemp's ridley, and loggerhead turtles. Witherington et al. (2012) confirmed the presence of surface-pelagic juvenile green, hawksbill, Kemp's ridley and loggerhead turtles within eastern Gulf of Mexico waters. The year-round persistence of SPDC

and the presence of surface-pelagic juvenile sea turtles indicate that the eastern Gulf of Mexico may serve as critical developmental habitat for surface-pelagic green, hawksbill, Kemp's ridley, and loggerhead turtles.

Literature Cited:

Alaska Oil and Gas Association, et al. v. Kenneth L. Salazar, et al. 2013. Case 3:11-cv-0025-RBB. United States District Court for the District of Alaska. 50 p.

Ban, N. C., S. M. Maxwell, D. C. Dunn, A. J. Hobday, N. J. Bax, J. Ardron, K. M. Gjerde, E. T. Game, R. Devillers, D. M. Kaplan, P. K. Dunstan, P. N. Halpin, and R. L. Pressey. 2014. Better integration of sectoral planning and management approaches for the interlinked ecology of the open oceans. Marine Policy 49:127–136.

Blumenthal, J. M., F. A. Abreu-Grobois, T. J. Austin, A. C. Broderick, M. W. Bruford, M. S. Coyne, G. Ebanks-Petrie, A. Formia, P. A. Meylan, A. B. Meylan, and B. J. Godley. 2009. Turtle groups or turtle soup: dispersal patterns of hawksbill turtles in the Caribbean. Molecular Ecology 18:4841–4853.

Bolten, A. B. 2003. Life history patterns of sea turtles: consequences of an oceanic juvenile stage. Pages 243–257 in P. L. Lutz, J. Musick, and J. Wyneken, editors. The biology of sea turtles, volume II. CRC Press, Boca Raton, FL.

Botsford L., and A. Parma. 2005. Uncertainty in marine management. Pages 375–392 in E. Norse and L. Crowder, editors. Marine conservation biology: the science of maintaining the sea's biodiversity. Island Press, Washington, D.C., USA.

Brost, B., B. Witherington, A. Meylan, E. Leone, L. Ehrhart, D. Bagley. *In press*. Sea turtle hatchling production from Florida (USA) beaches, 2002–2012, with recommendations for analyzing hatching success. Endangered Species Research.

Butler, J.N., B.F. Morris, J. Cadwallader, and A.W. Stoner. 1983. Studies of *Sargassum* and the *Sargassum* Community. Special Publication No. 22. Bermuda Biological Station for Research.

Butler, J. N., and A. W. Stoner. 1984. Pelagic *Sargassum*: has its biomass changed in the last 50 years? Deep Sea Research 31:1259–1264.

Carr, A.F. 1967. Adaptive aspects of the scheduled travel of Chelonia. Pages 35 - 55. In R.M. Storm, editor. Animal navigation and orientation. Oregon State University Press. Corvallis, Oregon.

Carr, A. F. 1982. *Sargassum*-raft reconnaissance. A final report on Project 1800 to the World Wildlife Fund.

Carr, A.F. 1987a. New perspectives on the pelagic stage of sea turtle development. Conservation Biology 1:103-121.

Carr, A. 1987b. Impact of nondegradable marine debris on the ecology and survival outlook of sea turtles. Marine Pollution Bulletin 18:352–356.

Carr, A.F. and A.B. Meylan. 1980. Evidence of passive migration of green turtle hatchlings in *Sargassum*. Copeia 1980:366-368.

Carr, A.F., M.H. Carr, and A.B. Meylan. 1978. The ecology and migrations of sea turtles, 7. The west Caribbean green turtle colony. Bulletin of the American Museum of Natural History 162:1-46.

Collard, S. B., and L. H. Ogren. 1990. Dispersal scenarios for pelagic post-hatchling sea turtles. Bulletin of Marine Science 47:233–243.

Coston-Clements, L., L. R. Settle, D. E. Hoss, and F. A. Cross. 1991. Utilization of the *Sargassum* habitat by marine invertebrates and vertebrates — a review. US Department of Commerce, NOAA Technical Memorandum NMFS-SEFSC-296, 32 pp.

Dooley, J. K. 1972. Fishes associated with the pelagic *Sargassum* complex, with a discussion of the *Sargassum* community. Contributions in Marine Science 16:1–32.

Ehrhart, L. M, D. A. Bagley, W. E. Redfoot. 2003. Loggerhead turtles in the Atlantic Ocean: Geographic distribution, abundance and population status. Pages 157–174 in A. B. Bolten and B. E. Witherington, editors. Loggerhead Sea Turtles. Smithsonian Institution, Washington, D.C., USA.

Fine, M. L. 1970. Faunal variation on pelagic *Sargassum*. Marine Biology 7:112–122.

Gower, J., C. Hu, G. Borstad, and S. King. 2006. Ocean color satellites show extensive lines of floating *Sargassum* in the Gulf of Mexico. IEEE Transactions on Geoscience and Remote Sensing 44:3619–3625.

Gower, J., E. Young, and S. King. 2013. Satellite images suggest a new *Sargassum* source region in 2011. Remote Sensing Letters 4:764–773.

Gower, J., and S. King. 2008. Satellite images show the movement of floating *Sargassum* in the Gulf of Mexico and Atlantic Ocean. Nature Precedings. http://hdl.handle.net/10101/npre.2008.1894.1.

Gower, J. F. R., and S. A. King. 2011. Distribution of floating *Sargassum* in the Gulf of Mexico and the Atlantic Ocean mapped using MERIS. International Journal of Remote Sensing 32:1917–1929.

Haney, J. C. 1986. Seabird Patchiness in Tropical Oceanic Waters : The Influence of *Sargassum* " Reefs ." The Auk 103:141–151.

Hu, C. 2009. A novel ocean color index to detect floating algae in the global oceans. Remote Sensing of Environment 113:2118-2129.

Hu, C., J. Cannizzaro, K. Carder, F. Muller-Karger, and R. Hardy. 2010. Remote detection of Trichodesmium blooms in optically complex coastal waters: examples with MODIS full-spectral data. Remote Sensing of Environment 114:2048-2058.

Hu, C., Z. Chen, T. D. Clayton, P. Swarzenski, J. C. Brock, and F. E. Muller–Karger. 2004. Assessment of estuarine water-quality indicators using MODIS medium-resolution bands: Initial results from Tampa Bay, FL. Remote Sensing of Environment 93:423–441.

Hu, C., X. Li, and W. G. Pichel. 2011. Case Study 1 Detection of Oil Slicks using MODIS and SAR Imagery. Pages 111–124 in T. P. and S. S. Jesus Morales, Venetia Stuart, editor. Handbook of satellite remote sensing image interpretation: Applications for marine living resources conservation and management. EU PRESPO Project and IOCCG, Dartmouth, Canada. <http://www.ioccg.org/handbook/>.

Hu, C., F. E. Mueller-Karger, C. (Judd) Taylor, D. Myhre, B. Murch, A. L. Odriozola, and G. Godoy. 2003. MODIS Detects Oil Spills in Lake Maracaibo, Venezuela. Eos, Transactions American Geophysical Union 84:313–319.

Kanamitsu, M., W. Ebisuzaki, J. Woollen, S. K. Yang, J. J. Hnilo, M. Fiorino, and G. L. Potter. 2002. NCEP-DOE AMIP-II reanalysis (R-2). Bulletin of the American Meteorological Society 83:1631–1643+1559.

Kemp, M.U., E.E. van Loon, J. Shamoun-Baranes, W. and Bouten. 2012. RNCEP: Global weather and climate data at your fingertips. Methods in Ecology and Evolution 3:65-70. R package version 1.0.6.

Johnson, D. R., D. S. Ko, J. S. Franks, P. Moreno, and G. Sanchez-Rubio. 2013. The *Sargassum* invasion of the eastern Caribbean and dynamics of the equatorial North Atlantic. Pages 102–103 in. Proceedings of the 65th Gulf and Caribbean Fisheries Institute. GCFI, Santa Marta, Colombia.

Laffoley, D. D., H. S. J. Roe, M. V. Angel, J. Ardron, N. R. Bates, I. L. Boyd, S. Brooke, K. N. Buck, C. A. Carlson, B. Causey, M. H. Conte, S. Christiansen, J. Cleary, J. Donnelly, S. A. Earle, R. Edwards, K. M. Gjerde, S. J. Giovannoni, S. Gulick, M. Gollock, J. Hallett, P. Halpin, R. Hanel, A. Hemphill, R. J. Johnson, A. H. Knap, M. W. Lomas, S. A. McKenna, M. J. Miller, F. W. Ming, R. Moffitt, N. B. Nelson, L. Parson, A. J. Peters, J. Pitt, P. Rouja, J. Roberts, D. A. Seigel, A. N. S. Siuda, D. K. Steinberg, A. Stevenson, V. R. Sumaila, W. Swartz, S. Thorrold, T. M. Trott, and V. Vats. 2011. The protection and management of the Sargasso Sea: The golden floating rainforest of the Atlantic Ocean. Summary Science and Supporting Evidence Case. Sargasso Sea Alliance. 44 pp.

Lapointe, B. E. 1986. Phosphorus-limited photosynthesis of growth of *Sargassum natans* and *Sargassum fluitans* (Phaeophycae) in the western North Atlantic. Deep-Sea Research 33:391–399.

Lapointe, B. E. 1995. A comparison of nutrient-limited productivity in *Sargassum natans* from neritic vs . oceanic waters of the western North Atlantic Ocean. Limnology & Oceanography 40:625–633.

Lapointe, B. E., L. E. West, T. T. Sutton, and C. Hu. 2014. Ryther revisited: Nutrient excretions by fishes enhance productivity of pelagic *Sargassum* in the western North Atlantic Ocean. Journal of Experimental Marine Biology and Ecology 458:46–56.

Marmorino, G. O., W. D. Miller, G. B. Smith, and J. H. Bowles. 2011. Airborne imagery of a disintegrating *Sargassum* drift line. Deep Sea Research Part I: Oceanographic Research Papers 58:316–321. Elsevier.

Meylan, P.A., A.B. Meylan, and J.A. Gray. 2011. The ecology and migrations of sea turtles, 8. Tests of the developmental habitat hypothesis. Bulletin of the American Museum of Natural History 357:1-70.

Moser, M. L., and D. S. Lee. 2012. Foraging over *Sargassum* by western North Atlantic seabirds. The Wilson Journal of Ornithology 124:66–72.

Musick, J. A., and C. Limpus. 1997. Habitat utilization and migration in juvenile sea turtles. Pages 137–163 in P. L. Lutz and J. A. Musick, editors. The biology of sea turtles, volume 1. CRC Press, Washington, D.C.

[NMFS] National Marine Fisheries Service. 2014 Endangered and threatened species: Critical habitat for the Northwest Atlantic Ocean loggerhead sea turtle distinct population segment (DPS) and determination regarding critical habitat for the North Pacific Ocean loggerhead DPS. Federal Register 79(132) 39856–39912, 10 July 2014.

[NMFS and USFWS] National Marine Fisheries Service and US Fish and Wildlife Service. 2007. Green sea turtle (*Chelonia mydas*) 5-year review: Summary and evaluation. National Marine Fisheries Service, Silver Spring, MD.

[NMFS and USFWS] National Marine Fisheries Service and U.S. Fish and Wildlife Service. 2008. Recovery plan for the Northwest Atlantic Population of the loggerhead sea turtle (*Caretta caretta*), Second Revision. National Marine Fisheries Service, Silver Spring, MD.

[NMFS, USFWS, and SEMARNAT] National Marine Fisheries Service, U.S. Fish and Wildlife Service, and SEMARNAT. 2011. Bi-national recovery plan for the Kemp's ridley sea turtle (*Lepidochelys kempii*), Second Revision. National Marine Fisheries Service. Silver Spring, Maryland 156 pp. + appendices.

Parr, A.E. 1939. Quantitative observations on the pelagic *Sargassum* vegetation of the western north Atlantic. Bulletin of the Bingham Oceanographic Collection 6:1-93.

Pearce, J. L., and M. S. Boyce. 2006. Modelling distribution and abundance with presence-only data. Journal of Applied Ecology 43:405–412.

[SAFMC] South Atlantic Fishery Management Council. 2002. Fishery management plan for pelagic *Sargassum* habitat of the South Atlantic region.

Shamblin, B. M., M. G. Dodd, D. a. Bagley, L. M. Ehrhart, A. D. Tucker, C. Johnson, R. R. Carthy, R. A. Scarpino, E. McMichael, D. S. Addison, K. L. Williams, M. G. Frick, S. Ouellette, A. B. Meylan, M. H. Godfrey, S. R. Murphy, and C. J. Nairn. 2011. Genetic structure of the southeastern United States loggerhead turtle nesting aggregation: evidence of additional structure within the peninsular Florida recovery unit. Marine Biology 158:571–587.

R Core Team. 2013. R: A language and environment for statistical computing. R Foundation for Statistical Computing, Vienna, Austria. http://www.R-project.org/.

Rooker, J. R., J. R. Simms, R. J. D. Wells, S. a Holt, G. J. Holt, J. E. Graves, and N. B. Furey. 2012. Distribution and habitat associations of billfish and swordfish larvae across mesoscale features in the Gulf of Mexico. PloS one 7:e34180.

Ryther, J. H. 1956. The Sargasso Sea. Scientific American 194:98–104.

Saba, V. S. 2013. Oceanic habits and habitats: *Dermochelys coriacea*. Pages 163–188 in J. Wyneken, K. J. Lohmann, J. A. Musick, editors. The biology of sea turtles, volume III. CRC Press, Boca Raton, FL.

Schuyler, Q., B. D. Hardesty, C. Wilcox, and K. Townsend. 2014. Global analysis of anthropogenic debris ingestion by sea turtles. Conservation biology : the journal of the Society for Conservation Biology 28:129–39.

Stoner, A. W. 1983. Pelagic *Sargassum*: Evidence for a major decrease in biomass. Deep-Sea Research 30:469–474.

Thiel, M. and L. Gutow 2005. The ecology of rafting in the marine environment. I. The floating substrata. Pages 181-264. In R.N. Gibson, R.J.A. Atkinson, J.D.M. Gordon, editors. Oceanography and marine biology: an annual review. Volume 42. CRC Press, USA.

[USFWS] United States Fish and Wildlife Service. 2010. Endangered and Threatened Wildlife and Plants; designation of critical habitat for the polar bear (*Ursus maritimus*) in the United States. Federal Register 75(234)76086–76137, 7 December 2010.

Weis, J.S. 1968. Fauna Associated with pelagic *Sargassum* in the Gulf Stream. American Midland Naturalist 80:554–558.

Witherington, B.E. 2002. Ecology of neonate loggerhead turtles inhabiting lines of downwelling near a Gulf Stream front. Marine Biology 140: 843-853.

Witherington, B. E., R. Herren, and M. Bresette. 2006. *Caretta caretta* – loggerhead sea turtle. Chelonian Research Monographs 3:74–89.

Witherington, B., S. Hirama, and R. Hardy. 2012. Young sea turtles of the pelagic *Sargassum*-dominated drift community: habitat use, population density, and threats. Marine Ecology Progress Series 463:1–22.

Yang, H., R. H. Weisberg, P. . Niiler, W. Sturges, and W. Johnson. 1999. Lagrangian circulation and forbidden zone on the West Florida Shelf. Continental Shelf Research 19:1221–1245.

Tables:

Table 1.1. Summary of eastern Gulf of Mexico Landsat scenes examined for the presence of surface-pelagic drift communities (SPDC). The scene index is provided as a combination of path and row numbers. The number of images within which SPDC was detected is noted. The average extent of searchable waters is also provided (km^2). The proportion of each image covered by SPDC is provided (values scaled to ‰, mean ±SD).

Landsat scene index	SPDC observed	Total images	Mean searched area km^2	SPDC coverage ‰ (mean ±SD)
p16r42	76	154	20082	0.086 ±0.338
p16r43	105	136	27258	0.137 ±0.277
p17r40	68	97	15319	0.422 ±0.826
p17r41	85	143	23179	0.082 ±0.191
p17r42	58	62	33630	0.056 ±0.108
p17r43	60	69	31622	0.163 ±0.311
p18r39	79	96	8354	0.812 ±1.430
p18r40	85	159	27551	0.086 ±0.272
p18r41	4	10	26884	0.012 ±0.005
p18r42	1	9	31666	0.002 ±0.004
p19r39	49	77	11558	0.059 ±0.141
p19r40	25	45	33101	0.085 ±0.161
p19r41	5	9	30488	0.004 ±0.005
p19r42	5	7	32368	0.005 ±0.005
p20r39	48	152	15320	0.090 ±0.268
p20r40	59	79	32624	0.161 ±0.377
p20r41	6	9	30127	0.022 ±0.022
p20r42	3	10	28718	0.006 ±0.012
Total (all images)	**821**	**1323**	**22631**	**0.171 ±0.553**

Table 1.2. Area of surface-pelagic drift communities (SPDC) observed within Landsat images from the eastern Gulf of Mexico. Landsat scenes used in this analysis are noted in the far left column. The mean, standard deviation and maximum area of SPDC (km^2) are provided for two time periods: May–October and July–October. These time periods correspond to the months when the density of surface-pelagic juveniles and post-hatchlings were estimated per area of SPDC (9.73 and 1.98 turtles km^{-2}, respectively). Those values are multiplied by mean SPDC area within the table below.

Landsat scene	Area of SPDC during May–October (km^2)			Surface-pelagic turtles (mean SPDC area x 9.73 turtles km^{-2} SPDC)	Area of SPDC during July–October (km^2)			Post-hatchling turtles (mean SPDC area x 1.98 turtles km^{-2} SPDC)
	Mean	SD	Maximum		Mean	SD	Maximum	
p16r42	1.82	5.04	38.22	17.71	1.73	5.62	38.22	3.43
p16r43	5.40	10.82	62.40	52.54	5.15	11.47	62.40	10.20
p17r40	7.91	15.41	90.84	76.96	10.75	18.24	90.84	21.29
p17r41	2.01	4.16	26.12	19.56	2.47	4.70	26.12	4.89
p17r42	2.14	4.47	24.09	20.82	3.02	5.53	24.09	5.98
p17r43	6.54	13.31	72.29	63.63	9.14	15.83	72.29	18.10
p18r39	9.52	12.01	48.53	92.63	10.94	12.49	48.53	21.66
p18r40	3.20	7.90	54.59	31.14	3.91	9.25	54.59	7.74
p18r41	0.19	0.27	0.74	1.85	0.19	0.19	0.44	0.38
p18r42	0.03	0.08	0.22	0.27	0.05	0.11	0.22	0.10
p19r39	0.77	2.14	12.94	7.49	0.81	2.55	12.94	1.60
p19r40	3.82	6.11	22.30	37.17	4.42	7.02	22.30	8.75
p19r41	0.12	0.16	0.44	1.17	0.16	0.18	0.44	0.32
p19r42	0.16	0.16	0.40	1.56	0.11	0.19	0.40	0.22
p20r39	1.72	4.19	25.43	16.74	1.36	4.00	25.43	2.69
p20r40	9.67	16.79	82.65	94.06	8.28	15.20	75.99	16.39
p20r41	0.63	0.78	2.07	6.13	0.45	0.64	1.56	0.89
p20r42	0.08	0.22	0.61	0.78	0.15	0.31	0.61	0.30

Figures:

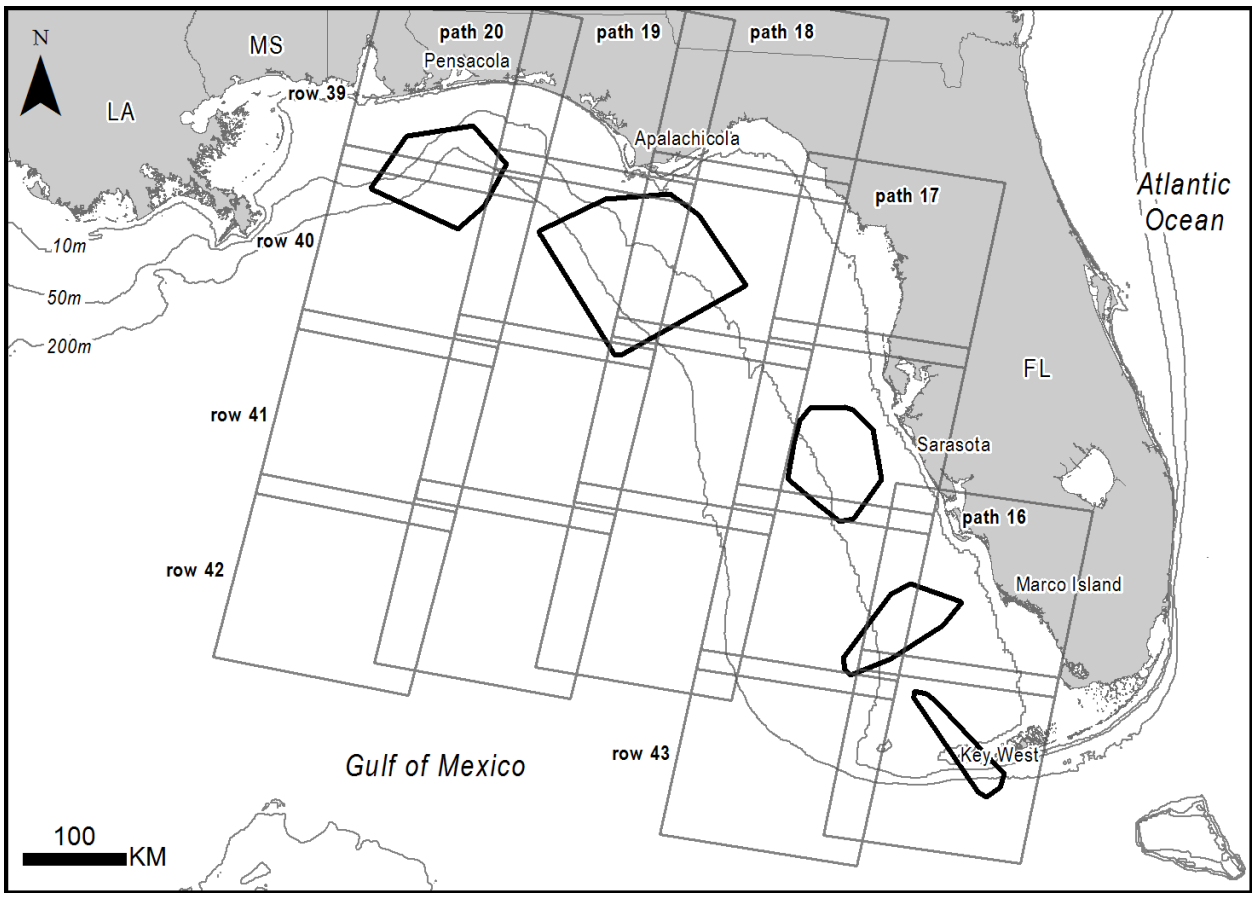

Figure 1.1. The extents of Landsat 5 and 7 scenes within the eastern Gulf of Mexico, paths 16–20 and rows 39–42. Paths are labeled at the top of each path and rows are labeled along the left side of each row. The extents of on-water transect surveys conducted by Witherington et al. (2012) are represented by the polygons (outlined in black).

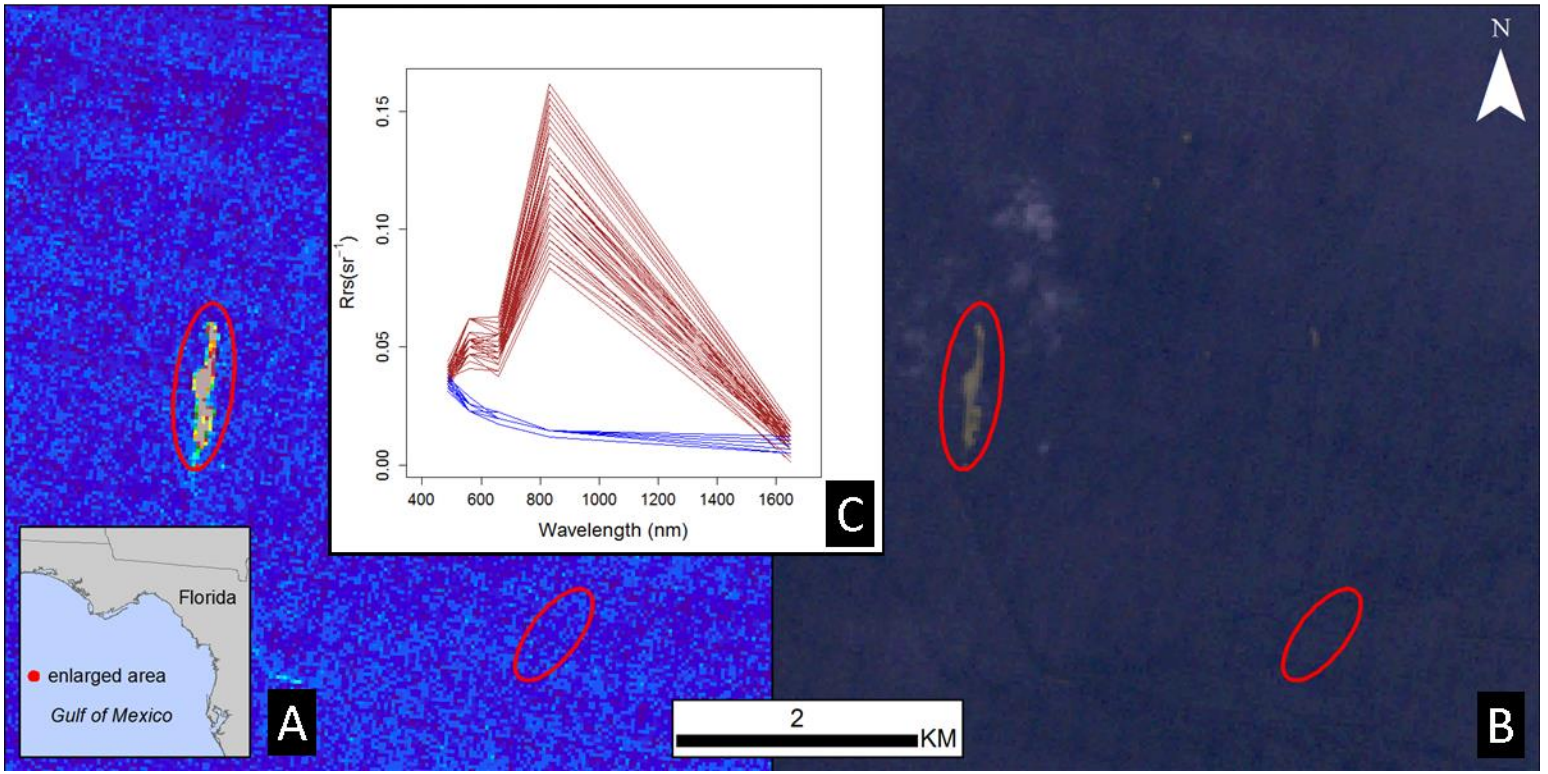

Figure 1.2. Landsat 5 image of path 19 row 40 collected on 1 August 2005 over waters southwest of Apalachicola, Florida. The Floating Algae Index (FAI, A) and true-color (B) images are shown at identical scales and extents. The images highlight a patch of *Sargassum* that was approximately 180 m wide (maximum) and 1,400 m long. The inset plot (C) shows the Rayleigh-corrected remote sensing reflectance values from bands 1–5 for pixels over the *Sargassum* patch (n=50, red lines) and nearby surface water pixels (n= 50, blue lines). The red ellipses within frames A and B identify the regions from which sample pixels representing *Sargassum* and surface water were extracted.

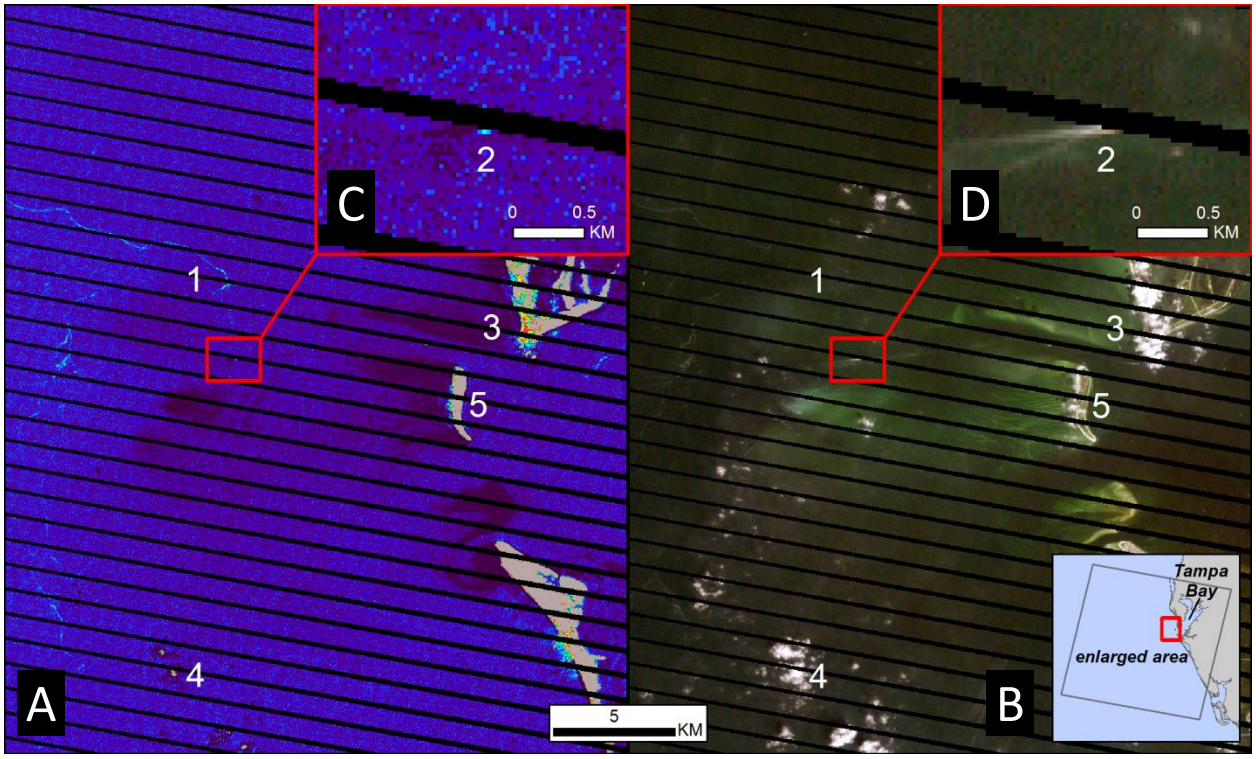

Figure 1.3. Landsat 7 image of path 17 row 41 collected on 15 September 2006, showing waters within the Tampa Bay region of west-central Florida. The Floating Algae Index (FAI, A) and true-color (B) images are shown at identical scales and extents. The images highlight *Sargassum* features (1) and some common anomalies present within Landsat imagery. The horizontal striping was present in Landsat 7 imagery, from 2003–present, as a result of the failed scan line corrector. The enlarged regions (frames C and D) show an underway vessel (2) that exhibited a high FAI response (C) and a V-shaped wake that is only apparent in the true color image (D). Clouds (3 and 4) may exhibit a relatively high (A, 3) FAI response or appear as saturated pixels within the FAI image (A, 4). These features can easily be identified as clouds using the coregistered true color image. Land areas appear as no data within the FAI image (5, Egmont Key at the mouth of Tampa Bay, FL).

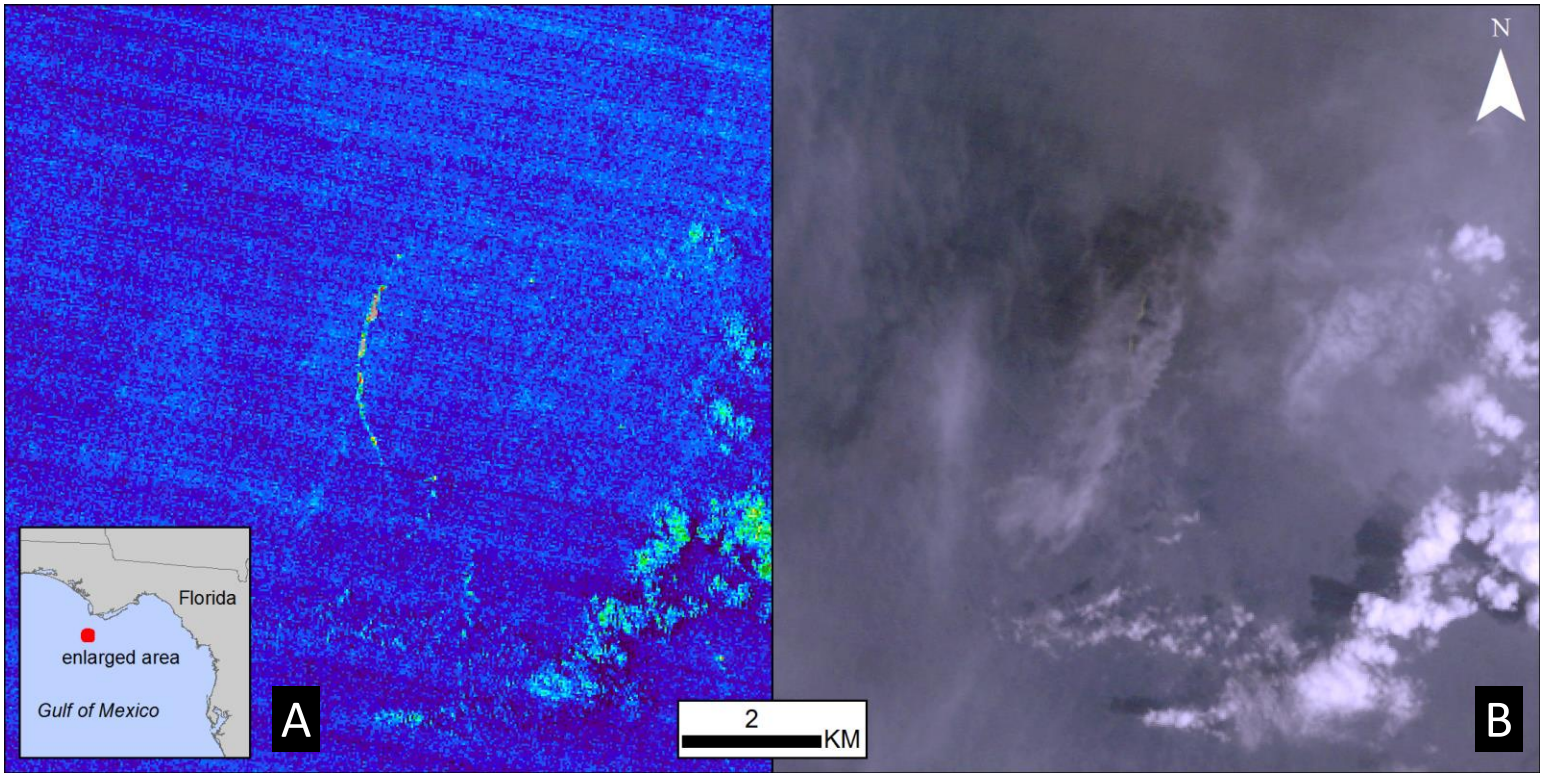

Figure 1.4. Landsat 5 image of path 19 row 40 collected on 1 August 2005 over waters southwest of Apalachicola, Florida. The Floating Algae Index (FAI, A) and true-color (B) images are shown at identical scales and extents. A line of *Sargassum* was clearly detected by the FAI and is shown within the center of the FAI image. Thin clouds obscured this feature within the accompanying true-color image.

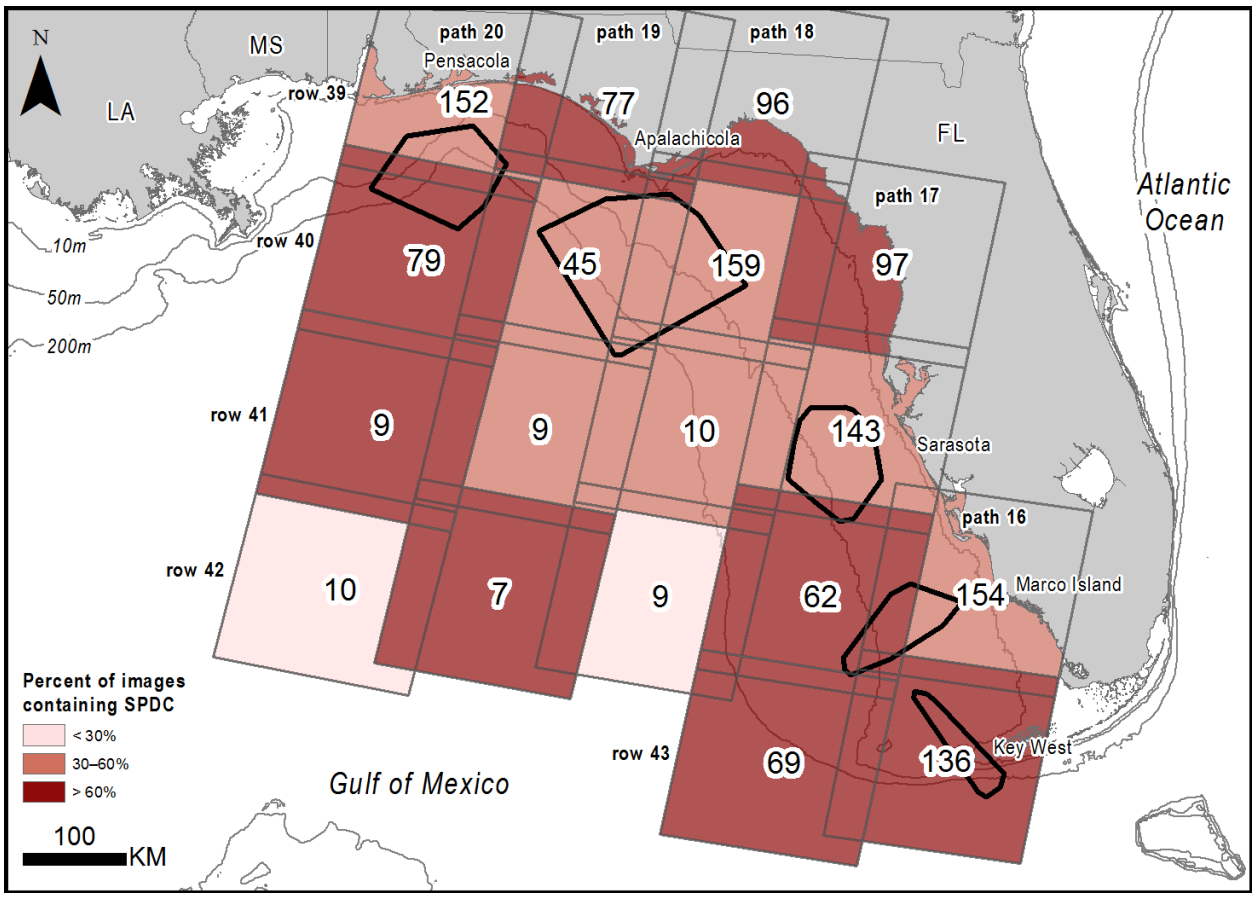

Figure 1.5. The extents of Landsat 5 and 7 scenes within the eastern Gulf of Mexico area of interest of the present study, paths 16–20 and rows 39–42. Paths are labeled at the top of each path and rows are labeled along the left side of each row. Colors represent the percent of images containing SPDC. The values within the center of each scene represent the total number of images examined for that scene. The extents of on-water transect surveys conducted by Witherington et al. (2012) are represented by the polygons (outlined in black).

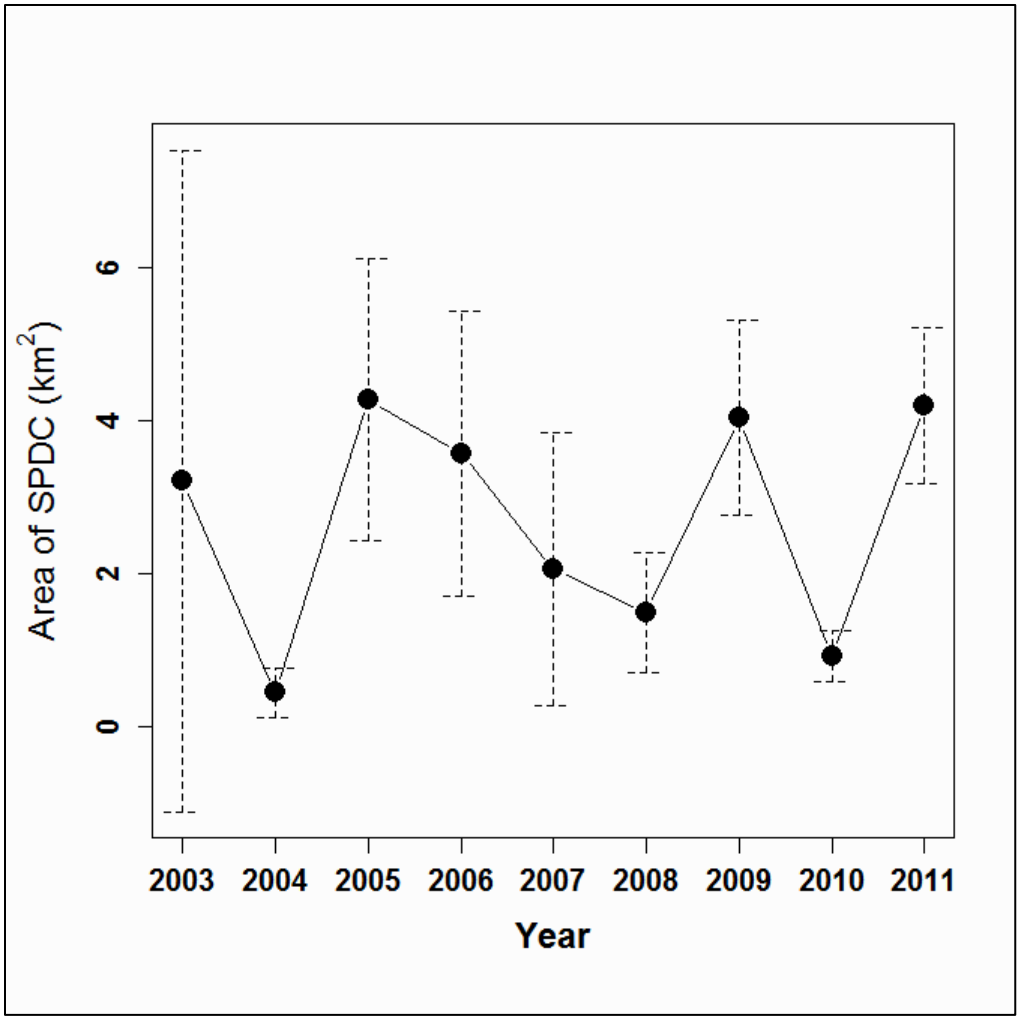

Figure 1.6. Annual mean area (km^2) of surface-pelagic drift communities (SPDC) observed within the eastern Gulf of Mexico. Error bars represent 95% confidence intervals surrounding the mean values.

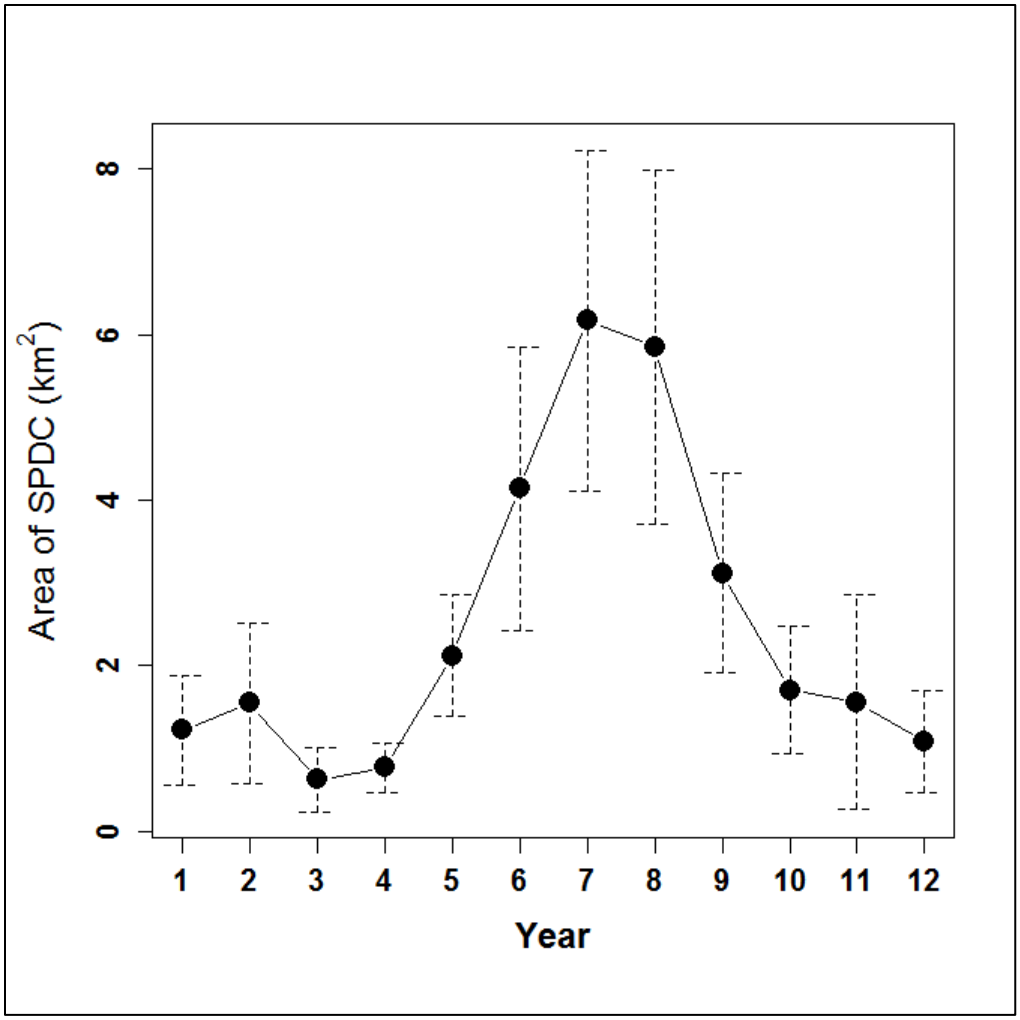

Figure 1.7. Monthly mean area (km^2) of surface-pelagic drift communities (SPDC) observed within the eastern Gulf of Mexico. Error bars represent 95% confidence intervals surrounding the mean values.

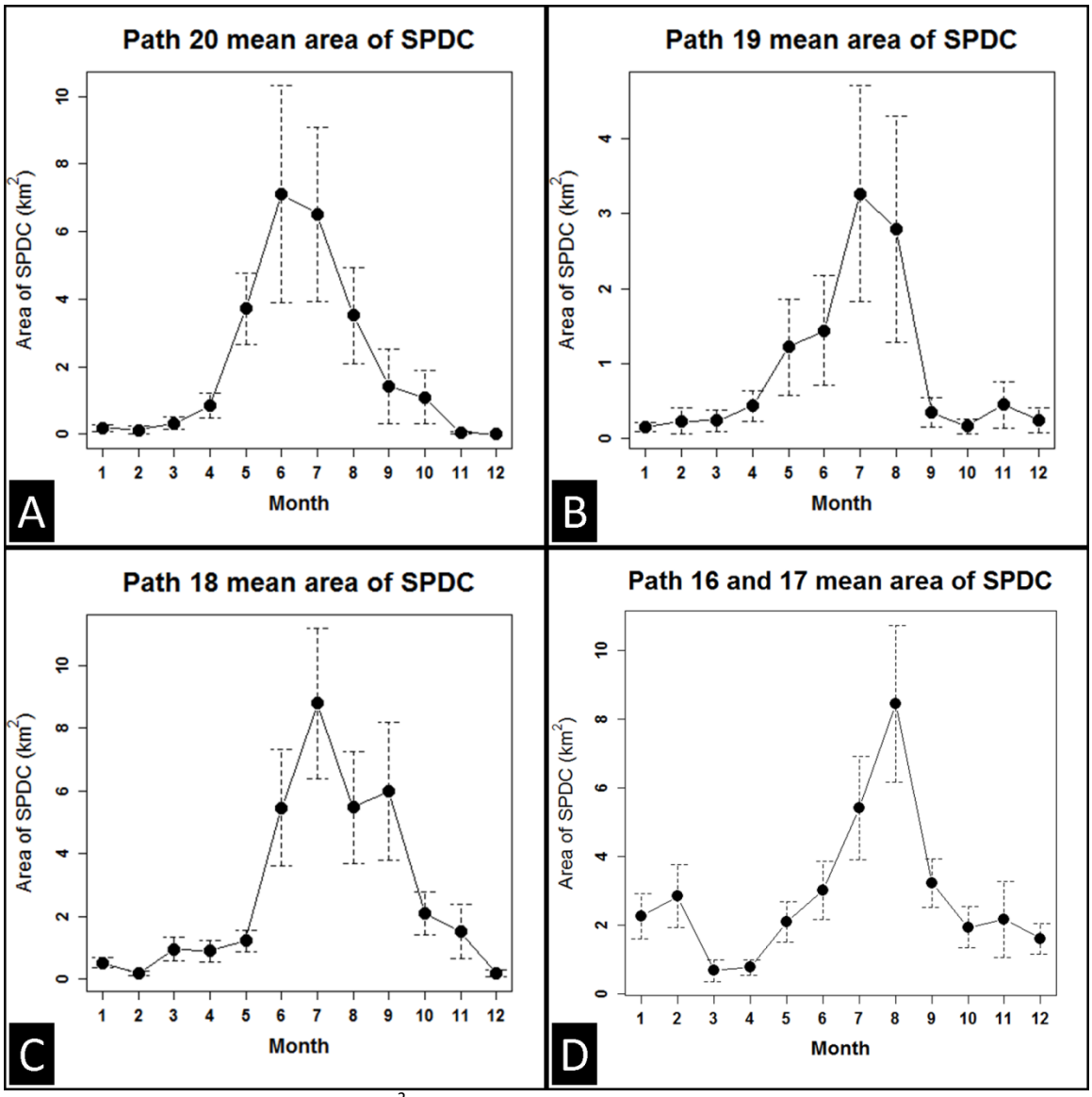

Figure 1.8. Monthly mean area (km^2) of surface-pelagic drift communities (SPDC) observed per Landsat path within the eastern Gulf of Mexico. Error bars represent 95% confidence intervals surrounding the mean values. Each plot represents the mean area of SPDC observed within selected Landsat paths. Figures are arranged with paths in decreasing order, from 20–16, which corresponds to their geographic order (west–east). Data from paths 16 and 17 were combined (D).

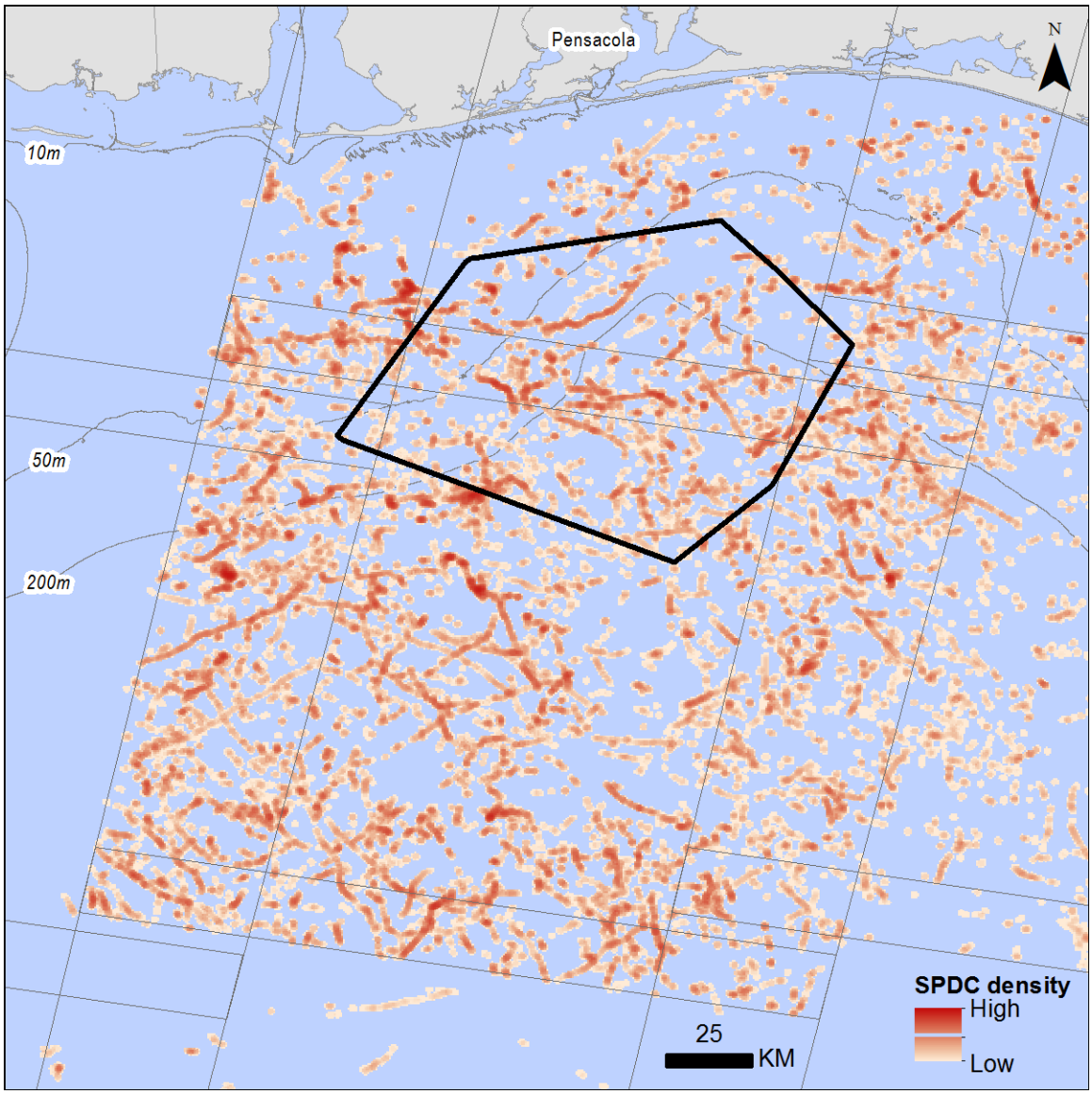

Figure 1.9. Density of surface-pelagic drift communities (SPDC) observed within Landsat path 20, rows 39 and 40 from 2003–2011. These Landsat scenes intersect with the on-water transect study area south of Pensacola, Florida (black polygon).

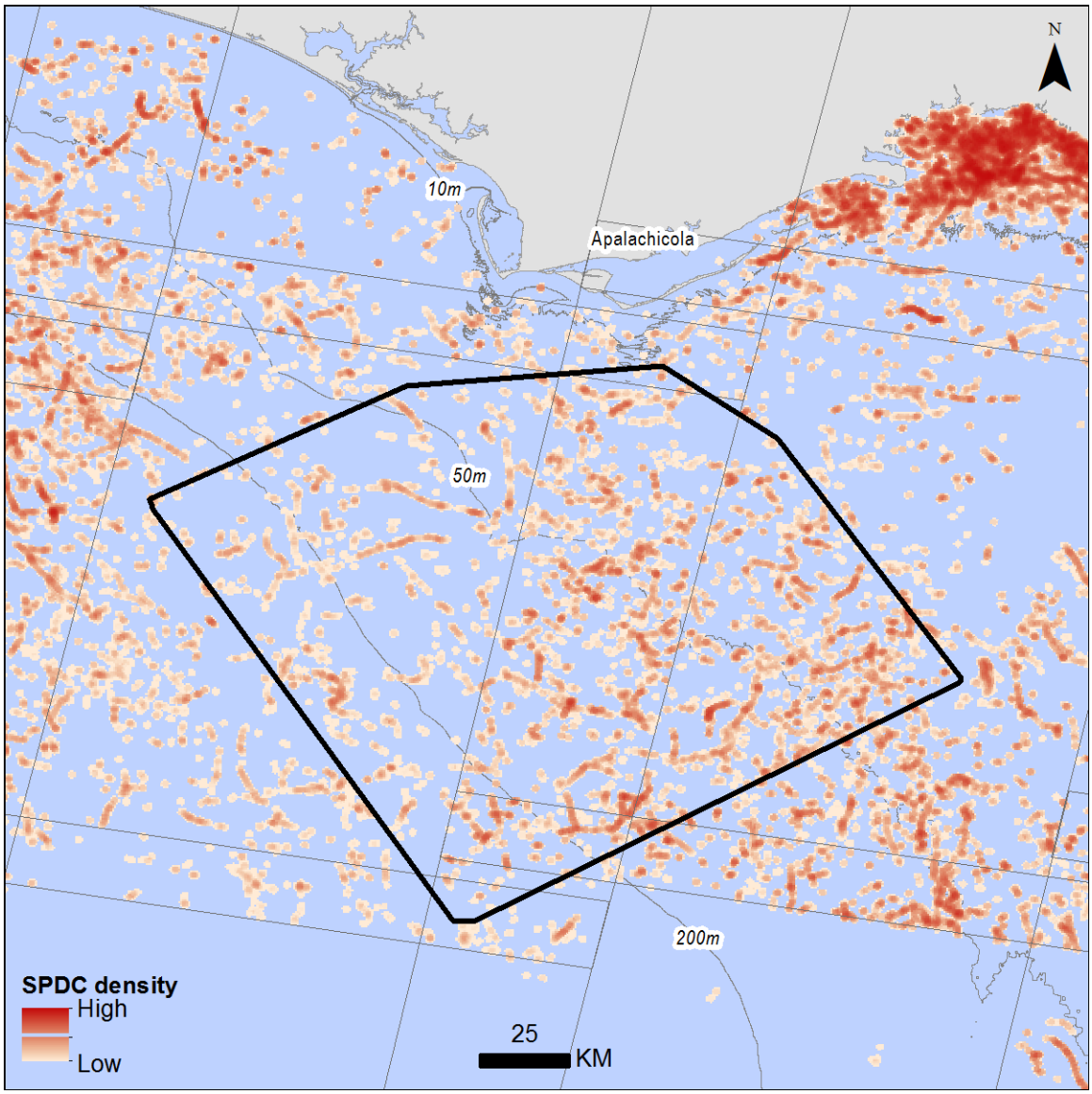

Figure 1.10. Density of surface-pelagic drift communities (SPDC) observed within Landsat paths 18 and 19, rows 39 and 40 from 2003–2011. These Landsat scenes intersect with the on-water transect study area south of Apalachicola, Florida (black polygon).

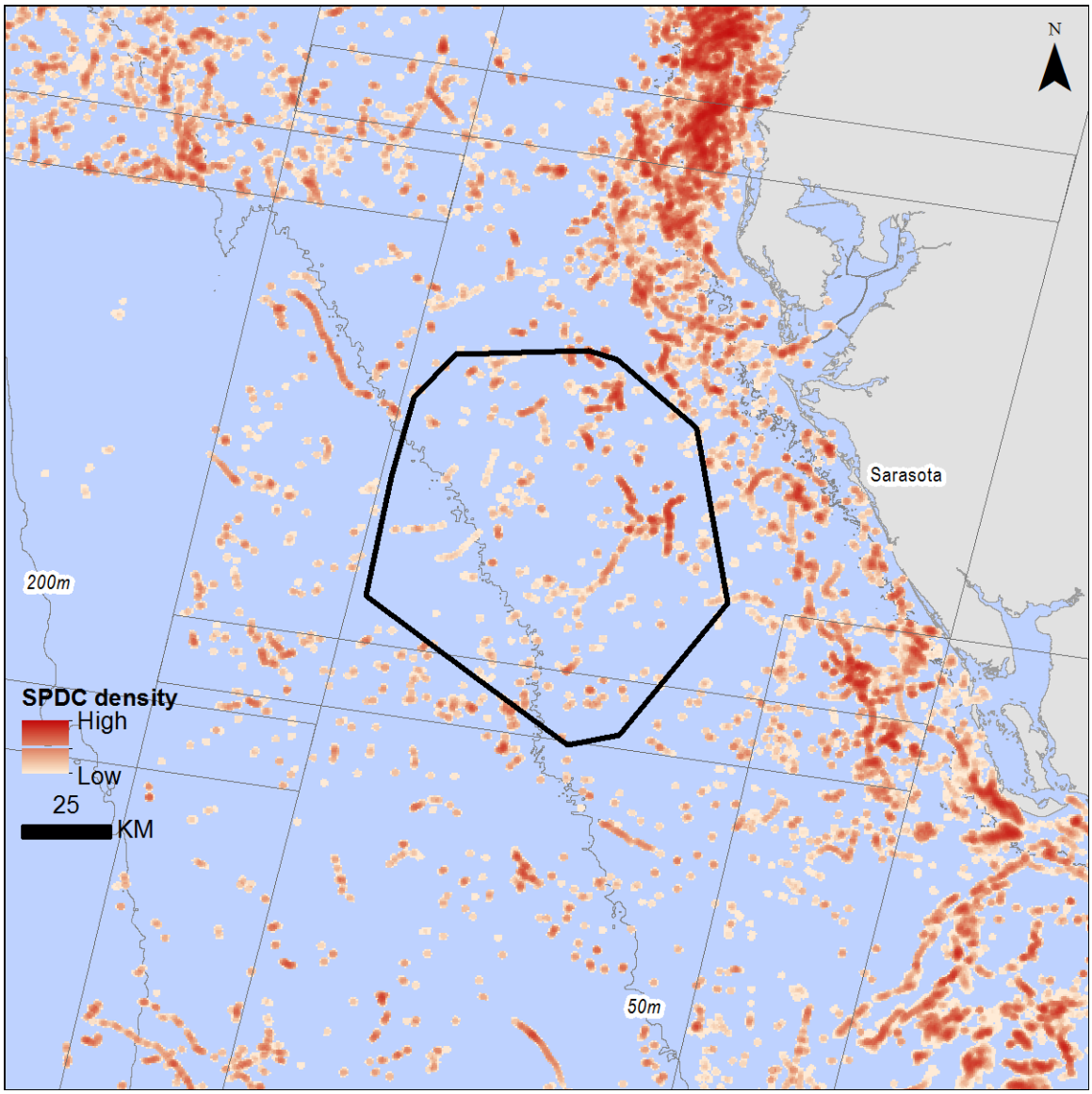

Figure 1.11. Density of surface-pelagic drift communities (SPDC) observed within Landsat path 17, row 41 from 2003–2011. This Landsat scene intersects with the on-water transect study area west of Sarasota, Florida (black polygon).

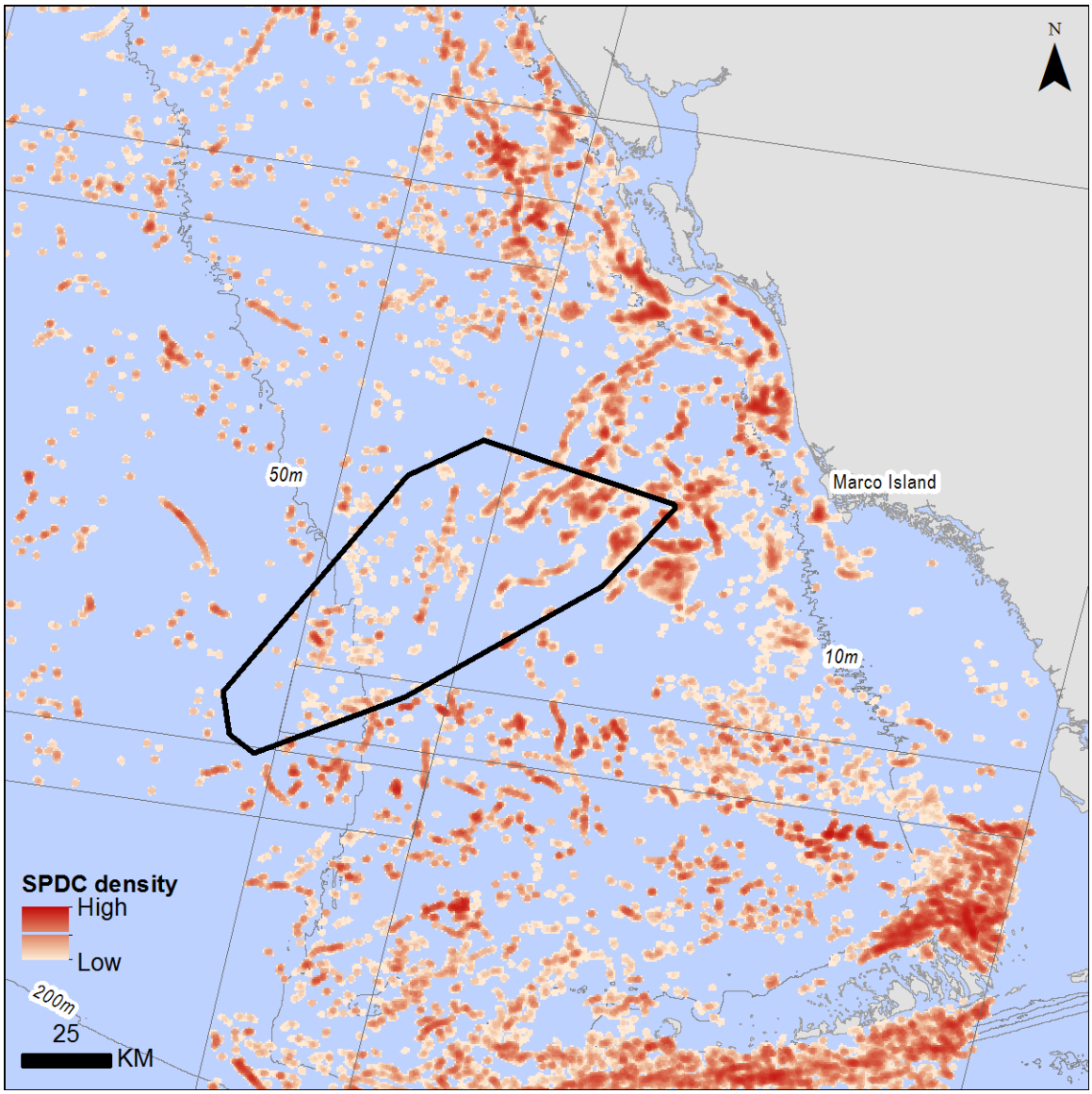

Figure 1.12. Density of surface-pelagic drift communities (SPDC) observed within Landsat path 16, row 42 from 2003–2011. This Landsat scene intersects with the on-water transect study area west of Marco Island, Florida (black polygon).

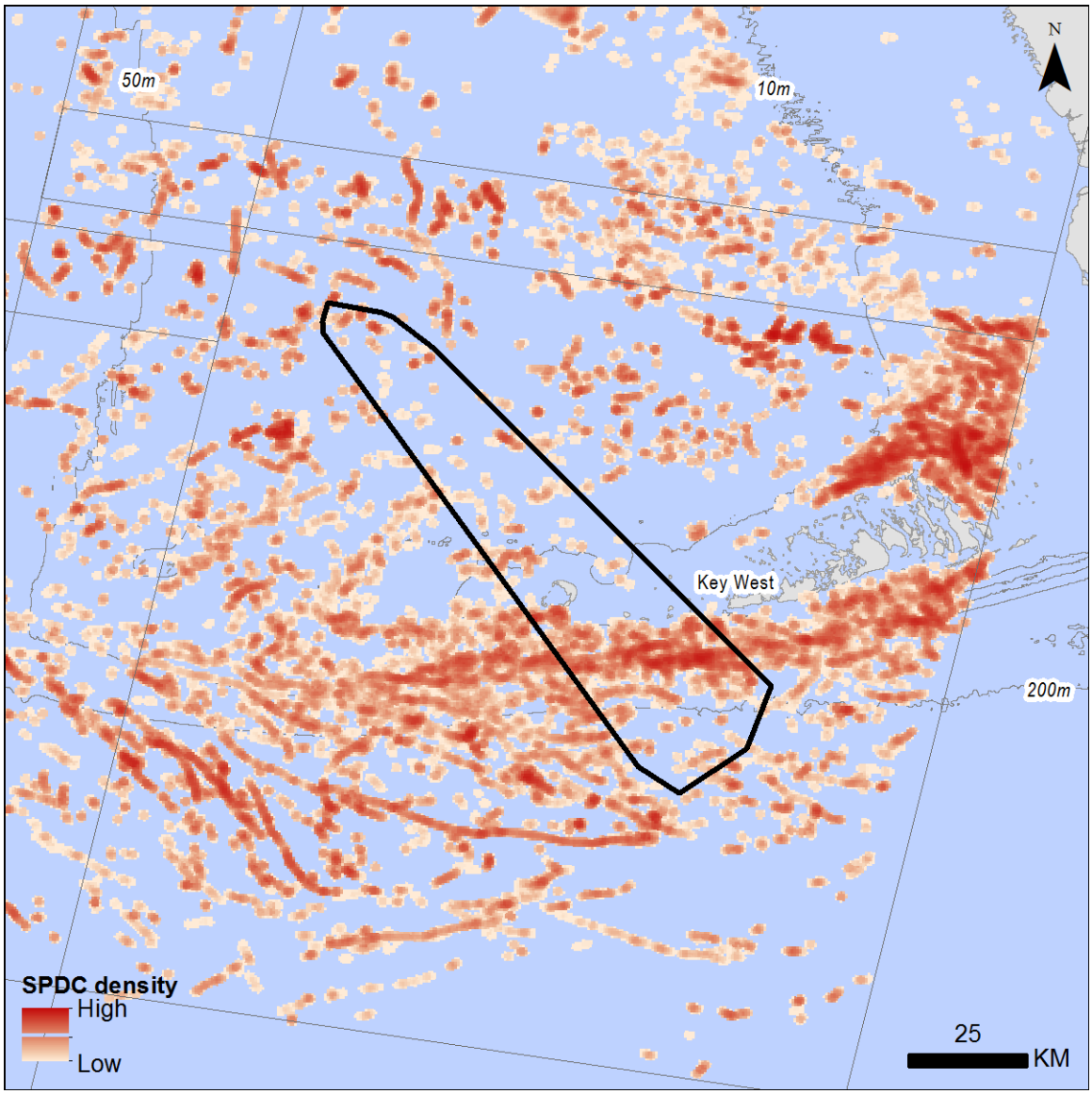

Figure 1.13. Density of surface-pelagic drift communities (SPDC) observed within Landsat path 16, row 43 from 2005–2011. This Landsat scene intersects with the on-water transect study area west of Key West, Florida (black polygon).

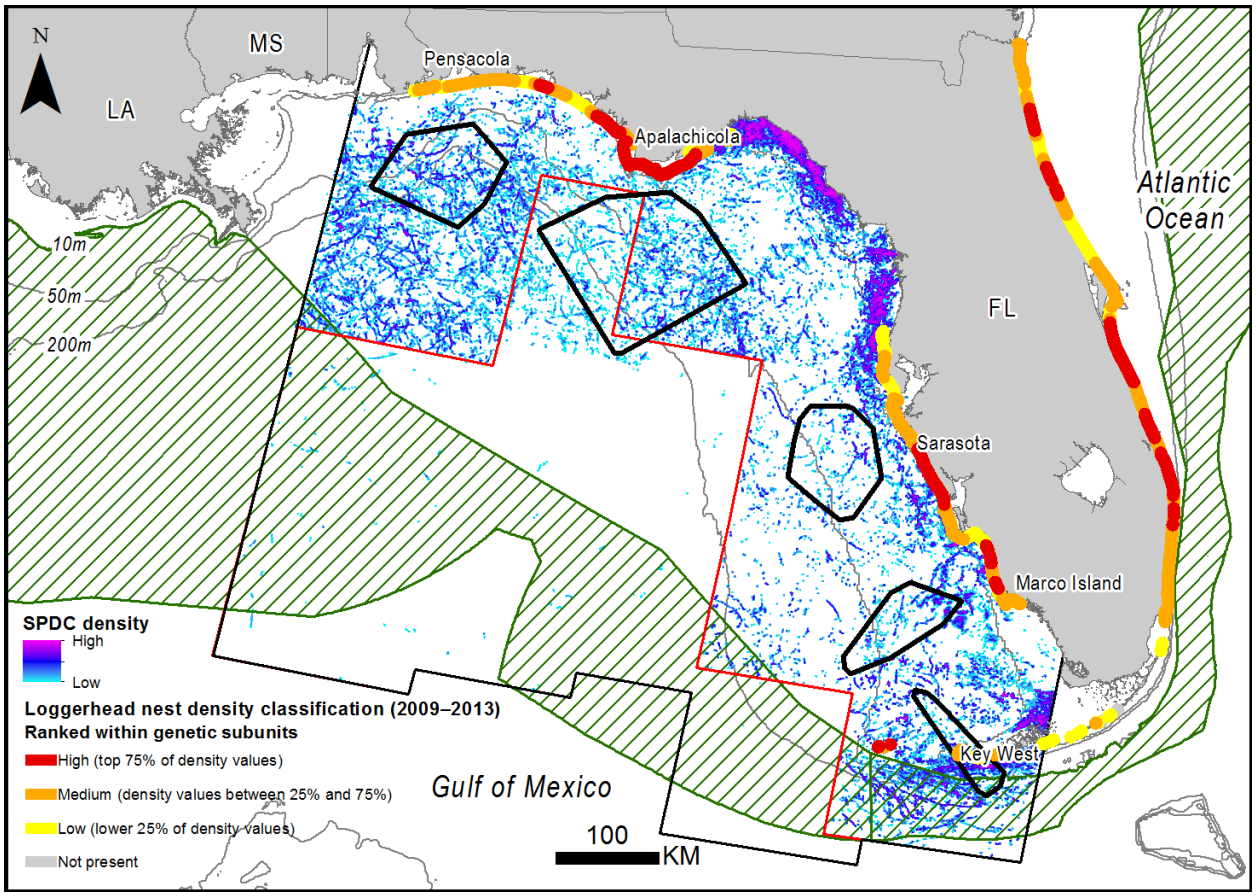

Figure 1.14. Density of surface-pelagic drift communities (SPDC) observed within the eastern Gulf of Mexico from 2003–2011. The hatched polygon shows the extent of the recently designated *Sargassum* critical habitat for loggerheads (NMFS 2014). The density of loggerhead nesting on Florida beaches from 2009–2013 is shown (Florida Fish and Wildlife Conservation Commission, Statewide Sea Turtle Nesting Beach Survey Program 2014). The black lines represent the extent of the eastern Gulf of Mexico study area. Within the study area, the red line represents the northern extent of the region where the availability of Landsat data was limited.

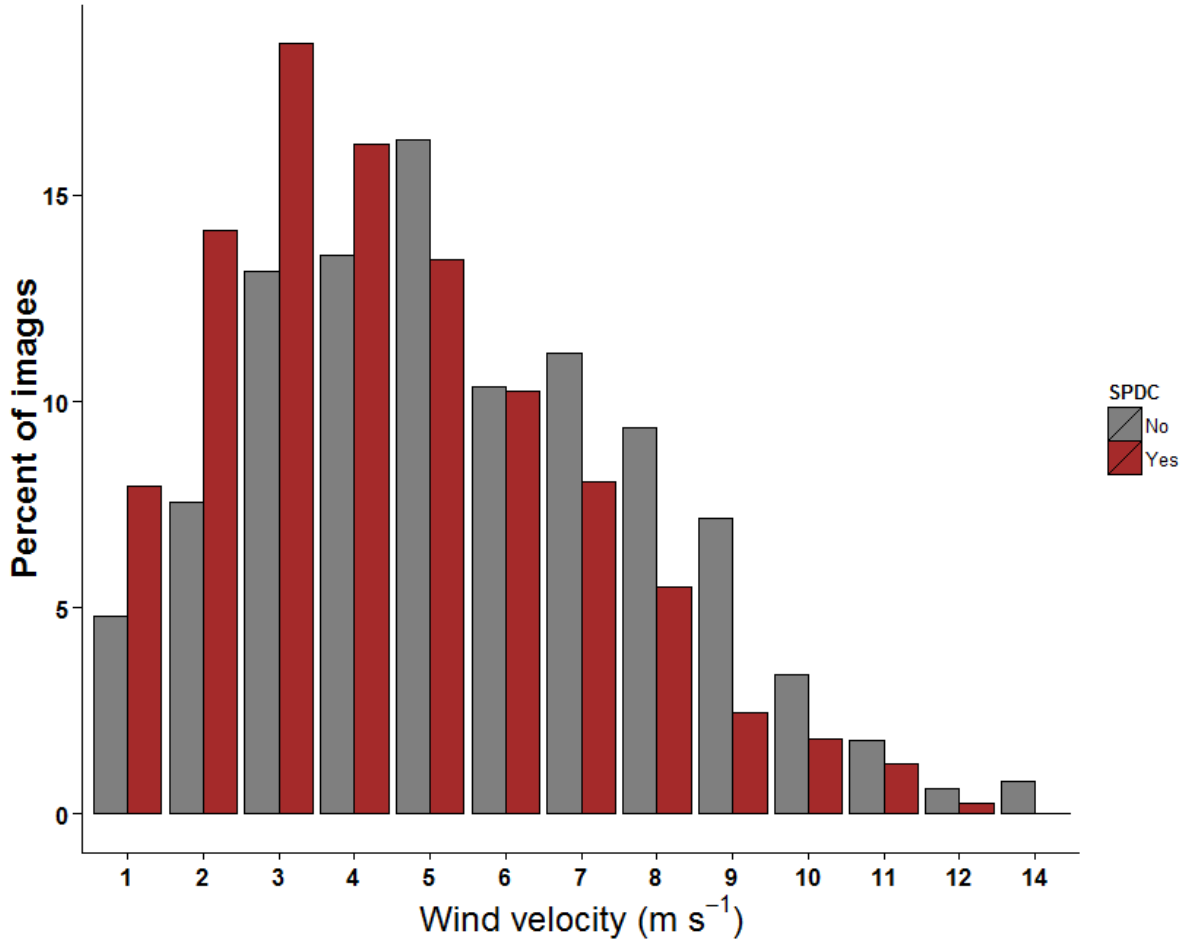

Figure 1.15. Wind velocity and the frequency of occurrence of surface-pelagic drift communities (SPDC) within eastern Gulf of Mexico Landsat images. Bars represent the percentage of images within which SPDC was (Yes) or was not (No) detected.

CHAPTER TWO:

MOVEMENTS AND HABITAT ASSOCIATIONS OF SURFACE-PELAGIC JUVENILE KEMP'S RIDLEYS (*LEPIDOCHELYS KEMPII*) WITHIN THE NORTHERN GULF OF MEXICO

1. Abstract

Information on the behavior and habitat associations of protected marine species is essential to their conservation. Within the North Atlantic and surrounding oceanic regions, early (surface-pelagic) juveniles of several sea turtle species are presumed to be principally passive drifters associated with surface-pelagic drift communities (SPDC). This information is supported by anecdotal observations, directed research, and oceanographic-based species distributional modeling. The present study used satellite telemetry to examine the movement characteristics and habitat associations of surface-pelagic juvenile Kemp's ridleys (*Lepidochelys kempii*) captured at sea within the northern Gulf of Mexico. Ocean surface habitats were described in terms of currents, winds, and temperature. Remotely-sensed observations of *Sargassum*-dominated SPDC were also used to characterize habitats. Tracked turtles exhibited mostly passive behavior, particularly when associated with SPDC or conditions favorable for its formation. Tracked turtles moved with, against, and across relatively weak surface currents (inferred from altimetry). Shallow waters (< 20 m) and the presence of SPDC were the only features that appeared to constrain the movements of tracked turtles. One individual appeared to transition from surface-pelagic habitats into nearshore neritic habitats. Results suggest that SPDC within the northern and eastern Gulf of Mexico serves as critical developmental habitat for surface-pelagic juvenile Kemp's ridleys. This information on the sea surface habitats used by this species and life-stage broadens

knowledge of their distribution and habitat requirements. Additionally, the long-term association observed between tracked turtles and SPDC illustrates the vulnerability of this life stage to anthropogenic threats, such as marine debris and oil spills.

2. Introduction

Many large marine vertebrates (e.g., mammals, seabirds, sea turtles, and sharks) share traits that challenge conservation efforts. These species are often long-lived and wide ranging; they also tend to have complex life-histories and diverse habitat associations (Hyrenbach et al. 2000). Conservation efforts for these species often depend on information regarding habitat selection, migratory patterns, and threats (Block et al. 2003; Wallace et al. 2010). Within the pelagic environment, information on the spatial or temporal distributions of a specific species or life-history stage may be particularly limited (Hyrenbach et al. 2000). Addressing these knowledge deficiencies through direct observation of marine vertebrates and their habitats may not always be feasible. The use of indirect observational methods (e.g., remote monitoring and tracking techniques) is now regularly used in marine conservation research and has helped fill critical data gaps (Hart and Hyrenbach 2009).

Sea turtles have a global distribution, and many species exhibit lengthy developmental and reproductive migrations. Their reproductive and foraging habitats may be on opposite sides of major ocean basins (Witt et al. 2011). Developmental migrations made by sea turtles may also span oceans and intersect with waters of several nations (Meylan et al. 2011). Satellite telemetry provides a method to understand the characteristics of lengthy sea turtle migrations and to identify potential areas of long-term residence at nodes within these movements (Godley et al. 2008). Satellite tracking is now increasingly used in conjunction with remotely-sensed oceanographic data to explain patterns of occurrence and habitat associations for some species, e.g., leatherback turtles (Bailey et al. 2012).

Satellite tracking and remotely-sensed oceanographic data have also been combined to identify discrete habitats used by juvenile loggerheads in the North Pacific (Polovina et al. 2004).

Once clear habitat associations have been established, those results can be used to predict species occurrence that can guide conservation management efforts. Leatherback turtles within the Atlantic and Pacific oceans have also been shown to associate with remotely-identifiable fronts or temperature gradients and within regions that may place them at increased risk for fisheries bycatch (Eckert et al. 2006; Bailey et al. 2012). Howell et al. (2008) combined loggerhead habitat preferences, remote sensing data, longline fishery characteristics, and bycatch patterns in order to develop "TurtleWatch", a tool designed to reduce interactions between loggerheads and pelagic longline fishing activities within the North Pacific. These examples demonstrate that linking marine animal movement patterns with remotely-sensed oceanographic features can lead to powerful marine conservation management tools.

It may also be possible to link the early juvenile life stages of some sea turtle species to discrete, remotely-identifiable habitat features. Witherington et al. (2012) found that young (surface-pelagic) juveniles of four North Atlantic sea turtle species closely associate with aggregations of the floating macroalgae *Sargassum* spp. The species found within *Sargassum* were green (*Chelonia mydas*), hawksbill (*Eretmochelys imbricata*), Kemp's ridley (*Lepidochelys kempii*), and loggerhead (*Caretta caretta*) turtles. *Sargassum*-dominated surface-pelagic drift communities (SPDC) are unique marine ecosystems within which a variety of organisms forage and find cover (Fine 1970). Under favorable conditions, SPDC tends to aggregate within lines that are of sufficient size to be detected within satellite images (Gower et al. 2006; Hu 2009). The ability to conduct remote habitat detection studies, coupled with recent advancements in satellite telemetry, provide an opportunity to examine questions of habitat association, behavior, and movements of surface-pelagic juvenile sea turtles.

After emerging from nests, sea turtle hatchlings enter the water and may spend the initial 24 hours in a period of continuous and rapid swimming, the "swim-frenzy" stage (Dalton 1979; Wyneken and

Salmon 1992). The swim-frenzy period may end when post-hatchlings seek shelter within SPDC or other flotsam (Carr 1986; Witherington 2002). By associating with SPDC, turtles likely decrease their risk of predation and increase their foraging opportunities (Musick and Limpus 1997; Witherington et al. 2012). Because of the availability of food and cover, sea turtles associated with SPDC are thought to spend a majority of the time drifting passively with the habitat; therefore, it is presumed that their distribution must be driven by ocean surface currents and winds that are responsible for distributing SPDC (Carr 1986; Collard and Ogren 1990; Bolten 2003b).

The Kemp's ridley has the smallest range of all North Atlantic sea turtles, and the oceanographic factors responsible for its distribution have been examined in detail (Collard and Ogren 1990; Putman et al. 2010). The principal Kemp's ridley nesting beaches are found in Tamaulipas, Mexico, along the western shoreline of the Gulf of Mexico (Marquez 1994). Based on Gulf circulation patterns, Collard and Ogren (1990) developed several scenarios to explain the distribution of surface-pelagic juvenile Kemp's ridleys. Kemp's ridleys may remain within the southwestern Gulf or be transported eastward. Turtles that are transported eastward may become entrained in westward drifting anticyclonic eddies or the southward-flowing Loop Current, which would transport them out of the Gulf. Recently, Putman et al. (2013) used particle drift simulations to predict the distributions of surface-pelagic juvenile Kemp's ridleys and found similar distributional patterns. Putman et al. (2013) also found support for the occurrence of surface-pelagic Kemp's ridleys within the eastern Gulf, an area where surface-pelagic juvenile Kemp's ridleys have been directly observed (Witherington et al. 2012). Increased accuracy of these distributional models awaits refinements on the behavior of surface-pelagic Kemp's ridleys and the distribution of their habitats (Putman et al. 2013).

The present study coupled telemetry and remotely-sensed habitat features to characterize the movements made by surface-pelagic juvenile Kemp's ridleys and to describe their habitat associations. Remotely-sensed data for winds, surface currents, surface temperature and SPDC were used to

characterize the habitats used by tracked turtles. The association of tracked turtles with SPDC was examined over multi-day time scales using remote sensing techniques. Within the North Atlantic, SPDC is known to vary spatially and temporally (Gower and King 2011). Additionally, large areas of SPDC may be dispersed into smaller patches or clumps at high wind speeds (Marmorino et al. 2011). The marine species closely associated with SPDC must have evolved an ability to locate habitat. For surface-pelagic juvenile sea turtles, this may result in a dichotomous behavioral strategy including an active, habitat searching phase and a relatively passive drift phase that occurs when habitat is located (Witherington 2002). A mixed strategy of active and passive movements has been proposed for juvenile loggerheads (Witherington 2002; Bolten 2003a) and leatherbacks (Gaspar et al. 2012). In addition to habitat characterization, this study sought to determine whether surface-pelagic juveniles exhibit both active and passive behavior and whether this behavioral response is predicted by availability of SPDC.

3. Methods

3.1 Satellite Transmitter Deployments

Satellite transmitter deployments were made by B. Witherington and S. Hirama (NMFS Permit 14726-01) from June–September 2011 as part of a long-term study of sea turtles within SPDC (Witherington et al. 2012). They deployed transmitters on a sample of 10 surface-pelagic juvenile Kemp's ridleys captured at three locations within the northeastern and eastern Gulf (Fig. 2.1). All turtles were captured within SPDC and returned to this habitat upon release (capture–release time was approximately 2 hours). Three transmitters were deployed on turtles captured within each of two northern Gulf study sites, south of Pensacola and Apalachicola, Florida. The remaining four transmitters were deployed at an eastern Gulf study site, within West Florida Shelf (WFS) waters near Sarasota, Florida. The transmitters were 9.5 g, solar-powered tags (Microwave Telemetry PTT-100) and were

attached using silicone adhesive following the methods of Mansfield et al. (2012) (Fig. 2.2). The activity of these units was controlled by duty cycles, not water conductivity as is common in other marine animal telemetry equipment. The duty cycle for five units was 10 hours on/48 hours off, and the other five had a duty cycle set to 10 hours on/24 hours off. Turtles were randomly assigned transmitters programmed with one of the two duty cycles. The transmitter manufacturer recommended relatively brief active periods followed by longer inactive times in order to allow time for the batteries to recharge.

3.2 Transmitter Temperature and Battery Voltage

Transmitters reported temperature and battery voltage data within Argos messages. Temperature and voltage data were decoded from two 8-bit message fields following the manufacturer's recommendations (MTI 2011). Spurious records from the temperature and voltage data were removed using the Hampel Filter implemented with the pracma package written by Borchers (2014) for the program R (R Core Team 2013). The Hampel Filter performs a median absolute deviation computation on an ordered subset of temperature records using a moving window technique. I used a window size of 6 records and 3 sigma threshold recommended by Pearson (1999). Outlying values were replaced with the median value of the subset.

3.3 Argos Positional Data Treatment

Raw Argos location estimates were subjected to plausibility filtering using the Douglas Argos Filter Algorithm (DAF; Douglas 2012), implemented using SAS Enterprise Guide 5.1 (SAS Institute, Inc. Cary, NC USA). The DAF evaluated positions based on rate, distance, angle, and quality. Similar to Eckert (2006), I set the travel rate parameter for the DAF by estimating the rate of travel between mean daily positions calculated from all Argos positions for each transmitter. I selected the value of 3 km hr^{-1}, which was

conservatively above 90% of the travel rate values for each turtle (Fig. 2.3). The DAF implemented a minimum-redundant distance test, which allows positions collected near in time and within a user-specified distance threshold to validate one another (Douglas et al. 2012). I set the distance threshold to 5 km, a value consistent with other local-scale analyses of sea turtle tracking data (Foley et al. 2014). Within Argos data, acute turn angles are often indicative of spurious positions (Douglas et al. 2012). The DAF established the minimum allowable turn angle at each position using the 'ratecoef' value (-25+ratecoef*ln(min(distA-B, distB-C; where dist = distance between pairs of positions, A and B, B and C). I set the ratecoef value to 25, a value that was consistent with other sea turtle studies involving examinations of movements (Eckert et al. 2006; Foley et al. 2013). Collecte Localisation Satellites (CLS, the company which operates the Argos system) provided accuracy estimates to accompany locations in the form of Location Class (LC) rankings. CLS is able to estimate positional error for locations solved from four or more messages. Class A and B locations are solved using one to three messages and error estimates cannot be estimated (CLS 2014). I considered LCs 2 and 3 to be of sufficient accuracy for the present study, and these locations were automatically retained by the DAF plausibility filtering step. CLS (2014) estimated the error radii for LCs 2 and 3 to be 250 and 500 m, respectively. Tracks began at the release position, which was recorded by the research vessel's GPS. The final positions collected from each tracked turtle were also retained. Travel rates (km hr^{-1}, mean ±SD) for each turtle were obtained from a selection of the highest quality Argos position collected for each day. I calculated the directness of turtles' path by dividing the distance between the deployment and final locations by the overall path distance (Batschelet 1981).

3.4 Positional Interpolation and State-Space Modeling

Travel paths were reconstructed by fitting a two-state-switching, correlated, random-walk model to Argos positions deemed plausible by the DAF routine. I interpolated positions at 12-hr intervals. This

model was implemented using WinBugs 1.4.3 (Lunn et al. 2000) and R following methods developed by Jonsen et al. (2005) with modifications by Breed et al. (2009). The model categorized positions as being in one of two behavioral states based on travel rate and turn angle. Breed et al. (2009) employed this method to distinguish between foraging and travel states within data collected from satellite-tracked adult gray seals. Recently, Hart et al. (2012) used similar methods to distinguish between migration and resident foraging behaviors using Argos data collected from post-nesting loggerhead turtles. For the present study, I applied this method to explore the possibility that surface-pelagic juveniles exhibited two behavioral states: passive (drift) and active (transit).

3.5 Remotely-Sensed Habitat Information

I overlaid positions with several remotely-sensed environmental datasets. Sea surface circulation velocity and direction data were obtained from Ssalto/Duacs sea surface height (SSH) data distributed by Aviso, with support from Cnes (http://www.aviso.altimetry.fr/duacs/). I obtained daily, 4 km spatial resolution sea surface temperature (SST) data from thermal infrared sensors onboard MODIS Aqua and Terra satellites. MODIS data were obtained from the Physical Oceanography Distributed Active Archive Center at the NASA Jet Propulsion Laboratory, Pasadena, CA (http://podaac.jpl.nasa.gov). I extracted spatially and temporally corresponding SSH and SST data at interpolated positions using the Marine Geospatial Ecology Tools for ArcGIS (Esri, Redlands, CA; Roberts et al. 2010). I obtained wind velocity values corresponding to each interpolated position from the global NCEP/NCAR Reanalysis 2 dataset using the RNCEP package written for the program R (Kanamitsu et al. 2002; Kemp et al. 2012). I attributed bathymetry values to interpolated positions using ArcGIS and the US Coastal Relief Model dataset (NOAA NGDC 2009).

I identified SPDC within Landsat 5 Thematic Mapper and Landsat 7 Enhanced Thematic Mapper Plus images using the Floating Algae Index (Hu 2009). Landsat imagery has a spatial resolution of 30 m. Each

satellite revisits scenes on 16-day intervals; together, Landsat 5 and 7 provided 8-day temporal resolution. Landsat primarily provided data for nearshore waters during the study period (Fig. 2.1). Using ArcGIS, I intersected satellite track positions with Landsat scene footprints to identify the dates that each tracked turtle intersected with specific Landsat scenes. I browsed the images and searched for dates of interest using the US Geological Survey's Global Visualization Viewer (Glovis; http://glovis.usgs.gov/). Using Glovis, I selected images collected on or within 1 day of a tracked turtle being observed within that scene. I downloaded and applied atmospheric correction to the level-1 reflectance data using a customized set of IDL routines (Hu et al. 2004; Exelis Visual Information Solutions, Boulder, CO). Next, I calculated the FAI using the corrected reflectance data from bands 3, 4, and 5 (Hu 2009). I examined FAI images, along with co-registered RGB images, within ENVI (Exelis Visual Information Solutions, Boulder, CO). I digitized SPDC features within ENVI, converted the SPDC features to vectors, and recorded those as feature classes within an ArcGIS geodatabase. Within ArcGIS, I estimated the distances from the nearest interpolated turtle position to the nearest SPDC feature.

3.6 Statistical Methods

In order to evaluate the effects of longer duty cycles on transmitter performance, I compared the duration of deployment and the number of days during which positions were collected (data days) for the two duty cycles using two sample t-tests. Using Watson's two sample test of homogeneity, I evaluated the similarity between turtle travel direction and surface circulation direction. I compared SST values provided by the transmitters to those obtained from MODIS using a two sample t-test. The aforementioned statistical tests were performed using R with alpha = 0.05. I compared wind velocity, surface current velocity and SST, values between behavioral states using a liner mixed-effects model implemented with the lme4 R package (Bates et al. 2014). Within the models, behavioral state was used

as a fixed effect, and turtle was incorporated as a random effect. Likelihood ratio tests were used to compare the model with behavioral state included to a null model, within which behavior was omitted.

4. Results

Turtles were tracked for an average of 36.5 days (±14.8 SD, range = 20–71) during June–October, 2011. During the tracking periods, transmitters provided locations for an average of 28 days (±10.5 SD, range 13–44). I received an average of 166.6 locations from each transmitter (±67 SD, range = 85–312). Argos positional data generated by these transmitters were dominated by the lower quality class 0–Z locations (91.9% of all positions received; Fig. 2.4). Most of these locations were classified as 0 or B (45% and 33%, respectively). Transmitters maintained consistent battery charges throughout the duration of deployments, the average voltage was 4.0 (±0.21 SD, range = 3.2–4.3). Battery voltages of four transmitters generally increased during the deployment while the remaining six units showed slightly declining charges (Fig. 2.5). The five transmitters with the shorter (24 hour) period of inactivity provided an average of 207 Argos locations while the units with the longer (48 hour) duty cycle provided an average of 126 locations, per deployment. The two duty cycles did not differ significantly in the quality of Argos locations ($p = 0.97$), number of data-days ($p = 0.09$), or length of deployments ($p = 0.65$; Table 2.1).

4.1 Movement Characteristics and Behavior

Of the six turtles released from the two northern Gulf study sites, five had eastward or southeastward travel paths (Fig. 2.6). The northern Gulf individuals also moved farther from their release position (mean displacement = 217.7 km) than turtles released on the WFS (mean displacement = 118.2 km; Table 2.2). Northern Gulf turtles had shorter overall travel path lengths and, as a result,

more direct paths (Table 2.2). The average travel rate was 0.91 km hr^{-1} (±1.68 SD). Northern Gulf turtles traveled an average of 0.3 km hr^{-1} faster than those released on the WFS (Table 2.2).

Turtles spent an average of 75% of the tracking period within the behavioral state characterized by slower travel rates and larger turn angles — the relatively passive behavioral state presumed to represent drift (Table 2.2). This behavioral state dominated the tracking period for all but two individuals, 105467 and 105471, both of which exhibited above average travel rates (Table 2.2). Turtle 105472 also exhibited high travel rates but had a sinuous travel path (Table 2.2). Two individuals (105468 and 105473) never entered behavioral state 2, the state marked by relatively fast and direct travel. Both individuals had low path straightness indices and low overall displacement, indicative of localized movements (Table 2.2).

Satellite-tracked turtles were released within or near to continental shelf waters (Fig. 2.1). The average depth of release positions was 120 m (±65 SD, range = 45–206). The average depths used by turtles was 318 m (±720 SD, range = <1–3241). Half of the turtles remained within continental shelf waters throughout the tracking period (Table 2.4). The 30 m contour constrained a majority of the movements made by tracked turtles (Fig. 2.6). All but one of the individuals remained in waters deeper than 19.8 m throughout their tracking period (Table 2.4). One individual, 105466, moved into shallow waters during the final month of tracking (minimum depth < 1 m).

4.2 Apparent Departure from the Surface-Pelagic Environment

Turtle 105466 was captured and tracked from SPDC found offshore of Sarasota, Florida on 13 August 2011 (Fig. 2.7). The animal remained offshore of the 30 m bathymetric contour during the initial month of the tracking period. On 10 September, this individual began a fairly direct movement toward the coastline of western peninsular Florida. This movement ended on 13 September, near the mouth of the Suwannee River, in approximately 4 m depth. From 14 September–14 October, this individual moved

northward, toward the Pepperfish Keys, then southward, past the Cedar Keys and into Waccasassa Bay, while remaining within an average depth of 6.1 m (±1.9 SD, range = 1.6–9.8). Prior to 14 September, the number of messages received during each Argos overpass was 4.2 (±3.5 SD, range = 1–13; Fig. 2.8). From 14 September – 14 October, the mean number of messages per overpass fell to 1.3 (±0.7 SD, range = 1–4; Fig. 2.8). On 15 October, turtle 105466 traveled shoreward, toward the mouth of the Withlacoochee River (Fig. 2.7). The final two locations from this unit were transmitted on 18 and 23 October from two nearshore (depth < 1 m) locations, the Withlacoochee Reefs and Crystal Bay, respectively.

4.3 Sea Surface Habitat

The average temperature reported by the transmitters' internal sensors was 33.6° C (±1.2 SD, range = 24.3 – 38.5). The average of remotely-sensed SST values corresponding to turtle positions was 29.7° C (±1.1 SD, range = 25.4 – 32.2). Transmitter-reported SST values were significantly higher than those obtained from MODIS satellites (t-test, $p < 0.01$). The temperature values reported by the transmitters and those derived from MODIS imagery are reported by transmitter in Fig. 2.9. The average surface current velocity encountered by tracked turtles was 0.37 km hr^{-1} (±0.20, range 0.08–1.18; Table 2.3). When averaged across the entire track, turtle travel direction and surface circulation direction differed significantly for each animal (Watson's two sample test for homogeneity, alpha = 0.05). A close inspection of the travel paths and direction of surface circulation corresponding to each position revealed that each individual exhibited periods of movement with, against or across the flow of prevailing surface currents (Fig. 2.10). Surface circulation velocity and SST values did not differ between behavioral states for these eight individuals. The average wind speeds experienced by tracked turtles was 3.4 m s^{-1} (±2.1 SD, range = 0.01–11.7). For the eight individuals observed in both behavioral states,

wind velocity values were significantly higher (1.1 m s^{-1} ±0.2 SE, $\chi^2 = 23.5$, $p = 0.001$) when turtles were in the behavioral mode characterized by faster and more direct travel.

I examined 30 Landsat 5 and 7 images collected during June–October 2011. Landsat imagery was available corresponding to the paths of all but one tracked turtle (Table 2.5). This turtle received transmitter number 105465 south of Apalachicola, Florida during July 2011. This capture and transmitter deployment occurred within a within a region where Landsat data were not available (Landsat path 19, row 40; Fig. 2.11). The turtle moved south-southeast through waters not imaged by Landsat, then traveled northeastward and into a Landsat scene that was imaged during the summer of 2011 (path 18, row 40). Turtle 105465 remained within this area from 27 July until the tag ceased transmissions on 7 August 2011. Landsat images were collected within this scene on 26 July and 11 August. Landsat 7 was scheduled to image the area on 3 August, but the image was not acquired (USGS EROS pers. comm. September 2014). As part of a complementary study, I examined the two Landsat 5 images nearest to this time period and found SPDC within both images (Fig. 2.11). Turtle 105465 switched relatively passive movements on 29 July. This behavioral change occurred when the turtle was within 10 km of the location where SPDC was observed three days prior, on 26 July (Fig. 2.11). From 29 July–7 August, this individual also did not experience winds in excess of 5 m s-1, the point above which larger areas of SPDC may disintegrate (Marmorino et al. 2011).

Four turtles were observed in close association with remotely-detected SPDC. Turtle number 105464 was released within SPDC southeast of Pensacola, Florida on 3 June 2011. SPDC was found within Landsat images collected on three days corresponding to this turtle's track (Fig. 2.12). On 6 June, SPDC was apparent approximately 15 km south of the location of turtle 105464. The turtle travelled southwestward between 6 and 14 June, into an area where lines of SPDC were observed on 6 June. Upon arrival in this area, the turtle's travel rate slowed, and its behavioral state switched to the passive state. A second Landsat image was collected on 14 June, and no SPDC was observed near to 105464.

Small patches of SPDC were observed approximately 40 km east of the turtle's position on that day. At this time the turtle had begun directed, eastward travel. A third Landsat image was collected on 23 June, and SPDC was observed approximately 30 km west of 105464.

Turtle 105468 was tracked from SPDC found south of Apalachicola, Florida on 7 July 2011. This individual was tracked for 20 days, during which time three Landsat images were collected and SPDC was observed in all images (Fig. 2.13). On 10 July, this individual was within 10 km of SPDC. On the following day, the turtle moved southward and through the area where SPDC was observed in the 10 July image. Turtle 105468 moved southward until 18 July, then turned and traveled northward, along a similar path. The area was imaged by Landsat 7 on 18 July and a small area of SPDC was observed approximately 40 km east of the turtle's positions. SPDC was again observed within the Landsat 5 image collected on 26 July. Patches of SPDC were found approximately 15 km northeast and southwest of the corresponding turtle positions.

Turtle 105469 was captured within and tracked from SPDC found west of Sarasota, Florida on 13 August 2011. This individual remained within the extent of Landsat path 17, row 41 throughout the tracking period. This Landsat scene was imaged seven times during the tracking period; SPDC was observed within 4 images (Table 2.5). On 13 September, a line of SPDC was observed slightly east of the path traveled by turtle 105469 (Fig. 2.14). Within the other three images, SPDC was present but distant (approx. 50–150 km) from the path of turtle 105469.

Turtle 105470 was tracked from SPDC found within waters south of Pensacola, Florida on 5 July 2011. The region was imaged by Landsat 5 the following day, 6 June, and 6.2 km^2 SPDC was observed within the image and overlapping with the location of turtle 105470 (Fig. 2.13). This individual remained within the area until 13 June, when it began directed eastward movements. This Landsat scene (path 20, row 39) was imaged again on 14 June and 0.2 km^2 of SPDC was observed within the image. Wind speeds corresponding to the locations of turtle 105470 increased to approximately 4.6 and 5.9 m s^{-1} by

13 and 14 June, respectively. From 15–19 June, turtle 105470 traveled eastward and south the extent of the nearby Landsat scene (path 19, row 39; Fig. 2.14). This scene was imaged on 15 June, and SPDC was present within this image, approximately 70 km from the corresponding position of the turtle. The average wind speed during the 15–19 June transit was 4.3 m s^{-1}. On 21 June, this individual's travel rate and direction changed; corresponding wind speeds fell to 2.4 m s^{-1}. The turtle spent the remainder of the tracking period in an area where SPDC was observed within Landsat images collected 24 June, 2 July, and 10 July (Fig. 2.14). The average wind speed corresponding to this time period (21 June–14 July) was 2.2 m s^{-1}.

The remaining five turtles were observed on or within one day of SPDC being present within the same Landsat scene for 74% of images examined (Table 2.5). Overall, the mean distance between tracked turtles and SPDC was 54 km. These records indicate that conditions were favorable for the presence of SPDC on those days. On 78% of these occasions, turtles were observed within the passive behavioral state.

5. Discussion

The surface-pelagic life stage, first classified by Carr et al. (1978) as the "lost year", remains one of the most poorly understood aspects of sea turtle biology. Research efforts focused on surface-pelagic juveniles have provided essential information on the species, size distribution, threats, behavior, and habitat associations (Witherington 2002; Witherington et al. 2012). For example, within the North Atlantic, we now know that four species of sea turtles spend their surface-pelagic juvenile phases within the region's *Sargassum*-dominated drift communities (Witherington et al. 2012). Knowledge of a strong association with a discrete habitat, and technological advancements within the field of oceanographic remote-sensing (Hu 2009) will help revise distributional patterns for these species and life stages.

Advancements in satellite tracking technology allowed us to build on this knowledge by evaluating habitat associations across longer periods of time.

The average transmitter deployment duration of 36.5 days was low relative to most sea turtle tracking studies. However, sea turtle tracking studies tend to involve larger, slower growing animals; larger transmitters; and longer-lasting attachment techniques (Balazs et al. 1996; Godley et al. 2008; Jones et al. 2013). The ability for smaller sized turtles to be tracked under the present study was made possible by the use of small transmitters initially developed for avian applications and flexible attachment techniques that would not prevent normal growth (developed by Mansfield et al. 2012). To date, one study has used similar methodology to satellite-track captive-reared loggerhead turtles (Mansfield et al. 2014). The present study represents the first application of this technique involving wild-captured surface-pelagic juvenile turtles. The differing tracking durations between the present study and Mansfield et al. (2014) could be a result deploying transmitters on a different species under field conditions.

Mansfield et al. (2014) experienced longer deployment durations (86.6 days) and received higher quality locations. The majority of Argos locations collected during the present study fell within classes 0–Z (91.9%). The quality of locations is a measure of the position's accuracy and largely depends on the number of messages received by satellites. CLS does not assign accuracy estimates to Argos locations derived from fewer than four messages (CLS 2014). Mansfield et al. (2014) received higher quality, mostly class 1, locations from lab-reared surface-pelagic juvenile loggerheads that were released within Gulf Stream waters off southeast Florida. The high percentage of class 0 locations in the present study was unexpected. Class 0 locations are those for which four or more messages were received but the upper limit of the error radius could not be determined (CLS 2014). This suggests that the transmitters were sending a sufficient number of messages, but failed plausibility checks resulted in the poor data quality observed by the present study. Similar to Mansfield et al. (2014), transmitters in the present

study exhibited stable battery voltage throughout the deployments. This suggests that sufficient solar radiation reached the transmitters' solar cells. An examination of the overall location quality for the present study may lead to the conclusion that the turtles were behaving differently than expected, i.e., spending less time at the surface. However, the frequency of Argos messages, consistent battery voltage, and transmitter temperatures consistently higher than SST suggested that the turtles were spending much of their time at the surface during daylight hours.

5.1 Behavior

The present study explored the use of state-space modeling techniques as a tool to determine whether the movements of surface-pelagic juveniles could be classified into periods of passive and active behavior. Overall, turtles were in the relatively passive behavioral state 75% of the time. Two individuals spent a majority of the time in a more active behavioral state, and their path characteristics (rate, path straightness, and displacement) supported this classification. Two other turtles were never identified by the model as being in the active behavioral state. Path characteristics also supported this passive-state classification because both individuals had indirect paths with small displacements. It is possible the tracking duration was not sufficient to capture a behavioral change; both were relatively brief deployments (20 and 24 days). One of these individuals (turtle 105473) had the second highest overall travel rate despite never having entered the relatively active behavioral state. Travel rates can be extremely high and not useful for plausibility tests when calculated among Argos positions collected near in time and space (< 5 km in the present study). Turtle 105473 moved the shortest overall distance during the deployment, and most locations were retained by plausibility filtering due to their close proximity, rather than based on travel rate. This case illustrates the utility of plausibility filtering and behavioral classification techniques that consider multiple travel-path metrics. Behavioral models may be further refined by the incorporation of sea surface habitat variables.

The exploratory application of behavioral classification techniques was supported by travel path characteristics and by habitat associations, i.e., proximity to SPDC. Support principally came from direct observations of SPDC or the occurrence of low wind velocity, presumably favorable for SPDC formation. The FAI applied to Landsat imagery has proven to be a suitable method for detecting SPDC within the eastern Gulf of Mexico (Hu 2009; Ch. 1, present volume). Landsat imagery was available on multiple occasions for 9 of 10 tracked turtles, and SPDC was present within most of the images (Table 2.5). Four turtles were observed closely associated with SPDC, and their behavior suggested passive drift during those instances (Fig. 2.12–2.15). This behavior may be similar to the state in which these animals have been discovered during field captures (Witherington et al. 2012). The remaining five turtles were observed within a Landsat scene that also contained SPDC on several occasions (scene size = 183 x 170 km). This suggests that conditions were favorable for SPDC formation on those days, within the areas occupied by tracked turtles. On these occasions, it is possible that the habitat-detection method missed small features with which the turtles were associated or that the turtles were not associated with SPDC during those days. Low wind speeds appear conducive to the formation of SPDC (Marmorino et al. 2011; Ch. 1, present volume). In the absence of direct habitat observations, wind velocity may be a suitable indicator of conditions favoring the aggregation of SPDC. Across all individuals, wind velocity values were lower when turtles were in the passive behavioral state. More research is needed to determine whether wind velocity can be used to predict the occurrence of aggregated SPDC. The coupled examination of behavioral state and habitat associations suggests that these turtles exhibited mixed, but principally passive, behavior. Additionally, passive behavior appears to be in response to the presence of SPDC.

The prevalence of relatively passive behavior was expected. By associating with SPDC, young turtles reduce their risk of predation and increase foraging opportunities (Musick and Limpus 1997; Witherington et al. 2012). Once a suitable habitat is located, it is advantageous for turtles to remain

associated with it. Therefore, the distribution and availability of SPDC must constrain the distribution of associated surface-pelagic juvenile turtles. However, SPDC may be found in areas not occupied by surface-pelagic turtles. A complementary study (Ch. 1, present volume) identified dense aggregations of SPDC along the northeastern Gulf shoreline of Florida and within shallower waters than were inhabited by turtles in the present study. With one exception, turtles in the present study used a range of continental shelf and slope water depths and did not venture into waters shallower than 19.8 m. This behavior may indicate that shallow waters are somehow unsuitable for surface-pelagic juvenile turtles even though habitat is present. Rooker et al. (2012) found that blue marlin, white marlin and swordfish larval density increased with depth. Larvae of those species are also *Sargassum* associates. They speculated that the physical properties (salinity or temperature) of nearshore waters may be unsuitable for larval development. Rooker et al. (2012) also noted that predation of larval fish may be higher in nearshore areas as a result of higher predator concentrations due to increased production. Being reptiles, sea turtles exhibit a response to temperature in many aspects of their biology including distribution (Mrosovsky 1980). Perhaps, nearshore water temperatures are similarly less favorable for development of surface-pelagic juveniles. Avoidance of nearshore waters requires a behavioral strategy that is capable of detecting shallow waters and adjusting travel accordingly. Although principally surface-dwelling, Kemp's ridleys of this life stage are capable of diving to 20 m depth and make regular dives to the scattering layer (Witherington et al. 2012). This diving behavior may provide a mechanism by which individuals are able to detect and avoid shallow waters. Further satellite tracking and in-situ observations would help determine the extent to which water depth constrains movements of surface-pelagic juvenile turtles. This information is critical to generating distributional estimates for surface-pelagic juvenile Kemp's ridleys and is worthy of further study.

5.2 Evidence for Recruitment

One individual crossed the 20 m bathymetric contour and moved into nearshore waters of the northeastern Gulf (Fig. 2.7). Musick and Limpus (1997) speculated that as new recruits into neritic environments, Kemp's ridleys may first settle in shallow waters as a strategy to avoid large predators. Turtle 105466 moved into a shallow region where neritic juvenile-through-subadult Kemp's ridleys are known to occur. Thus, support for the observed event being a transition into neritic habitats, rather than a nearshore movement made by a surface-pelagic juvenile, can be found within previous research. Carr and Caldwell (1956) examined the commercial sea turtle fishery that operated near the Cedar Keys and within Waccasassa Bay. They found that neritic-stage Kemp's ridleys were commonly captured within the fishery. Schmid (1998) conducted net-capture studies focused on the Waccasassa Bay reefs and identified the area as an important developmental habitat for neritic-stage Kemp's ridleys. Additional research has identified Kemp's ridleys within other areas along the western peninsular Florida coastline (see review by Schmid and Barichivich 2006). Neritic-stage Kemp's ridleys (23.2–60.0 cm, straight carapace length, SCL) have been recorded within the intake canal of the nearby nuclear power plant (data reported to FWC by Progress Energy Florida, reviewed by Eaton et al. 2008). This canal is approximately 10 km from the final location recorded for turtle 105466 (Fig. 2.7). This individual was relatively large (26.2 cm SCL), compared to the mean size of surface-pelagic Kemp's ridleys found within the eastern Gulf of Mexico (23.3 cm, Witherington et al. 2012).

Further evidence in support of this being a recruitment event comes from the behavioral shift that was detected by the behavioral model and by examining transmitter messaging rates. This individual made directed movements northward from the vicinity of its capture location to a nearshore location where it exhibited a change in movement behavior. After 13 September, the path characteristics switched from directed movements to wandering movements in a northward and southward direction along the shoreline (Fig. 2.7). The daily Argos messaging rates also fell on 13 September (Fig. 2.8).

Abrupt changes in messaging rates from Argos transmitters attached to sea turtles have been used to indicate extreme events, such as mortality. For example, Nero et al. (2013) examined the satellite track of a neritic juvenile Kemp's ridley that died under unusual circumstances. They used the change in Argos messaging rates and location quality to identify the likely place and time of mortality for the animal in question. The case presented by Nero et al. (2013) involved a neritic juvenile for which tracking data prior to mortality were characterized by poor quality positions derived from infrequent messaging. Such a pattern is characteristic of satellite-tracking animals that spend a majority of the time underwater (Vincent et al. 2002). Nero et al. (2013) noted that after a brief period of no data, message counts and location quality increased, and the subsequent track was explained by surface drift. The current case used the marked shift in Argos messaging to support somewhat of an inverse scenario—tracking a known surface-dwelling individual through its transition to a principally subsurface lifestyle. As hypothesized by Witherington et al. (2012), these results suggest that surface-pelagic juvenile Kemp's ridleys within the northeastern and eastern Gulf could remain within SPDC for prolonged periods, ultimately recruiting to nearshore habitats along the western Florida coastline.

5.3 Distribution and Habitat Association

The present study identified several points that can be used to refine knowledge of the distribution of Kemp's ridleys within the Gulf of Mexico. Turtles appeared principally constrained by the availability of SPDC and by shallow waters (< 20 m). Within the northwestern Atlantic, the Gulf Stream Current or its meanders likely constrain the distribution of surface-pelagic juvenile turtles (Mansfield et al. 2014). The Gulf Stream has been shown to deflect the migrations of adult loggerheads departing eastern Florida nesting beaches and encounter northward-flowing surface current velocities in excess of 1 m s^{-1} (Foley et al. 2013). Surface-pelagic juveniles may not be capable of traveling in a direction counter to such fast-moving currents. Within the northern Gulf, turtles in the present study appeared capable of

moving freely with, across, or against the low velocity currents they encountered. Most of the directed movements appeared to involve traveling perpendicular to the movement of surface waters (Fig. 2.11). Perhaps, this strategy increases the animals' likelihood of encountering SPDC.

The regions encountered by turtles tracked in the present study are areas where SPDC is found year-round (Ch. 1, present volume). An examination of available Landsat FAI imagery indicated that SPDC was frequently present near to or within the general area occupied by tracked turtles. Additionally, wind data indicated that when turtles were in the passive behavioral state, conditions were favorable for SPDC accumulation. Similar to Mansfield et al. (2014), turtles in the present study may have achieved body temperatures that exceeded SST by an average of 3.9°C (Fig. 2.9). Marmarino et al. (2011) demonstrated that the temperature of *Sargassum* may differ from surrounding waters by as much as 0.5°C but is typically 0.1°C higher than SST. Basking behavior has been demonstrated to elevate sea turtle body temperatures 3.75°C above that of surrounding sea water (Sapsford and van der Riet 1979). Assuming transmitter temperatures are suitable proxies for the body temperature of the turtles to which they are affixed, the temperature difference between the transmitters and SST might be largely due to solar radiation with *Sargassum* heat transduction and storage being secondary. As suggested by Mansfield et al. (2014), the principal role of SPDC in the thermal environment may be to offer a location for young sea turtles to bask with reduced risk of predation.

The findings of this and previous studies can be combined to estimate the threat of marine pollution to surface-pelagic juvenile sea turtles: 1) Surface-pelagic juveniles of four sea turtle species are closely associated with SPDC (Witherington et al. 2012). 2) These habitats are often impacted by pollution in the form of persistent marine debris or spilled petroleum products (Carr 1987; Witherington 2002; Schuyler et al. 2014). 3) Post-hatchling and juvenile sea turtles found within SPDC are known to ingest various types of anthropogenic debris and pollutants (Witherington 2002; Witherington et al. 2012).

Collectively, these findings suggest that anthropogenic debris may be having severe impacts on surface-pelagic juvenile sea turtles throughout their range.

5.4 Conclusions

Based on direct observations, Witherington et al. (2012) demonstrated that surface-pelagic juveniles green, hawksbill, Kemp's ridley, and loggerhead turtles are closely associated with SPDC. The present study followed surface-pelagic stage Kemp's ridleys for periods up to 71 days and found a linkage between tracked turtles and SPDC. Tracked turtles showed evidence of both active and, mostly, passive behavior. When in a passive behavioral state, turtles were likely drifting in association with SPDC. In the absence of habitat, tracked turtles underwent directed movements that terminated near locations of SPDC. The behavioral information presented herein supports the hypothesis that surface-pelagic juvenile Kemp's ridleys are principally passive associates of SPDC for long periods of time until the completion of the initial surface-pelagic developmental phase (Musick and Limpus 1997; Witherington et al. 2012). They also appear capable of directed travel, presumably to relocate the ephemeral habitats on which they depend. The abundance of Gulf of Mexico SPDC varies spatially and seasonally, but the habitat appears to be present year-round throughout much of the region (Gower and King 2011; Ch. 1, current volume). Surface-pelagic drift habitats within continental shelf waters of the eastern Gulf may provide critical habitats for juvenile Kemp's that are on the cusp of transitioning to neritic habitats. Future work addressing the movements of Kemp's ridleys from other parts of the Gulf of Mexico will help determine if other regions of the Gulf also serve such a role in the life history of Kemp's ridleys.

Literature Cited:

Bailey, H., S. R. Benson, G. L. Shillinger, S. J. Bograd, P. H. Dutton, S. A. Eckert, S. J. Morreale, F. V Paladino, T. Eguchi, D. G. Foley, B. A. Block, R. Piedra, C. Hitipeuw, R. F. Tapilatu, and J. R. Spotila. 2012. Identification of distinct movement patterns in Pacific leatherback turtle populations influenced by ocean conditions. Ecological Applications 22:735–747.

Balazs, G. H., R. K. Miya, S. C. Beavers. 1996. Procedures to attach a satellite transmitter to the carapace of an adult green turtle, Chelonia mydas. In: J. A. Keinath, D. E. Barnard, J. A. Musick, B. A. Bell (comps). Proceedings of the 15th annual symposium on sea turtle biology and conservation. US Department of Commerce, NOAA Technical Memorandum NMFS-SEFSC-387, 355 pp.

Bates, D., M. Maechler, B. Bolker, S. Walker. 2014. lme4: Linear mixed-effects models using Eigen and S4. R package version 1.1-7. http://CRAN.R-project.org/package=lme4.

Batschelet, E. 1981. Circular statistics in biology. Academic Press, New York, NY, USA.

Block, B. A., D. P. Costa, G. W. Boehlert, and R. E. Kochevar. 2003. Revealing pelagic habitat use : the tagging of Pacific pelagics program. Oceanologica Acta 25:255–266.

Bolten, A. B. 2003a. Active swimmers – passive drifters: The oceanic juvenile stage of loggerheads in the Atlantic system. Pages 63–78 in A.B. Bolten and B.E. Witherington, editors. Loggerhead Sea Turtles. Smithsonian Institution Press. Washington D.C.

Bolten, A. B. 2003b. Life history patterns of sea turtles: consequences of an oceanic juvenile stage. Pages 243–257 in P. L. Lutz, J. Musick, and J. Wyneken, editors. The biology of sea turtles, Volume II. CRC Press, Boca Raton, FL.

Borchers, H. W. 2014. Pracma: Practical numerical math functions, v. 1.7.0. http://cran.r-project.org/web/packages/pracma/index.html

Breed, G. A., I. D. Jonsen, R. A. Myers, W. D. Bowen, and M. L. Leonard. 2009. Sex-specific , seasonal foraging tactics of adult grey seals (*Halichoerus grypus*) revealed by state-space analysis. Ecology 90:3209–3221.

Carr, A. 1987. Impact of nondegradable marine debris on the ecology and survival outlook of sea turtles. Marine Pollution Bulletin 18:352–356.

Carr, A. 1986. Rips, FADS, and little loggerheads. BioScience 36:92–100.

Carr, A., and D. K. Caldwell. 1956. The ecology and migrations of sea turtles, 1. Results of field work in Florida, 1955. American Museum Novitates 1793:1–24.

Carr, A., M. H. Carr, and A. B. Meylan. 1978. The ecology and migrations of sea turtles, 7. The west Caribbean green turtle colony. Bulletin of the American Museum of Natural History 162:1–46.

[CLS] Collecte Localisation Satellites. 2014. Argos user's manual. Collecte Localisation Satellites, Toulouse, France.

Collard, S. B., and L. H. Ogren. 1990. Dispersal scenarios for pelagic post-hatchling sea turtles. Bulletin of Marine Science 47:233–243.

Dalton, S. 1979. Temporal patterns of locomotor activity in hatchling sea turtles. Ph.D. Dissertation. University of Florida, Gainesville, Florida, USA.

Douglas, D. C., R. Weinzierl, S. C. Davidson, R. Kays, M. Wikelski, and G. Bohrer. 2012. Moderating Argos location errors in animal tracking data. Methods in Ecology and Evolution 3:999–1007.

Eaton, C., E. McMichael, B. Witherington, A. Foley, R. Hardy, and A. Meylan. 2008. In-water sea turtle research in Florida: review and recommendations. US Department of Commerce, NOAA Technical Memorandum NMFS-OPR-38, 233pp.

Eckert, S. A. 2006. High-use oceanic areas for Atlantic leatherback sea turtles (*Dermochelys coriacea*) as identified using satellite telemetered location and dive information. Marine Biology 149:1257–1267.

Eckert, S. A., D. Bagley, S. Kubis, L. Ehrhart, C. Johnson, K. Stewart, and D. DeFreese. 2006. Internesting and postnesting movements and foraging habitats of leatherback sea turtles (*Dermochelys coriacea*) nesting in Florida. Chelonian Conservation and Biology 5:239–248.

Fine, M. L. 1970. Faunal variation on pelagic *Sargassum*. Marine Biology 7:112–122.

Foley, A. M., B. A. Schroeder, R. Hardy, S. L. MacPherson, M. Nicholas, and M. S. Coyne. 2013. Postnesting migratory behavior of loggerhead sea turtles *Caretta caretta* from three Florida rookeries. Endangered Species Research 21:129–142.

Foley, A. M., B. A. Schroeder, R. Hardy, S. L. MacPherson, and M. Nicholas. 2014. Long-term behavior at foraging sites of adult female loggerhead sea turtles (*Caretta caretta*) from three Florida rookeries. Marine Biology 161:1251–1262.

Gaspar, P., S. R. Benson, P. H. Dutton, A. Réveillère, G. Jacob, C. Meetoo, A. Dehecq, and S. Fossette. 2012. Oceanic dispersal of juvenile leatherback turtles: going beyond passive drift modeling. Marine Ecology Progress Series 457:265–284.

Godley, B., J. Blumenthal, A. Broderick, M. Coyne, M. Godfrey, L. Hawkes, and M. Witt. 2008. Satellite tracking of sea turtles: Where have we been and where do we go next? Endangered Species Research 4:3–22.

Gower, J., C. Hu, G. Borstad, and S. King. 2006. Ocean Color Satellites Show Extensive Lines of Floating *Sargassum* in the Gulf of Mexico. IEEE Transactions on Geoscience and Remote Sensing 44:3619–3625.

Gower, J. F. R., and S. A. King. 2011. Distribution of floating *Sargassum* in the Gulf of Mexico and the Atlantic Ocean mapped using MERIS. International Journal of Remote Sensing 32:1917–1929.

Hart, K., and K. D. Hyrenbach. 2009. Satellite telemetry of marine megavertebrates: The coming of age of an experimental science. Endangered Species Research 10:9–20.

Hart, K. M., M. M. Lamont, I. Fujisaki, A. D. Tucker, and R. R. Carthy. 2012. Common coastal foraging areas for loggerheads in the Gulf of Mexico: Opportunities for marine conservation. Biological Conservation 145:185–194.

Howell, E. A., D. R. Kobayashi, D. M. Parker, G. H. Balazs, and J.J. Polovina. 2008. TurtleWatch: a tool to aid in the bycatch reduction of loggerhead turtles *Caretta caretta* in the Hawaii-based pelagic longline fishery. Endangered Species Research 5:267–278.

Hu, C. 2009. A novel ocean color index to detect floating algae in the global oceans. Remote Sensing of Environment 113: 2118-2129.

Hu, C., Z. Chen, T. D. Clayton, P. Swarzenski, J. C. Brock, and F. E. Muller–Karger. 2004. Assessment of estuarine water-quality indicators using MODIS medium-resolution bands: Initial results from Tampa Bay, FL. Remote Sensing of Environment 93:423–441.

Hyrenbach, K. D., K. A. Forney, and P. K. Dayton. 2000. Marine protected areas and ocean basin management. Aquatic Conservation: Marine and Freshwater Ecosystems 458:437–458.

Jones, T. T., K. S. Van Houtan, B. L. Bostrom, P. Ostafichuk, J. Mikkelsen, E. Tezcan, M. Carey, B. Imlach, and J. A. Seminoff. 2013. Calculating the ecological impacts of animal-borne instruments on aquatic organisms. Methods in Ecology and Evolution. doi: 10.1111/2041-210X.12109.

Jonsen, I. D., J. M. Flemming, and R. A. Myers. 2005. Robust state-space modeling of animal movement data. Ecology 86:2874–2880.

Kanamitsu, M., W. Ebisuzaki, J. Woollen, S. K. Yang, J. J. Hnilo, M. Fiorino, and G. L. Potter. 2002. NCEP-DOE AMIP-II reanalysis (R-2). Bulletin of the American Meteorological Society 83:1631–1643+1559.

Kemp, M.U., E.E. van Loon, J. Shamoun-Baranes, W. and Bouten. 2012. RNCEP: Global weather and climate data at your fingertips. Methods in Ecology and Evolution 3:65-70. R package version 1.0.6.

Lunn, D.J., Thomas, A., Best, N., and Spiegelhalter, D. 2000. WinBUGS -- a Bayesian modelling framework: Concepts, structure, and extensibility. Statistics and Computing, 10:325--337.

Mansfield, K. L., J. Wyneken, W. P. Porter, and J. Luo. 2014. First satellite tracks of neonate sea turtles redefine the 'lost years' oceanic niche. Proceedings of the Royal Society, Biological Sciences 281: 20133039.

Mansfield, K., J. Wyneken, D. Rittschof, M. Walsh, C. Lim, and P. Richards. 2012. Satellite tag attachment methods for tracking neonate sea turtles. Marine Ecology Progress Series 457:181–192.

Marmorino, G. O., W. D. Miller, G. B. Smith, and J. H. Bowles. 2011. Airborne imagery of a disintegrating *Sargassum* drift line. Deep Sea Research Part I: Oceanographic Research Papers 58:316–321.

Marquez-M., R. 1994. Synopsis of Biological Data on the Kemp's Ridley Turtle, *Lepidochelys kempi* (Garman, 1880). US Department of Commerce, NOAA Technical Memorandum, NMFS-SEFSC-343, 91 pp.

Meylan, P. A., A. B. Meylan, and J. A. Gray. 2011. The Ecology and Migrations of Sea Turtles, 8. Tests of the developmental habitat hypothesis. Bulletin of the American Museum of Natural History 357:1–70.

[MTI] Microwave Telemetry Inc. 2011. Solar PTT-100 Field Manual. Columbia, MD, USA. http://microwavetelemetry.com

Mrosovsky, N. 1980. Thermal biology of sea turtles. American Zoologist, 20:531–547.

Musick, J. A., and C. Limpus. 1997. Habitat utilization and migration in juvenile sea turtles. Pages 137–163 in P. L. Lutz and J. A. Musick, editors. The biology of sea turtles, volume 1. CRC Press, Washington, D.C.

[NOAA NGDC] National Oceanic and Atmospheric Administration, National Geophysical Data Center. 2009. US Coastal Relief model. http://www.ngdc.noaa.gov/mgg/coastal/crm.html.

Nero, R., M. Cook, A. Coleman, M. Solangi, and R. Hardy. 2013. Using an ocean model to predict likely drift tracks of sea turtle carcasses in the north central Gulf of Mexico. Endangered Species Research 21:191–203.

Pearson, R. K. 1999. Data cleaning for dynamic modeling and control. European Control Conference, ETH Zurich, Switzerland.

Polovina, J. J., G. H. Balazs, E. A. Howell, D. M. Parker, M. P. Seki, and P. H. Dutton. 2004. Forage and migration habitat of loggerhead (*Caretta caretta*) and olive ridley (*Lepidochelys olivacea*) sea turtles in the central North Pacific Ocean. Fisheries Oceanography 13:36–51.

Putman, N. F., T. J. Shay, and K. J. Lohmann. 2010. Is the geographic distribution of nesting in the Kemp's ridley turtle shaped by the migratory needs of offspring? Integrative and Comparative Biology 50:305–14.

Putman, N. F., K. L. Mansfield, R. He, D. J. Shaver, and P. Verley. 2013. Predicting the distribution of oceanic-stage Kemp's ridley sea turtles. Biology Letters 9:20130345.

R Core Team. 2013. R: A language and environment for statistical computing. R Foundation for Statistical Computing, Vienna, Austria. http://www.R-project.org/.

Roberts, J. J., B. D. Best, D. C. Dunn, E. A. Treml, and P. N. Halpin. 2010. Marine Geospatial Ecology Tools: An integrated framework for ecological geoprocessing with ArcGIS, Python, R, MATLAB, and C++. Environmental Modelling & Software 25:1197–1207.

Rooker, J. R., J. R. Simms, R. J. D. Wells, S. A. Holt, G. J. Holt, J. E. Graves, and N. B. Furey. 2012. Distribution and habitat associations of billfish and swordfish larvae across mesoscale features in the Gulf of Mexico. PloS one 7:e34180.

Sapsford, C. W. and M. van der Riet. 1979. Uptake of solar radiation by the sea turtle, *Caretta caretta*, during voluntary surface basking. Comparative Biochemistry and Physiology 63: 471–474.

Schmid, J. R. 1998. Marine turtle populations on the west-central coast of Florida: Results of tagging studies at the Cedar Keys, Florida, 1986–1995. Fishery Bulletin 96:589–602.

Schmid, J. R., and W. J. Barichivich. 2006. *Lepidochelys kempii* – Kemp's Ridley. Pages 128–141 in P. A. Meylan, editor. Biology and Conservation of Florida Turtles. Chelonian Research Monographs. Volume 3. Chelonian Research Foundation.

Schuyler, Q., B. D. Hardesty, C. Wilcox, and K. Townsend. 2014. Global analysis of anthropogenic debris ingestion by sea turtles. Conservation Biology 28:129–39.

Vincent, C., B. J. McConnell, V. Ridoux, and M. A. Fedak. 2002. Assessment of Argos location accuracy from satellite tags deployed on captive gray seals. Marine Mammal Science 18:156–166.

Wallace, B. P., A. D. DiMatteo, B. J. Hurley, E. M. Finkbeiner, A. B. Bolten, M. Y. Chaloupka, B. J. Hutchinson, F. A. Abreu-Grobois, D. Amorocho, K. A. Bjorndal, J. Bourjea, B. W. Bowen, R. B. Dueñas, P. Casale, B. C. Choudhury, A. Costa, P. H. Dutton, A. Fallabrino, A. Girard, M. Girondot, M. H. Godfrey, M. Hamann, M. López-Mendilaharsu, M. A. Marcovaldi, J. A. Mortimer, J. A. Musick, R. Nel, N. J. Pilcher, J. A. Seminoff, S. Troëng, B. Witherington, and R. B. Mast. 2010. Regional management units for marine turtles: A novel framework for prioritizing conservation and research across multiple scales. PloS one 5:e15465.

Witherington, B. E. 2002. Ecology of neonate loggerhead turtles inhabiting lines of downwelling near a Gulf Stream front. Marine Biology 140:843–853.

Witherington, B., S. Hirama, and R. Hardy. 2012. Young sea turtles of the pelagic *Sargassum*-dominated drift community: habitat use, population density, and threats. Marine Ecology Progress Series 463:1–22.

Witt, M. J., E. Augowet Bonguno, A. C. Broderick, M. S. Coyne, A. Formia, A. Gibudi, G. A. Mounguengui Mounguengui, C. Moussounda, M. NSafou, S. Nougessono, R. J. Parnell, G.-P. Sounguet, S. Verhage, and B. J. Godley. 2011. Tracking leatherback turtles from the world's largest rookery: Assessing threats across the South Atlantic. Proceedings of the Royal Society, Biological Sciences 278:2338–2347.

Wyneken, J., and M. Salmon. 1992. Frenzy and postfrenzy swimming activity in loggerhead, green, and leatherback hatchling sea turtles. Copeia 1992:478–484.

Tables:

Table 2.1. Satellite transmitter deployment characteristics for 10 surface-pelagic juvenile Kemp's ridleys tracked from capture locations in the northern and eastern Gulf of Mexico. The table provides the transmitter's duty cycle (off hours), date of deployment, and date of the final Argos location. Also included are the length of time that turtles were remotely-tracked (duration) and the number of days during which Argos locations were received (data days).

Turtle	Off hours	Deployment	Final location	Argos locations	Duration	Data days
105464	48	6/3/2011	7/10/2011	131	37	22
105465	48	7/6/2011	8/7/2011	129	32	20
105466	48	8/13/2011	10/23/2011	141	71	37
105467	48	7/6/2011	8/9/2011	146	34	20
105468	48	7/7/2011	7/27/2011	85	20	13
105469	24	8/13/2011	9/27/2011	312	45	44
105470	24	6/6/2011	7/14/2011	247	39	37
105471	24	6/5/2011	6/26/2011	97	22	22
105472	24	9/16/2011	10/29/2011	208	43	39
105473	24	7/12/2011	8/5/2011	170	24	24
Transmitters with 48 h off time				126.4	38.8	22.4
Transmitters with 24 h off time				206.8	34.6	33.2
All transmitters				**166.6**	**36.7**	**27.8**

Table 2.2. Summary of duration, behavior, and movements observed from satellite transmitter deployments on 10 surface-pelagic Kemp's ridleys. The percentage of days spent in each behavioral state (passive and active) is presented as a percentage of the total days. Distance traveled is expressed as the cumulative (path) distance and the distance between the deployment and final position (displacement). Subscripts identify the turtles' release location as one of two northern Gulf study sites (n) or the West Florida Shelf study site (w).

Turtle	Days at large	Days in passive state (%)	Days in active state (%)	Cumulative distance travelled (KM)	Distance from deployment to final position (KM)	Path straightness index	Travel rate (km hr^{-1}, mean ±SD)
105464_n	37	75.7	27.0	642.69	77.83	0.12	0.64 ±0.44
105465_n	32	87.5	18.8	534.19	179.78	0.34	2.03 ±5.12
105466_w	71	85.9	16.9	839.92	204.96	0.24	0.66 ±0.88
105467_n	34	2.9	97.1	843.36	237.26	0.28	1.55 ±3.00
105468_n	20	100.0	0.0	361.33	88.93	0.25	0.95 ±0.65
105469_w	45	86.7	13.3	913.91	67.63	0.07	0.64 ±0.64
105470_n	39	89.7	10.3	593.27	281.28	0.47	0.66 ±0.62
105471_n	22	27.3	77.3	632.51	440.88	0.70	1.12 ±0.73
105472_w	43	97.7	4.7	1016.71	170.37	0.17	1.03 ±1.27
105473_w	24	100.0	0.0	406.57	29.72	0.07	0.76 ±0.77
NGOM	**30.7**	**63.9**	**38.4**	**601.23**	**217.66**	**0.36**	**1.16**
WFS	**45.8**	**92.6**	**8.7**	**794.28**	**118.17**	**0.14**	**0.77**

Note: Percent of days within behavioral states sum to > 100% for individuals observed in both behavioral states on the same day.

Table 2.3. Summary of travel path direction, surface circulation direction and, surface circulation velocity for 10 satellite-tracked surface-pelagic Kemp's ridleys. Surface circulation direction and velocity were estimated at interpolated satellite track positions.

Turtle	Travel direction (degrees, mean ±sd)	Surface circulation direction (degrees, mean ±sd)	Surface circulation velocity (km hr-1)
105464	204.8 ±1.9	197.8 ±1.0	0.20 ±0.10
105465	150.2 ±1.4	186.2±1.1	0.30 ±0.14
105466	63.6 ±2.3	211.0 ±1.0	0.41 ±0.24
105467	238.5 ±1.4	220.2 ±1.0	0.52 ±0.28
105468	112.5 ±2.1	186.6 ±1.0	0.36 ±0.10
105469	49.4 ±2.6	219.2 ±1.9	0.35 ±0.08
105470	91.0 ±1.3	247.2 ±0.7	0.22 ±0.05
105471	137 ±0.8	196.2 ±1.0	0.33 ±0.10
105472	214.7 ±2.2	277.3 ±1.2	0.48 ±0.14
105473	350.4 ±2.2	87.3 ±1.1	0.56 ±0.08

Table 2.4. Summary of depths (m) occupied by satellite-tracked surface-pelagic Kemp's ridleys. Depth values at interpolated satellite track positions were obtained from the US Coastal Relief Model (NOAA NGDC 2009).

Turtle	Mean	SD	Minimum	Maximum
105464	162.7	135.0	40.4	420.6
105465	308.0	265.2	42.6	874.4
105466	35.7	42.1	0.6	141.6
105467	1887.1	1152.0	193.2	3241.0
105468	92.1	19.0	52.4	135.0
105469	38.8	6.0	31.0	55.3
105470	81.6	75.2	19.8	247.3
105471	1066.7	1124.9	77.1	3234.6
105472	59.9	18.7	39.4	130.0
105473	43.7	3.0	38.4	51.2

Table 2.5. The occurrence of surface-pelagic drift communities (SPDC) within eastern Gulf of Mexico Landsat scenes corresponding to satellite tracks from 10 surface-pelagic juvenile Kemp's ridleys. The number of images examined and the number of images within which SPDC was observed are noted. Asterisks indicate instances of close associations between tracked turtles and SPDC.

Turtle	Days tracked	Landsat overpasses	SPDC observations
105464	37	3	3*
105465	32	0	0
105466	71	7	5
105467	34	2	1
105468	20	3	3*
105469	45	7	4*
105470	39	4	4*
105471	22	2	2
105472	43	4	3
105473	24	4	3

Figures:

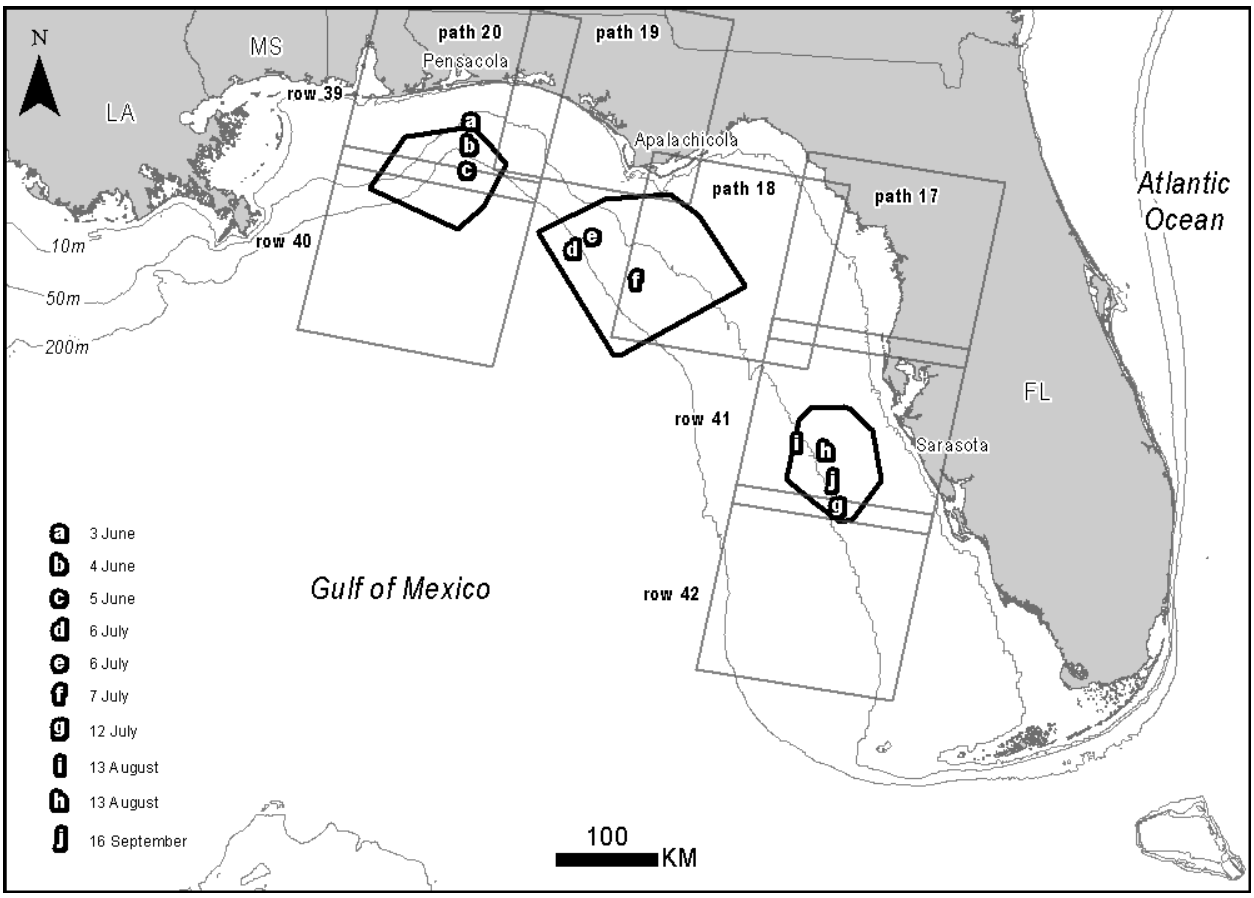

Figure 2.1. The locations where satellite-tracked surface-pelagic juvenile Kemp's ridley turtles were released within the northern and eastern Gulf of Mexico during 2011. Black polygons represent the transect survey study areas of Witherington et al. (2012) within which turtles were captured and released. Grey polygons represent the extents of Landsat 5 and 7 scenes that were available corresponding to the dates and locations of tracked turtles. Landsat paths are labeled at the top of each path and rows are labeled along the left side of each row.

Figure 2.2. A surface-pelagic juvenile Kemp's ridley bearing a 9.5 g solar-powered satellite transmitter attached with silicone adhesive. Photograph provided by Blair E. Witherington (NMFS Permit 14726-01).

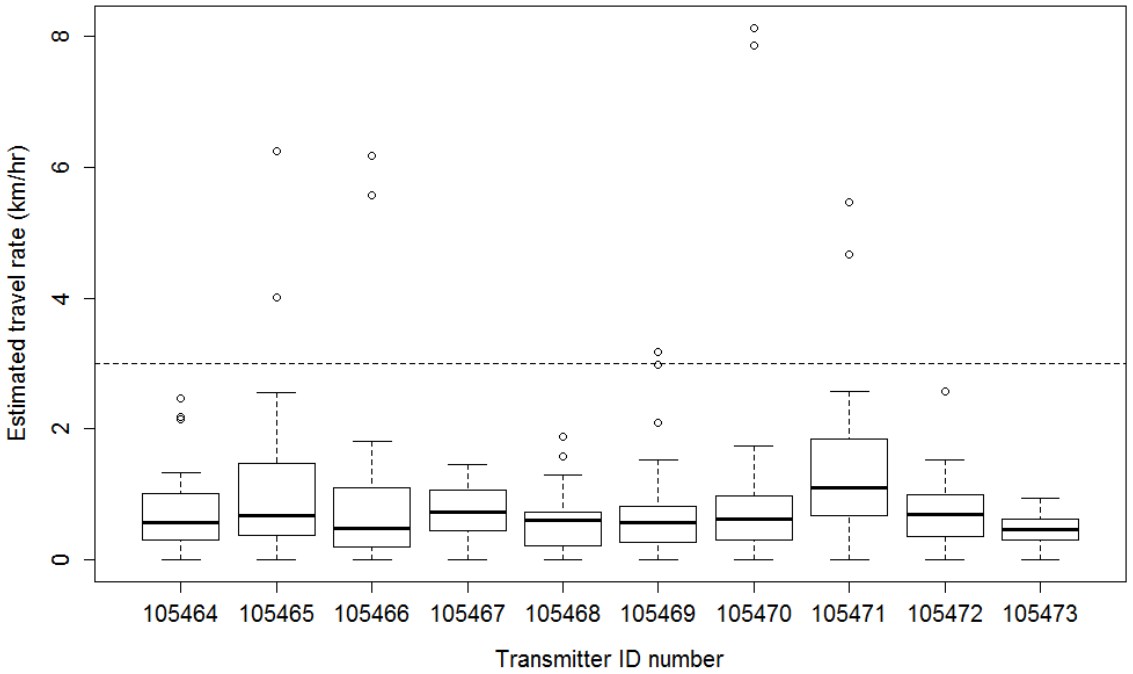

Figure 2.3. Estimated travel rates (km hr^{-1}) among mean daily Argos positions collected for each satellite-tracked Kemp's ridley. The horizontal solid line represents the value of 3 km hr^{-1} that was used within the plausibility filtering step applied by the Douglas Argos Filter (Douglas et al. 2012).

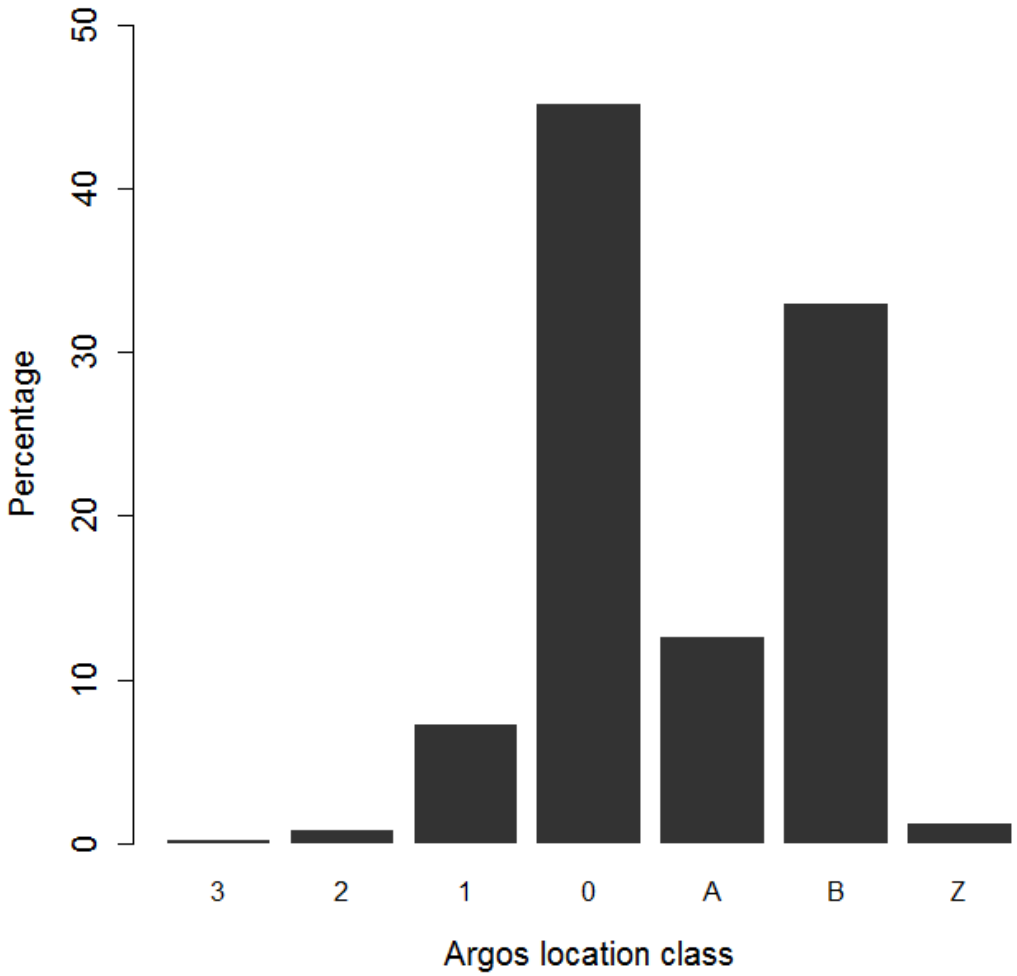

Figure 2.4. The quality of Argos locations received from satellite transmitters deployed on 10 surface-pelagic juvenile Kemp's ridleys. Location quality is expressed as the percent occurrence of each Argos location class within data received from tracked turtles. Turtles were tracked during summer and fall 2011 from locations within the northern and eastern Gulf of Mexico.

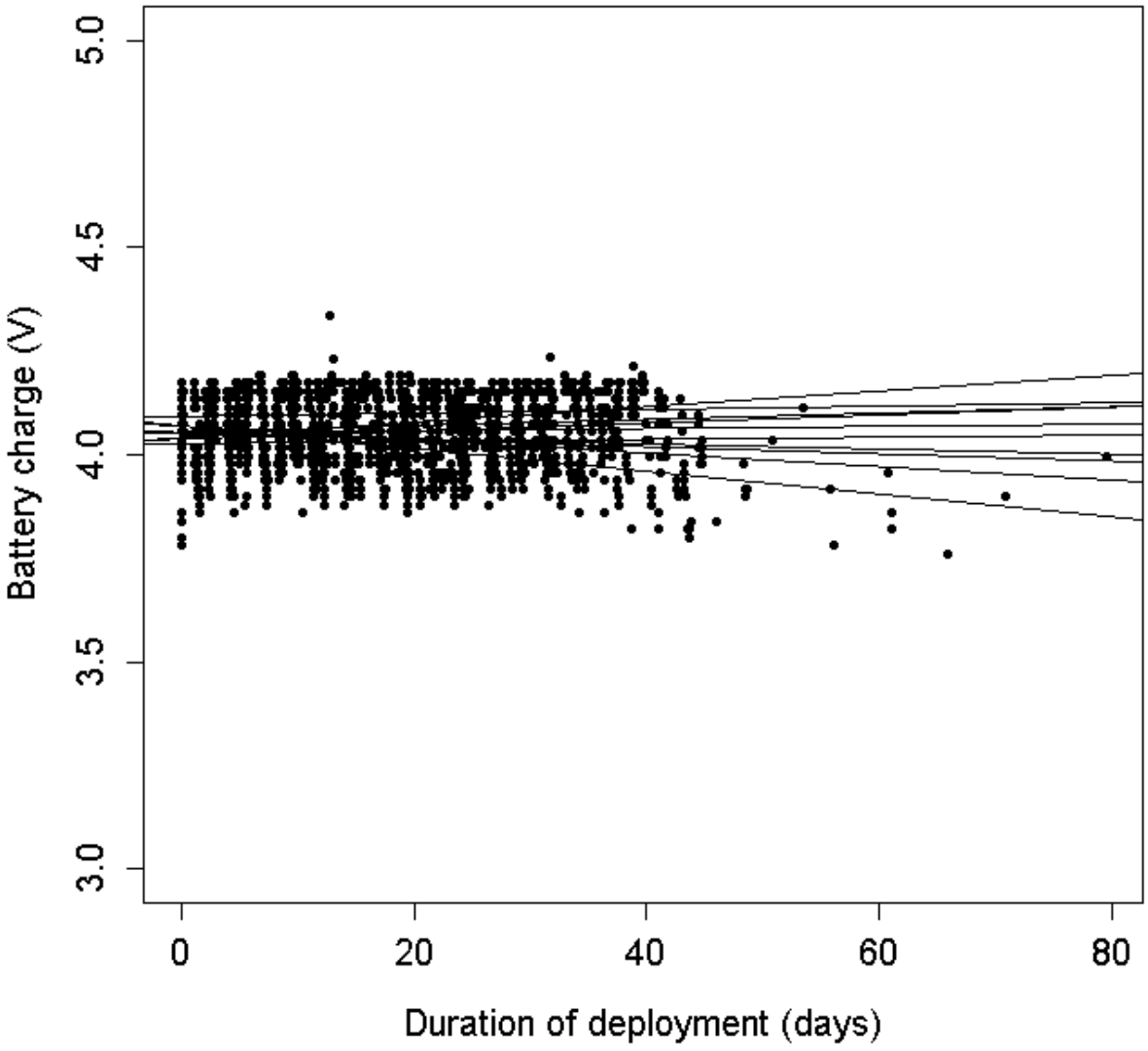

Figure 2.5. Transmitter battery voltage reported by satellite transmitters attached to 10 surface-pelagic juvenile Kemp's ridleys. Lines (1 per turtle) represent the trend battery voltage across the entire deployment. The minimum operational charge is 3.0 (manufacturer (MTI), pers. comm.).

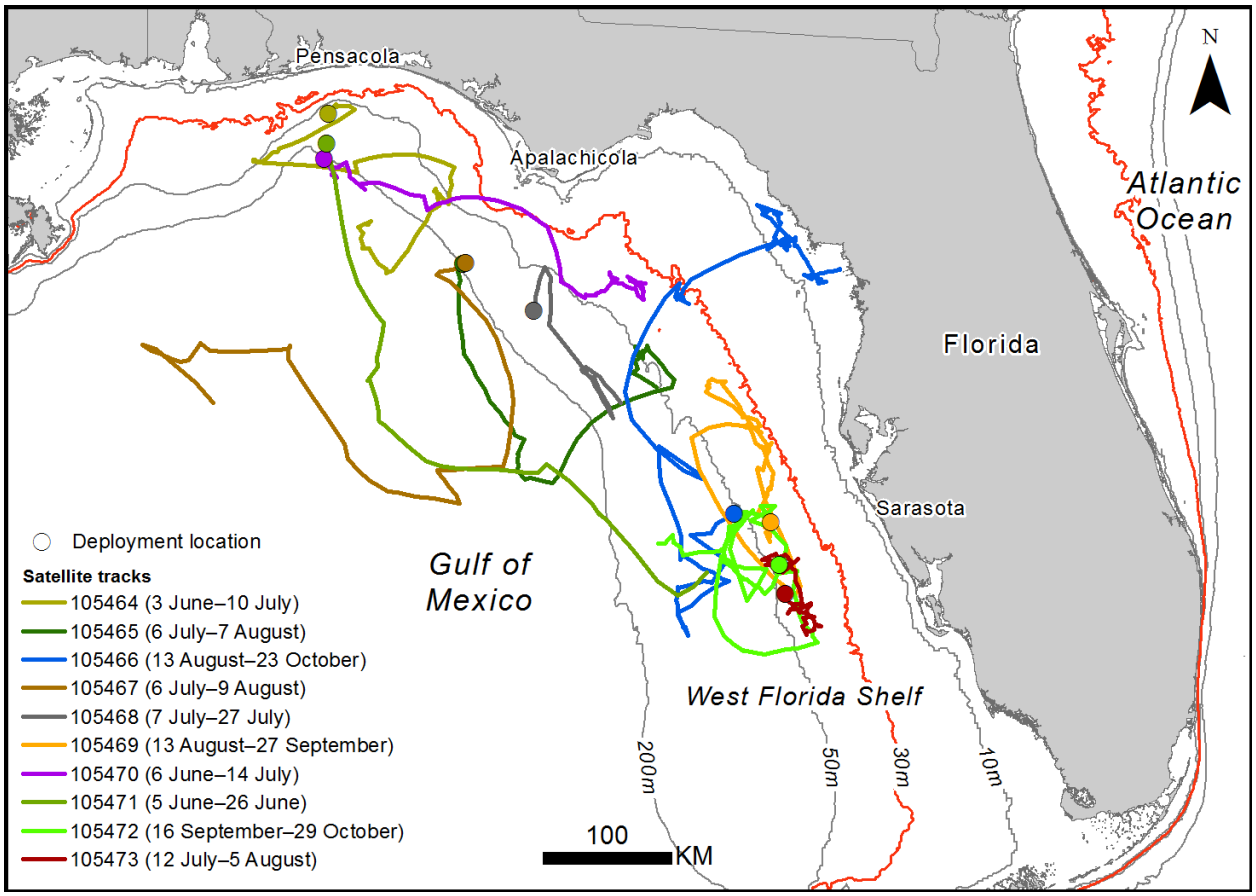

Figure 2.6. Interpolated travel paths of 10 surface-pelagic juvenile Kemp's ridley turtles that were satellite-tracked during 2011. The 30 m bathymetric contour (red line) constrained a majority of the movements made by tracked turtles.

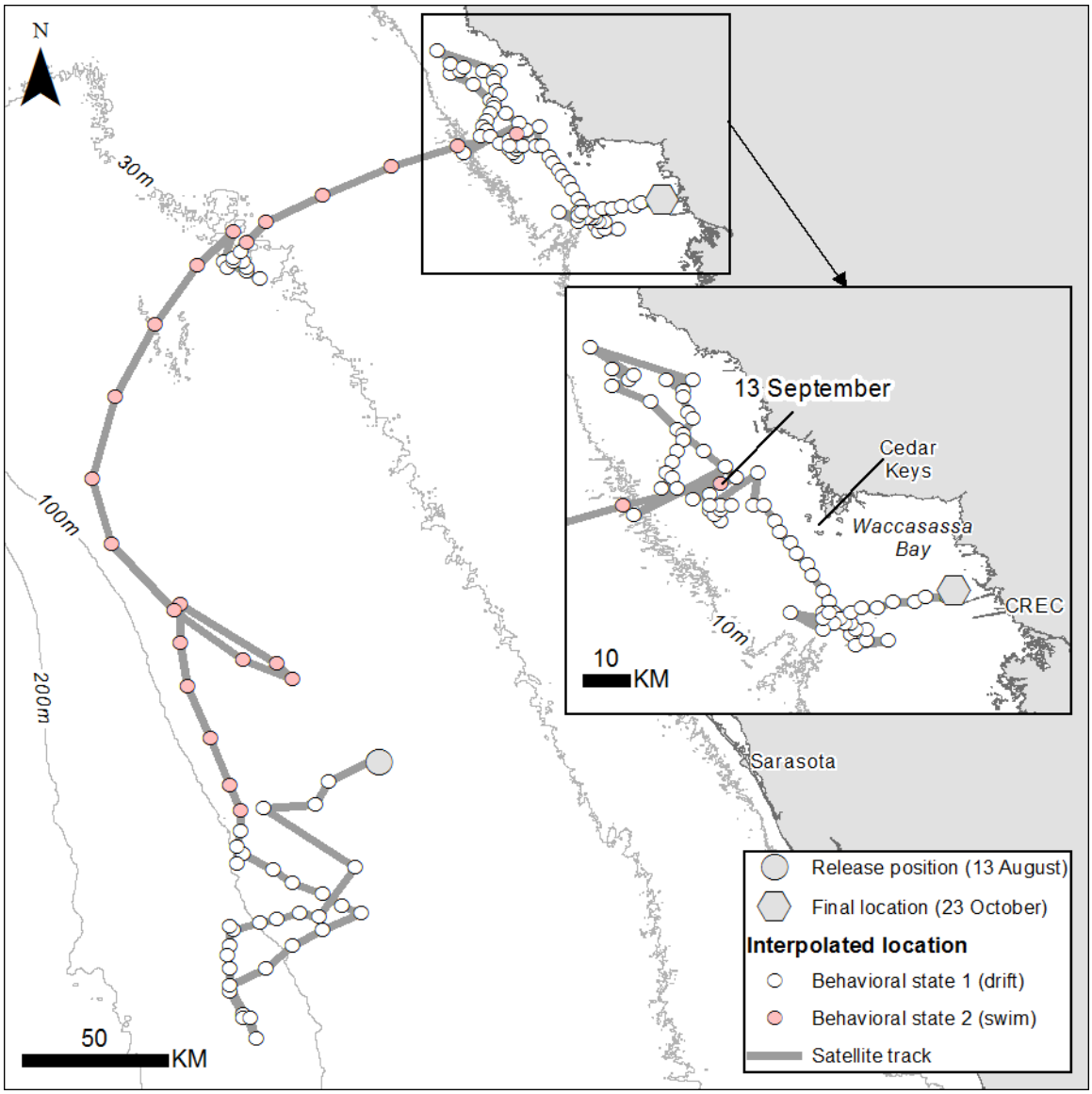

Figure 2.7. Interpolated positions and travel path for the surface-pelagic juvenile Kemp's ridley, turtle 105466. This individual was tracked from surface-pelagic drift habitats found during August 2011 west of Sarasota, Florida. This individual's tracking period ended within Waccasassa Bay (Levy County, Florida; inset). The location of the Crystal River Energy Complex (CREC) is shown within the inset map.

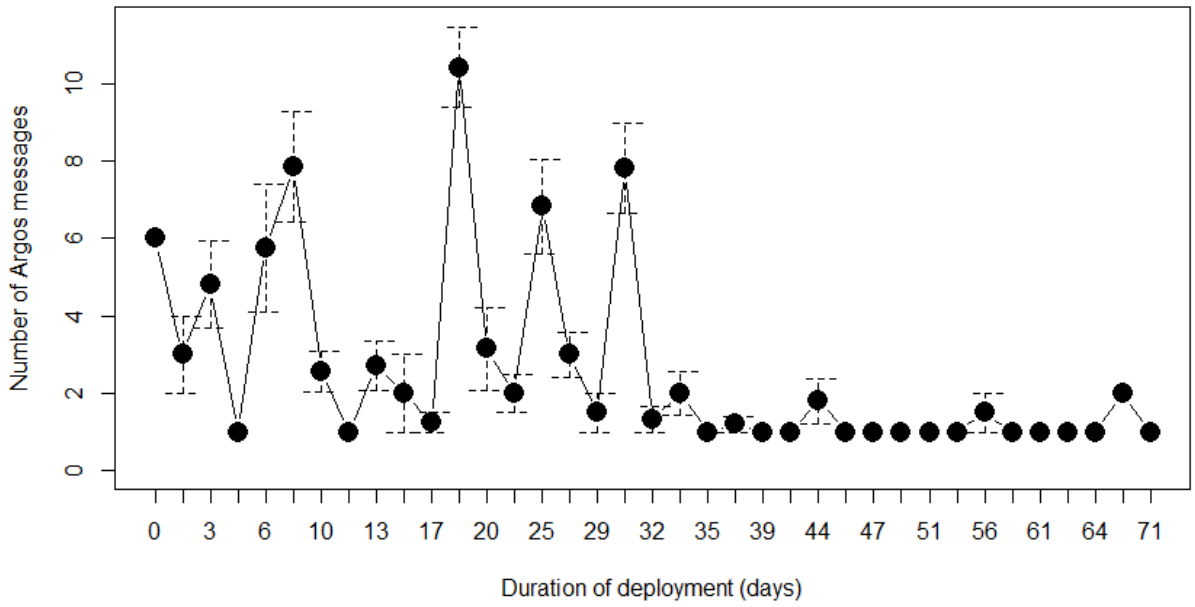

Figure 2.8. Daily mean number of Argos messages received from the transmitter affixed to turtle 105466. Bars represent the standard errors for the mean daily message counts. On 14 September 2011, 32 days post deployment, a marked decline was observed in the mean daily number of Argos messages received from this transmitter.

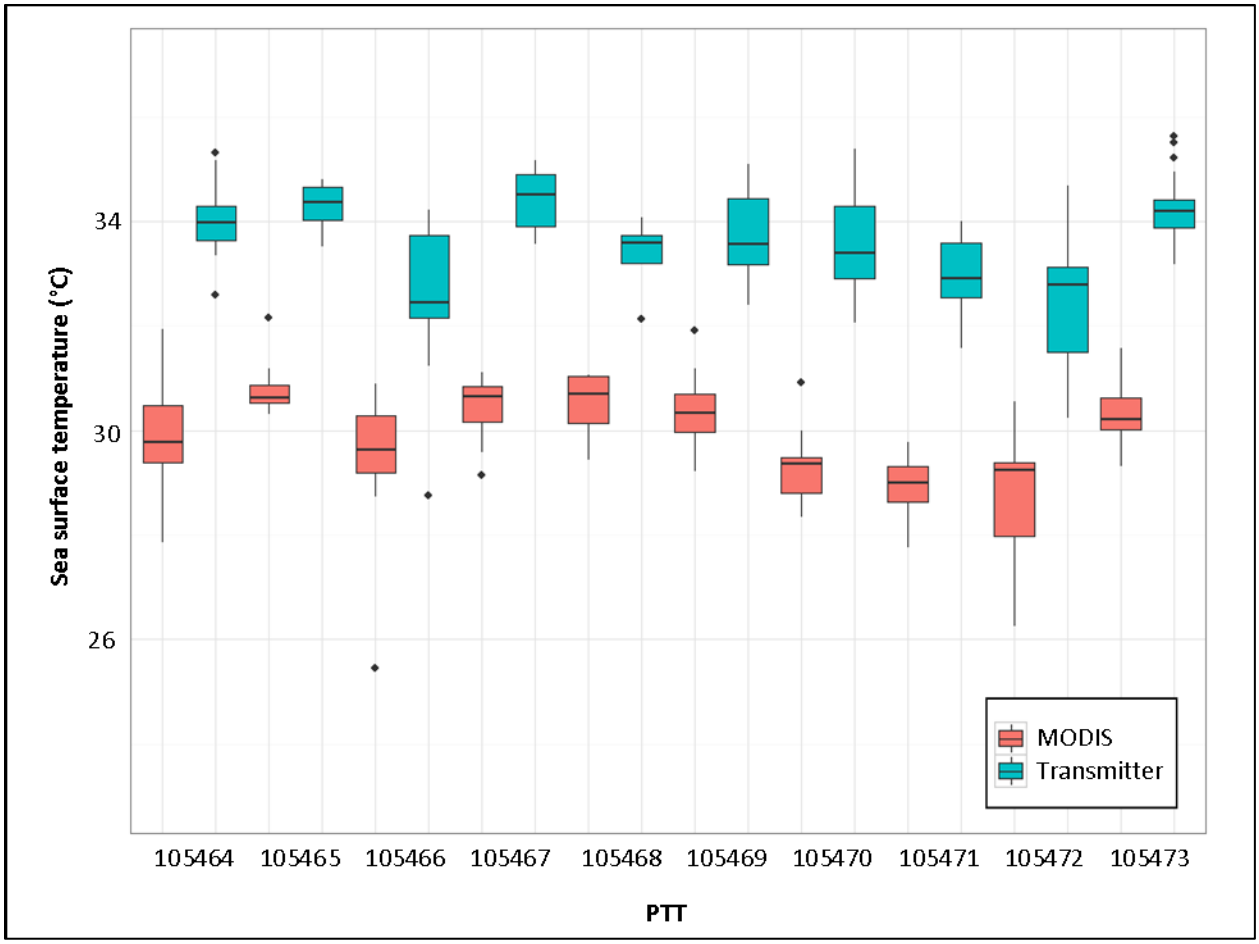

Figure 2.9. Sea surface temperature (SST) values corresponding to satellite-tracked surface-pelagic juvenile Kemp's ridleys. For each platform terminal transmitter (PTT), remotely-sensed SST (red) and the temperature reported by the transmitter's internal sensor (blue) temperature data are shown.

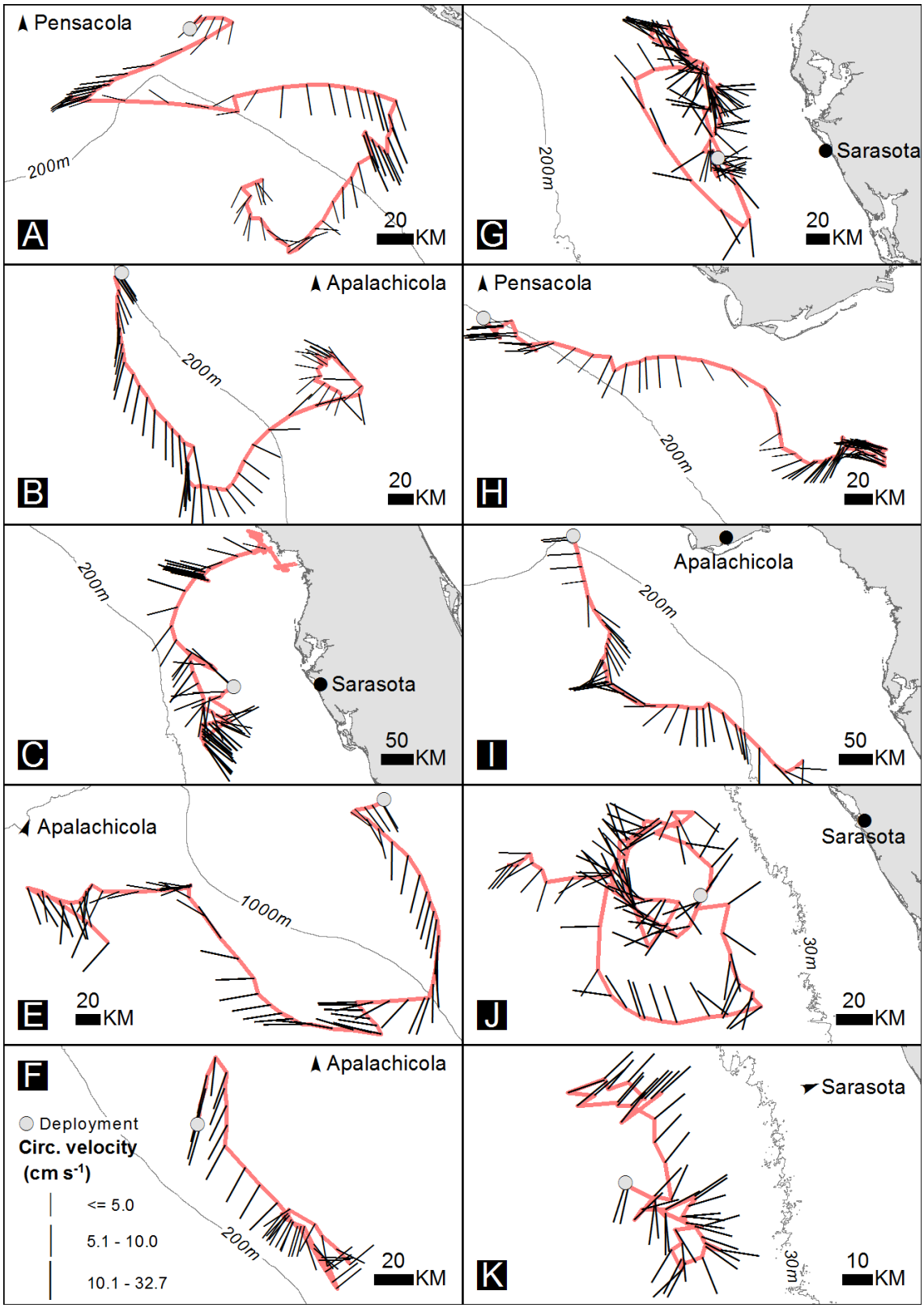

Figure 2.10. Interpolated travel paths for 10 surface-pelagic juvenile Kemp's ridleys. Vectors originating from positions along tracks represent the direction and velocity of surface currents. The ports of departure for the three study areas are labeled by points or arrows (indicating direction to the port).

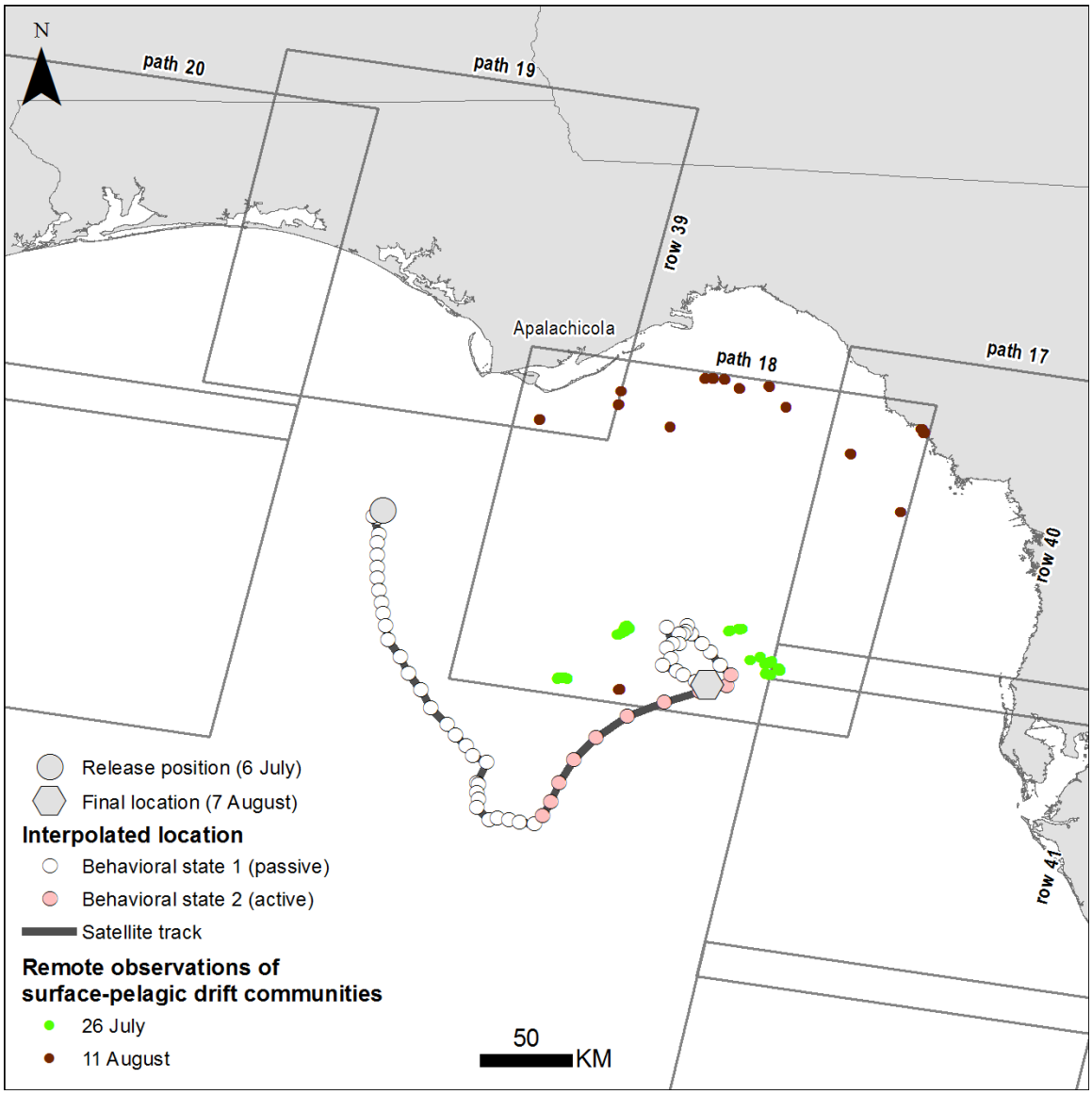

Figure 2.11. Interpolated positions and travel path for the surface-pelagic juvenile Kemp's ridley, turtle 105465. This individual was tracked from surface-pelagic drift habitats found during July 2011 within waters southwest of Apalachicola, Florida. During late July, this individual moved within Landsat path 18, row 40 within which surface-pelagic drift communities were observed during July and August 2011.

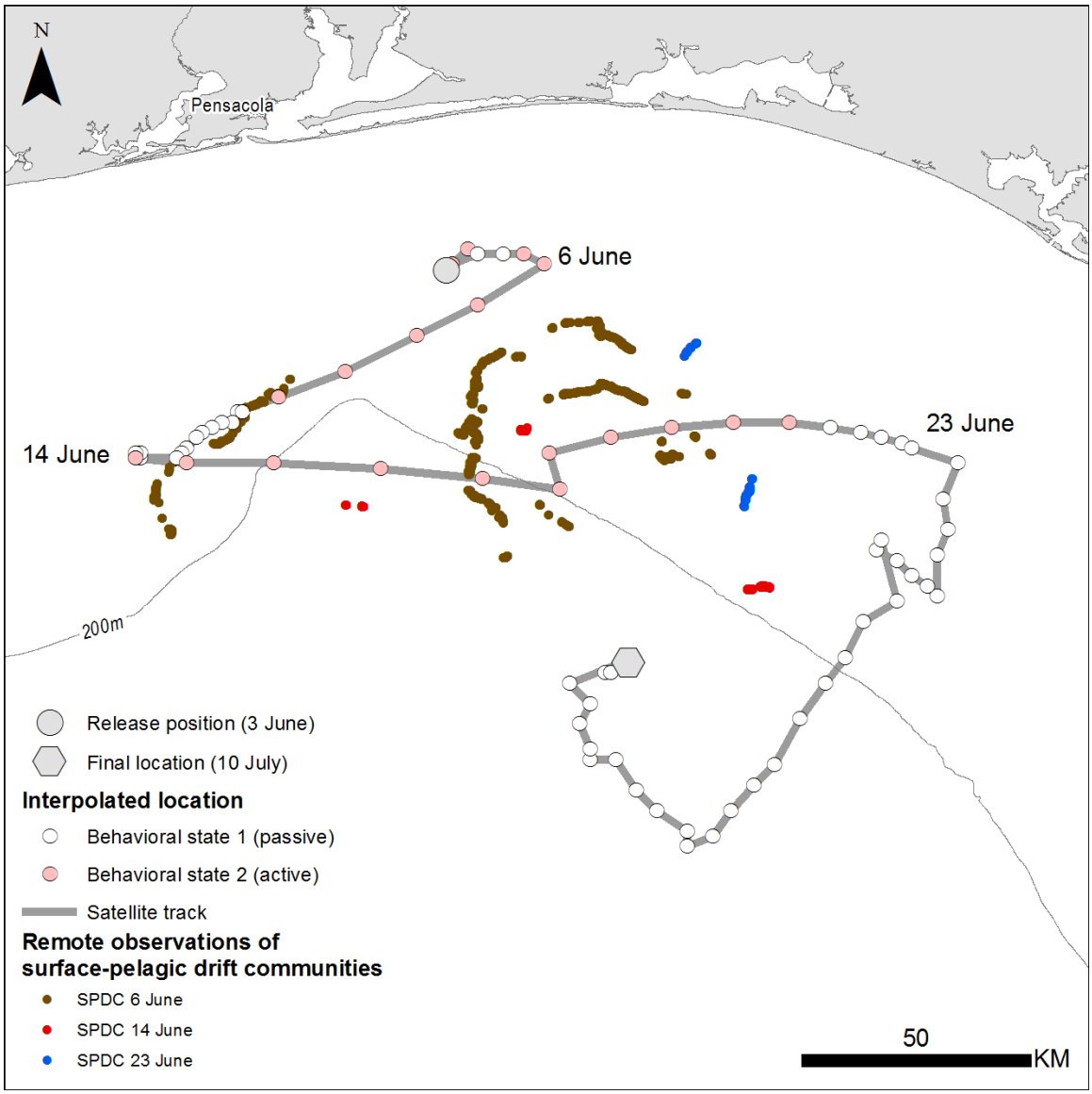

Figure 2.12. Interpolated positions and travel path for the surface-pelagic juvenile Kemp's ridley, turtle 105464. This individual was tracked from surface-pelagic drift habitats found during June 2011 within waters southeast of Pensacola, Florida. Landsat images were collected on three dates corresponding to the turtle's locations. Surface-pelagic drift communities were observed within the region on 6, 14 and 23 June 2011.

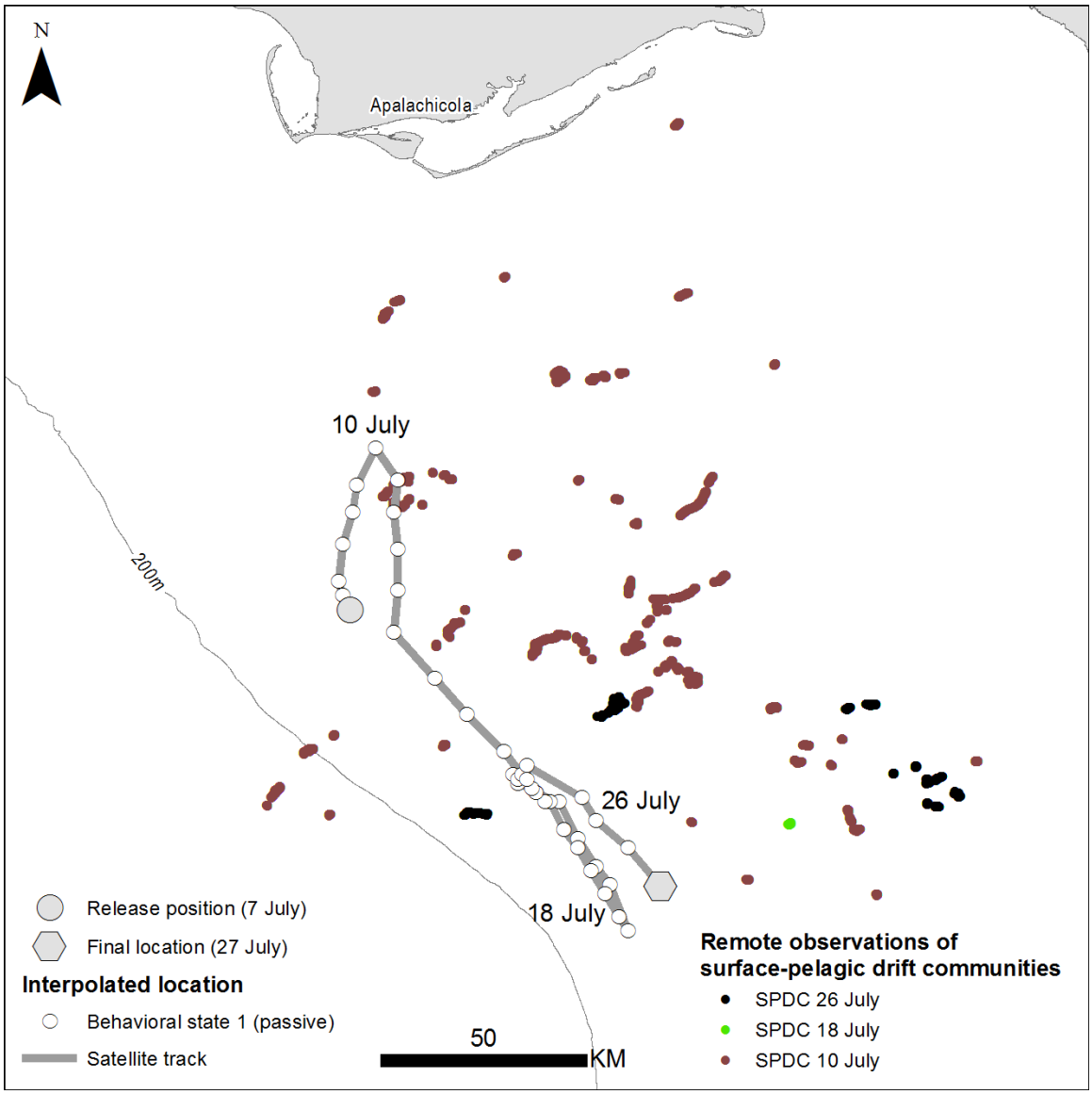

Figure 2.13. Interpolated positions and travel path for the surface-pelagic juvenile Kemp's ridley, turtle 105468. This individual was tracked from surface-pelagic drift habitats found on 7 July 2011 within waters south of Apalachicola, Florida. Landsat images were collected on three dates corresponding to the turtle's locations. Surface-pelagic drift communities (SPDC) were observed within the region on 10, 18 and 26 July 2011.

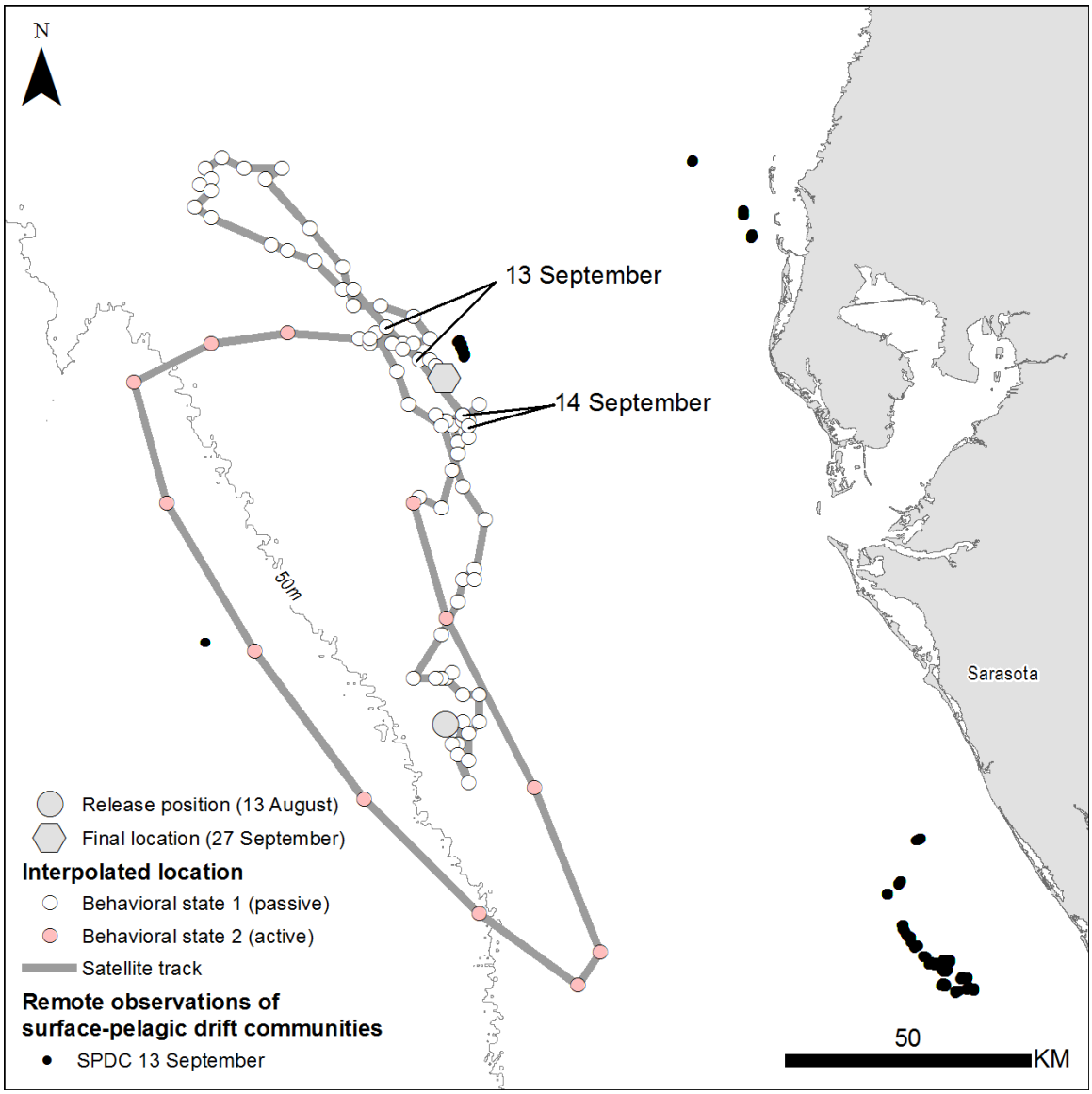

Figure 2.14. Interpolated positions and travel path for the surface-pelagic juvenile Kemp's ridley, turtle 105469. This individual was tracked from surface-pelagic drift habitats found on 13 August 2011 within waters west of Sarasota, Florida. Landsat images were collected on four dates corresponding to the turtle's locations. Surface-pelagic drift communities (SPDC) were close to the path of turtle 105469 on 13 September 2011.

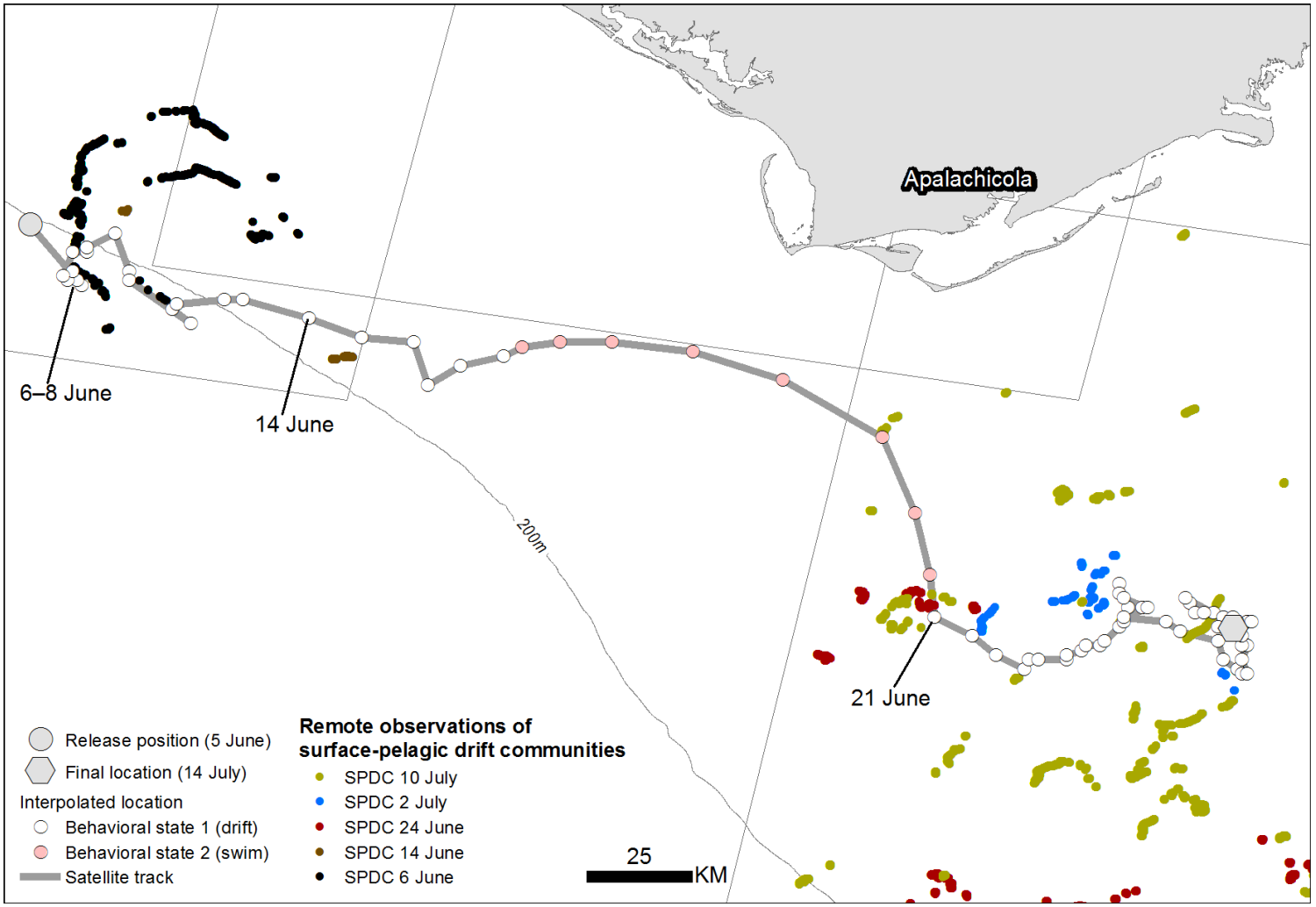

Figure 2.15. Interpolated positions and travel path for the surface-pelagic juvenile Kemp's ridley, turtle 105470. This individual was tracked from a surface-pelagic drift community (SPDC) found during June 2011 within waters southeast of Pensacola, Florida. Landsat images were collected on five dates corresponding to the turtle's locations and SPDC was found within all images. The extents of Landsat scenes are represented by the boxes. This individual was within Landsat path 20, row 39 from 5–14 June. After 14 June, the turtle traveled eastward through an area not imaged by Landsat satellites during June 2011. The turtle spent final portion of the tracking period within path 18, row 40, which was imaged on three days corresponding to the turtle's path.

CHAPTER THREE:

ASSESSMENT OF SURFACE-PELAGIC DRIFT COMMUNITIES WITHIN THE NORTHERN GULF OF MEXICO USING LANDSAT OBSERVATIONS COLLECTED FROM 2009–2011

1. Abstract

Surface-pelagic drift communities (SPDC) are an important habitat for many marine organisms; for example, SPDC has been identified as critical to the survival of loggerhead turtles. The surface-pelagic juvenile life stages of three other sea turtles have been found within Gulf of Mexico SPDC, including the critically endangered Kemp's ridley. Thus, understanding the regional patterns of SPDC is crucial to conservation management efforts for these species. SPDC is highly dynamic, both spatially and temporally, making it difficult to assess its abundance using traditional ship surveys. Remote sensing techniques have been shown effective in such assessments. The present study examined 30 m resolution Landsat imagery collected from 2009–2011 (1,202 images), representing approximately 750,000 km^2 of northern and eastern Gulf of Mexico waters. The abundance of SPDC peaked during late spring and early summer across the region. Seasonal SPDC peaks occurred earlier in the year within the western Gulf of Mexico, typically during May and June. The abundance of SPDC peaked during July and August within the eastern Gulf of Mexico. Western Gulf of Mexico waters had significantly higher amounts of SPDC than waters east of the Mississippi River Delta. The regional differences in abundance and seasonality support the hypothesis that the western Gulf of Mexico is a source region for SPDC. Assessments of SDPC using Landsat imagery after 2011 may be useful in evaluating the impacts of major anthropogenic disturbances, such as the Deepwater Horizon oil spill.

2. Introduction

The distribution and origins of drifting *Sargassum* macroalgae within the North Atlantic Ocean have been of interest to sailors since Columbus' transit to the Americas (Butler et al. 1983). Early research focused on identifying the boundaries of the region within which accumulations of drifting *Sargassum* were most frequently encountered. Butler et al. (1983) provided a review of the mapping efforts that led to the delineation of the Sargasso Sea within the North Atlantic Gyre. Bounded by major surface currents, rather than shorelines, the extent of the Sargasso Sea is dynamic. Efforts to refine the Sargasso Sea's boundaries have continued, buoyed by findings of ecological and marine pollution research (Fine 1970; Butler et al. 1983). The distribution of *Sargassum* now has geopolitical relevance with the formation of the multinational Sargasso Sea Alliance and the United States' declaration of *Sargassum* as critical developmental habitat for the threatened loggerhead turtle (Caretta caretta; Laffoley et al. 2011; NMFS 2014).

Accumulations of *Sargassum* within the open ocean, surface-pelagic drift communities (SPDC; Witherington et al. 2012) are now known to be indicators of a distinct marine ecosystem (Fine 1970). Associates of SPDC range from invertebrates to top predators, including fish and seabirds (Coston-Clements et al. 1991; Haney 1986). Other vertebrates may only use SPDC during specific developmental phases. SPDC provides developmental habitat for the larval forms of several fishes and sea turtles (Dooley 1972; Witherington et al. 2012). Given the ecological significance of SPDC, knowledge of the distribution, abundance, and seasonality of SPDC is crucial to understanding the biogeography of many marine species.

Parr (1939) provided the first quantitative assessments of the relative abundance and distribution of *Sargassum* within the North Atlantic, Caribbean, and Gulf of Mexico. Parr's estimates were based on neuston net tows conducted along transects throughout the region. Following Parr's estimates (1939), ship-based *Sargassum* surveys continued and were reviewed by Butler et al. (1983).

Quantitative shore-based surveys of *Sargassum* have also been conducted in an attempt to describe seasonal and interannual variability in abundance (Butler et al. 1983).

Recent advances in optical remote sensing have provided the tools necessary to conduct synoptic assessments of *Sargassum.* Gower et al. (2006) demonstrated that moderate-resolution satellite imagery could be used to detect and quantify *Sargassum* at the ocean basin scale. This work led to the identification of *Sargassum* bloom events and potential source regions within the North Atlantic (Gower and King 2011; Gower et al. 2013). Hu (2009) developed an optical method for detecting *Sargassum* using higher resolution Landsat satellite imagery. Using this method, detailed assessments of *Sargassum* are now possible and can be directly related to *in situ* observations of SPDC (Witherington et al. 2012; Ch. 1, present volume). The detailed mapping approach has proven essential when mapping *Sargassum* as habitat (i.e., SPDC) within regions where its abundance is low but its ecological value is high (Ch. 1, present volume).

Within the eastern Gulf of Mexico, SPDC is present year-round and serves as critical developmental habitat for four sea turtle species (Witherington et al. 2012; Ch. 1, present volume). Despite its year-round presence, SPDC within the eastern Gulf of Mexico is rarely perceptible within moderate resolution (e.g., 250 m–1 km) remotely-sensed imagery (Gower and King 2011). Broad scale mapping of SPDC has provided an unprecedented review of the distribution and potential source regions of SPDC within the North Atlantic (Gower et al. 2013); though, two recent conservation issues within the Gulf of Mexico have highlighted the need for multi-scale assessments of SPDC: (1) The Deepwater Horizon oil spill during 2010 and (2) the designation of *Sargassum* as critical developmental habitat for loggerhead turtles (NMFS 2014). The impacts of oil spills cannot be adequately assessed without knowledge of the dynamics of the ecosystems, species, and life-stages that would be affected (Lubchenco et al. 2012). Similarly, delineations of habitats critical to the survival of a species must also integrate detailed species occurrence and habitat information. Considering that protected species

conservation regulations are based on the occurrence of SPDC, it is imperative that mapping approaches are conducted at multiple spatial scales.

The present study examined the distribution and abundance of SPDC within the northern and eastern Gulf of Mexico using 30 m resolution Landsat satellite imagery. The objective was to describe the distribution and seasonality of SPDC within the region during 2009–2011. The time period and study area overlap with the Deepwater Horizon oil spill, which occurred in April 2010. Results are placed in the context of a previous assessment of SPDC and surface-pelagic juvenile turtles within the eastern Gulf of Mexico (Ch. 1, present volume).

3. Methods

The northern Gulf of Mexico study area was determined based on the availability of Landsat imagery collected from 2009–2011 (Fig. 3.1). Imagery from Landsat 5 Thematic Mapper (TM) and Landsat 7 Enhanced Thematic Mapper Plus (ETM+) were used in the present study. Both TM and ETM+ sensors collect reflectance data at 660, 825, and 1650 nm (bands 3, 4 and 5; respectively). The spatial resolution of Landsat imagery is 30 m. Each Landsat scene is approximately 180 km (length) by 185 km (width). Landsat scenes are arranged into paths (vertical) and rows (horizontal). Landsat scenes are referred to based on their unique path and row position and are abbreviated as p##r## (scenes are labeled in Fig. 3.1). The temporal resolution of each Landsat satellite is 16 days; combined, Landsat 5 and 7 provide 8-day temporal resolution. I obtained Landsat 5 and 7 from the US Geological Survey's Global Visualization Viewer (Glovis; http://glovis.usgs.gov/). I selected a minimum of one image per month for analysis. Using Glovis, I selected relatively cloud-free imagery for analysis (i.e., images within which a majority of sea surface waters appeared visible).

Image processing involved several steps. Atmospheric correction was applied to the raw reflectance data using a customized set of IDL routines (Hu et al. 2004; Exelis Visual Information Solutions, Boulder,

CO). Next, I calculated the FAI using the corrected reflectance data from bands 3, 4, and 5 (Hu 2009). I searched output FAI images and co-registered RGB images for SPDC within ENVI (Exelis Visual Information Solutions, Boulder, CO). Using ENVI, I digitized SPDC and recorded the pixel counts in a Microsoft Access database. I converted the SPDC pixels to vectors (shapefiles) and recorded those as feature classes within an ArcGIS geodatabase (Esri, Redlands, CA). Using ArcGIS, I calculated the density of SPDC at a spatial scale suitable for regional visualization (within a 1.5 km search radius of 500 m cells). I standardized estimates of SPDC across scenes by calculating the extent of "searchable waters" for each Landsat scene using a customized set of Python and R routines (R Core Team 2013). I defined searchable waters as the extent of the image with a clear view of surface ocean waters; i.e., land masses, vessels, thick clouds and scan line corrector failures (present only in Landsat 7 ETM+ imagery) were excluded (Ch. 1, Fig. 1.3, present volume). For each image, I calculated a scaled density of SPDC as follows: SPDC coverage ‰ = (SPDC pixels / searchable water pixels) * 1000.

I extracted wind velocity values for the dates and locations corresponding to each image using the RNCEP package written for the program R (Kemp et al. 2012). The RNCEP package provided wind velocity values from the global NCEP/NCAR Reanalysis 2 dataset (Kanamitsu et al. 2002). Using ArcGIS, I excluded land from the scene footprint polygons prior to estimating a geographically central location for each Landsat scene. Zonal and meridional wind velocity values were extracted at the scene's center location for days corresponding to image collections. Within R, I converted zonal and meridional velocity values to wind speed and direction. I examined the correlation between wind velocity and the amount of observed SPDC using Pearson's product-moment correlation test. I also compared mean wind velocities for scenes when SPDC was and was not observed using a two sample t-test.

4. Results

Across the northern Gulf of Mexico, 1,202 Landsat images, collected from 29 scenes were examined for the presence of SPDC. During the three-year period, a mean of 41 images were available for each scene — approximately 1 per month. SPDC was found in approximately 74% of images (Table 3.1). The mean coverage of SPDC was highest within the following scenes: p25r41, p25r40, and p18r39 (Table 3.1). The highest amounts of SPDC were found within the western Gulf of Mexico paths (p22–p26; Table 3.2). The mean area of SPDC across all Landsat images was 5.64 km^2 (±22.78 SD; range = 0–390.10; Table 3.2). The mean area of SPDC was highest within p25r41 (38.45 km^2) and p25r40 (25.51 km^2).

The amounts of SPDC fluctuated annually and monthly. SPDC was most abundant within the northern Gulf of Mexico during 2011 (9.20 km^2 per image) followed by 2009 (4.59 km^2). During 2010, the overall area of SPDC within the northern Gulf of Mexico was 3.65 km^2 per image, the lowest of the three-year period. The area of SPDC peaked during June and a second peak occurred during November (Fig. 3.2).

The monthly peaks in abundance of SPDC varied spatially. Within the southeastern most portion of the study area, paths 16 and 17, the abundance of SPDC peaked during August (Fig. 3.3 E, F). SPDC peaked during July or August within the central portions of the West Florida Shelf (Fig. 3.3 C, D, E). SPDC peaked during June and July within the northeastern Gulf, offshore of the Florida Panhandle (Fig. 3.3 B). SPDC peaked during June within most of the northern Gulf waters offshore of Louisiana (Fig. 3.3 A; Fig. 3.4 C, D). The area of SPDC typically peaked during May and June within waters offshore of eastern Texas. SPDC also peaked outside of the spring and summer time periods. A peak occurred during November 2009 within paths 21 and 22, near the Mississippi River Delta (Fig. 3.3 A; Fig. 3.4 E) and within path 25 offshore of Galveston Bay (Fig. 3.4 B). In the eastern Gulf of Mexico, an SPDC peak occurred during February 2011, primarily within paths 17 and 16 (Fig. 3.3 D, E). This spatial pattern in monthly

peaks is interpreted across the study area within Fig. 3.5. SPDC peaked during January 2011 along the Texas coastline, within path 26 (Fig. 3.4 A).

The density of SPDC increased west of 89° W longitude, near the Mississippi River Delta (Fig. 3.6). The boundary at 89° W longitude roughly coincides with the division between Landsat p21r40 and p22r40 (Fig. 3.1). The mean area of SPDC per image was significantly higher west of this location, when all scenes west and east of this location were grouped and compared ($t = 4.55$, $p < 0.01$). The mean area of SPDC detected within scenes from paths 22–26 was 19.52 km^2. The mean area of SPDC detected within eastern Gulf of Mexico scenes (paths 16–21) was 2.91 km^2. The continental shelf waters off of Louisiana and eastern Texas had higher concentrations of SPDC. Within this region, SPDC was least abundant within the shallowest continental shelf waters (< 10 m). This differs from much of the northeastern Gulf of Mexico where SPDC appeared most abundant inshore of the 10 m bathymetric contour (Fig. 3.6). In addition to a change in density, the waters near the Mississippi River Delta appeared to be an area where the timing of monthly SPDC abundance peaks shift. This division is used hereafter to separate the western and eastern portions of the Gulf of Mexico study area. SPDC peaks occurred within the western Gulf of Mexico during April–June each year (Fig. 3.7 A). Within the eastern Gulf of Mexico, SPDC abundance peaks occurred during July–August of 2009 and 2011, but not during 2010 (Fig. 3.7 B).

Wind speeds were significantly lower when SPDC was detected than when SPDC was not detected ($t = 4.04$, $p < 0.01$, Fig. 3.8). The mean wind speed was 5.42 m s^{-1} (±2.82 SD, n = 318 images) when no SPDC was detected. The mean wind speed was 4.68 m s^{-1} (±2.75 SD, n = 884 images) corresponding to images in which SPDC was detected. The maximum wind speed recorded for an image when SPDC was present was 13.3 m s^{-1} (1 m s^{-1} = 1.9 knots). Within images where SPDC was not found, wind speeds ranged from < 1–14.2 m s^{-1}. Within most Landsat scenes, the area of SPDC detected decreased as wind speeds increased (Fig. 3.10). High amounts of SPDC were found within some western Gulf of Mexico

scenes at wind speeds > 8 m s^{-1}. Across all images, the relationship between the area (km^2) of SPDC observed and wind speed was not significant (r = -0.05, p = 0.08).

5. Discussion

This study provides the first detailed assessment of SPDC that focused on the northern and eastern Gulf of Mexico. SPDC was most abundant and widespread within northern Gulf waters west of the Mississippi River Delta. High amounts of SPDC were distributed throughout the western portion of the study area except for the shallow waters offshore of Louisiana. Conversely, within the eastern Gulf of Mexico, high concentrations of SPDC were found within nearshore waters off of the northern Florida peninsula. Nearshore circulation may explain these SPDC density patterns. Countercurrents flow northward along the Florida peninsula and westward along the Louisiana coastline. Throughout the northern Gulf of Mexico, the amount of SPDC was greatest during late spring and summer. The SPDC distributional patterns and seasonality generally agreed with the findings of another assessment of SPDC that included the northern Gulf of Mexico, conducted by Gower and King (2011).

During 2009 and 2011, the SPDC abundance peaks within the western Gulf appeared to precede or coincide with abundance peaks within the eastern Gulf (Fig. 3.7). This suggests that a general eastward drift of SPDC may occur within the northern Gulf of Mexico. This finding is consistent with those of Gower and King (2011) who proposed that SPDC forming within the northwestern Gulf may drift eastward during summer months. A similar eastward drift pattern has been proposed for surface-pelagic juvenile Kemp's ridley turtles (Collard and Ogren 1990). An eastern Gulf SPDC abundance peak was not detected during 2010 despite the apparent abundance of SPDC within the western Gulf during June–August 2010. The Deepwater Horizon oil spill impacted northern Gulf of Mexico surface waters from April–August 2010 (Fig. 3.9). Based on the location and timing of the event, it is possible that eastward drifting SPDC became entrained within the spill area and did not arrive within eastern Gulf

waters (Powers et al. 2013). It should be noted that the presence of oil within surface waters of some Landsat images prevented those images from being fully examined for the presence of SPDC. The methods of the present study did not allow for effective discrimination between oil and SPDC. The spill principally affected analyses of imagery collected within paths 20 and 21 during May–July 2010. If SPDC peaks occurred during July and August 2010 within the eastern Gulf, as they have during other years (Fig. 3.3; Ch. 1, this volume), they should have been detected.

The abundance of SPDC was lowest in most areas during winter and early spring, particularly December and January (Fig. 3.2). The timing of peaks in SPDC abundance varied across years within some regions. For example, SPDC abundance peaked during November 2009 in three Landsat paths: paths 21 and 22, near the Mississippi River Delta; and within path 25, off of Galveston Bay, Texas. These peaks followed a period during which record rainfall was recorded for portions of eastern Texas, Louisiana and Mississippi that lie upstream of these northern Gulf waters (NOAA NCDC 2011). Perhaps this unusual rainfall event led to an influx of nutrients into these regions that fueled the growth of *Sargassum*. This observation is consistent with the findings of Lapointe et al. (2014) who suggested that new production of *Sargassum* may occur within nutrient-rich waters of northern Gulf of Mexico. Similarly, Gower et al. (2013) noted that 2011 was a period when SPDC was abundant throughout the North Atlantic, particularly within the Caribbean and equatorial regions. They suggested that the La Niña-associated rainfall anomaly may have contributed to nutrient runoff and subsequent *Sargassum* blooms. The late spring and early summer of 2011 was also a period when SPDC was highest within the northern Gulf of Mexico regions examined by the present study (Fig. 3.7).

The present study identified late spring and summer periods of peak SPDC abundance and an eastward shift in the timing of peak SPDC abundance. These findings are consistent with those of the broader assessment conducted by Gower and King (2011). It should be noted that considerable variability existed in the timing of peak SPDC abundance for some regions. For example, SPDC peaked

during June within paths 20, 21, 23 and 24, while SPDC peaked during August within path 22 (Fig. 3.3 A, B; Fig. 3.4 C–E). A selection of only 1–2 images per month was necessary to complete the present assessment due to the intense processing time associated with this effort. Considering the observed dissipative effects of winds, the infrequent sampling strategy likely contributed to the observed variation in seasonality.

The SPDC distribution and abundance estimates presented herein could be refined by addressing the potential for over- and under-estimates of SPDC that are inherent within the methods. Landsat imagery was collected as the satellites descended along paths. Image data were divided into scenes of equal length. A portion of the northern and southern extents of the scenes overlap (approximately 20%). Thus, opportunity for double-counting SPDC existed if it was detected within adjacent scenes on the same day and within the region of overlap. However, imagery used in the present study was typically limited to one or two nearshore scenes and most overlapped with no or one additional scene (Fig. 3.1). An exception occurred during the summer of 2010 when more imagery was made available for offshore scenes. Increased coverage of marine regions is provided by the new Landsat 8 satellite, launched during February 2013. The increased availability of overlapping scenes will means similar mapping efforts will need to account for image overlap. A method to account for this overlap was developed and evaluated as part of the present study. Similarly, the eastern and western edges of Landsat paths overlap. When using all data from Landsat 5 and 7, or Landsat 7 and 8, it is possible to obtain partially overlapping imagery collected 24 hours later. This was minimal in the present study, which used 1–2 images per month. Underestimation of SPDC is also possible. The present study detected SPDC within the eastern Gulf of Mexico where moderate resolution remote sensing methods have not proven reliable for SPDC detection. This difference was most likely due to the spatial resolution of the methods and suggests that the present methods may have missed SPDC that was not detectable within 900 m^2 Landsat pixels. Validation using *in situ* surveys and high-resolution imagery (e.g., 1 m) are needed to

identify minimum mapping units for SPDC and to provide correction factors for existing data. Field studies are also needed to determine the extent to which western Gulf of Mexico SPDC serves as habitat for surface-pelagic juvenile sea turtles. Such efforts are underway, expanding the work of Witherington et al. (2012) to regions considered by the present study.

The moderate resolution methods employed by Gower and King (2011) are ideal for conducting a broad-scale assessment of SPDC. The higher resolution approach of the present study is most appropriate for describing localized patterns of abundance. Both methods have a role in identifying SPDC, and both should be considered when developing conservation strategies or assessing anthropogenic impacts to this marine ecosystem.

Mapping efforts alone cannot serve as the sole source of information for conservation management actions focused on SPDC. The ecological role of SPDC should be addressed within distinct regions. For example, eastern Gulf of Mexico SPDC is established as developmental habitat for early juvenile sea turtles (Witherington et al. 2012). The western and eastern Gulf of Mexico appeared to differ in the abundance and distributional patterns of SPDC. Given the marked change in SPDC density, the density of surface-pelagic juveniles in waters within Gulf waters west of the Mississippi River Delta should also be examined. Conducting in-situ surveys would also provide an opportunity to validate remotely-sensed estimates of SPDC. Ship-based observations, potentially coupled with higher resolution imagery (from satellite or aerial platforms), would serve to correct SPDC estimates made by Landsat or other remote sensing methods.

5.1 Conclusions

SPDC was present year-round throughout the northern Gulf of Mexico. The abundance and distribution of SPDC differed significantly between the eastern and western portions of the northern Gulf of Mexico. SPDC abundance peaked during late spring and summer. In addition to high

concentrations of SPDC in the western Gulf of Mexico, seasonal peaks in SPDC abundance occurred later in the year within the eastern Gulf of Mexico. Eastern Gulf of Mexico SPDC appears to provide critical habitat for surface-pelagic juvenile sea turtles (Witherington et al. 2012; Ch. 1, present volume). Additional study is necessary to determine if the western Gulf of Mexico, where SPDC is more abundant, also serves as habitat for surface-pelagic juvenile sea turtles. The patterns of SPDC distribution presented herein could advise the locations of focused, in-situ efforts where surface-pelagic habitat and juvenile sea turtles could be monitored.

Literature Cited:

Butler, J.N., B.F. Morris, J. Cadwallader, and A.W. Stoner. 1983. Studies of *Sargassum* and the *Sargassum* community. Special Publication No. 22. Bermuda Biological Station for Research.

Collard, S. B., and L. H. Ogren. 1990. Dispersal scenarios for pelagic post-hatchling sea turtles. Bulletin of Marine Science 47:233–243.

Coston-Clements, L., L. R. Settle, D. E. Hoss, and F. A. Cross. 1991. Utilization of the *Sargassum* habitat by marine invertebrates and vertebrates - A review. US Department of Commerce, NOAA Technical Memorandum NMFS-SEFSC-296, 32 pp.

Dooley, J. K. 1972. Fishes associated with the pelagic *Sargassum* complex, with a discussion of the *Sargassum* community. Contributions in Marine Science 16:1–32.

Gower, J., C. Hu, G. Borstad, and S. King. 2006. Ocean color satellites show extensive lines of floating *Sargassum* in the Gulf of Mexico. IEEE Transactions on Geoscience and Remote Sensing 44:3619–3625.

Gower, J. F. R., and S. A. King. 2011. Distribution of floating *Sargassum* in the Gulf of Mexico and the Atlantic Ocean mapped using MERIS. International Journal of Remote Sensing 32:1917–1929.

Gower, J., E. Young, and S. King. 2013. Satellite images suggest a new *Sargassum* source region in 2011. Remote Sensing Letters 4:764–773.

Fine, M. L. 1970. Faunal variation on pelagic *Sargassum*. Marine Biology 7:112–122.

Haney, J. C. 1986. Seabird patchiness in tropical oceanic waters : The influence of *Sargassum* "Reefs." The Auk 103:141–151.

Hu, C. 2009. A novel ocean color index to detect floating algae in the global oceans. Remote Sensing of Environment 113:2118-2129.

Hu, C., Z. Chen, T. D. Clayton, P. Swarzenski, J. C. Brock, and F. E. Muller–Karger. 2004. Assessment of estuarine water-quality indicators using MODIS medium-resolution bands: Initial results from Tampa Bay, FL. Remote Sensing of Environment 93:423–441.

Kanamitsu, M., W. Ebisuzaki, J. Woollen, S. K. Yang, J. J. Hnilo, M. Fiorino, and G. L. Potter. 2002. NCEP-DOE AMIP-II reanalysis (R-2). Bulletin of the American Meteorological Society 83:1631–1643+1559.

Kemp, M.U., E.E. van Loon, J. Shamoun-Baranes, W. and Bouten. 2012. RNCEP: Global weather and climate data at your fingertips. Methods in Ecology and Evolution 3:65-70. R package version 1.0.6.

Laffoley, D. D., H. S. J. Roe, M. V. Angel, J. Ardron, N. R. Bates, I. L. Boyd, S. Brooke, K. N. Buck, C. A. Carlson, B. Causey, M. H. Conte, S. Christiansen, J. Cleary, J. Donnelly, S. A. Earle, R. Edwards, K. M. Gjerde, S. J. Giovannoni, S. Gulick, M. Gollock, J. Hallett, P. Halpin, R. Hanel, A. Hemphill, R. J. Johnson, A. H. Knap, M. W. Lomas, S. A. McKenna, M. J. Miller, F. W. Ming, R. Moffitt, N. B. Nelson, L. Parson, A. J. Peters, J. Pitt, P. Rouja, J. Roberts, D. A. Seigel, A. N. S. Siuda, D. K. Steinberg, A. Stevenson, V. R. Sumaila, W. Swartz, S. Thorrold, T. M. Trott, and V. Vats. 2011. The protection and management of the Sargasso Sea: The golden floating rainforest of the Atlantic Ocean. Summary Science and Supporting Evidence Case. Sargasso Sea Alliance. 44 pp.

Lapointe, B. E., L. E. West, T. T. Sutton, and C. Hu. 2014. Ryther revisited: Nutrient excretions by fishes enhance productivity of pelagic *Sargassum* in the western North Atlantic Ocean. Journal of Experimental Marine Biology and Ecology 458:46–56.

Lubchenco, J., M. K. McNutt, G. Dreyfus, S. A. Murawski, D. M. Kennedy, P. T. Anastas, S. Chu, and T. Hunter. 2012. Science in support of the Deepwater Horizon response. Proceedings of the National Academy of Sciences of the United States of America 109:20212–21.

[NMFS] National Marine Fisheries Service. 2014 Endangered and Threatened Species: Critical Habitat for the Northwest Atlantic Ocean Loggerhead Sea Turtle Distinct Population Segment (DPS) and Determination Regarding Critical Habitat for the North Pacific Ocean Loggerhead DPS. Federal Register 79(132) 39856–39912, 10 July 2014.

[NOAA NCDC] National Oceanic and Atmospheric Administration, National Climatic Data Center. 2011. State of the Climate: National Overview for Annual 2011, published online December 2011, retrieved on October 7, 2014; http://www.ncdc.noaa.gov/sotc/national/2011/13.

Parr, A. E. 1939. Quantitative observations on the pelagic *Sargassum* vegetation of the western North Atlantic. Bulletin of the Bingham Oceanographic Collection 6:1–94.

Powers, S. P., F. J. Hernandez, R. H. Condon, J. M. Drymon, and C. M. Free. 2013. Novel pathways for injury from offshore oil spills: direct, sublethal and indirect effects of the Deepwater Horizon oil spill on pelagic *Sargassum* communities. PloS one 8:e74802.

R Core Team. 2013. R: A language and environment for statistical computing. R Foundation for Statistical Computing, Vienna, Austria. http://www.R-project.org/.

Witherington, B., S. Hirama, and R. Hardy. 2012. Young sea turtles of the pelagic *Sargassum*-dominated drift community: habitat use, population density, and threats. Marine Ecology Progress Series 463:1–22.

Tables:

Table 3.1. The occurrence and coverage of surface-pelagic drift communities (SPDC) within the northern Gulf of Mexico from 2009–2011. For each Landsat scene, the number of images containing SPDC and the number of images examined are provided. The mean search area for each scene was used to estimate the fractional coverage of SPDC.

Landsat scene index	SPDC observed	Total images	Mean searched area (km^2)	SPDC coverage ‰ (mean ±SD)
p16r42	47	69	21913	0.062 ±0.148
p16r43	56	67	30263	0.216 ±0.355
p17r40	68	72	15362	0.429 ±0.831
p17r41	41	62	24207	0.098 ±0.227
p17r42	58	62	33630	0.056 ±0.108
p17r43	60	69	31622	0.163 ±0.311
p18r39	79	96	8354	0.812 ±1.429
p18r40	51	70	31014	0.070 ±0.108
p18r41	4	10	26884	0.012 ±0.006
p18r42	1	9	31666	0.002 ±0.004
p19r39	47	72	11620	0.060 ±0.143
p19r40	5	9	30774	0.039 ±0.052
p19r41	5	9	30488	0.004 ±0.005
p19r42	5	7	32368	0.005 ±0.005
p20r39	18	69	17440	0.015 ±0.054
p20r40	21	34	29588	0.051 ±0.063
p20r41	6	9	30127	0.022 ±0.021
p20r42	3	10	28718	0.006 ±0.012
p21r39	42	83	16866	0.041 ±0.098
p21r40	40	57	30059	0.098 ±0.235
p21r41	10	11	30947	0.047 ±0.069
p21r42	7	10	29379	0.032 ±0.059
p22r40	34	39	25368	0.316 ±0.654
p23r40	33	45	27152	0.336 ±0.841
p24r40	35	39	28281	0.527 ±1.336
p24r41	3	4	24526	0.045 ±0.054
p25r40	32	36	21430	1.169 ±2.728
p25r41	37	37	28985	1.320 ±2.927
p26r41	36	36	21924	0.578 ±1.163
Total (all images)	**884**	**1202**	**23435**	**0.300 ±1.032**

Table 3.2. Area of surface-pelagic drift communities (SPDC) detected within northern Gulf of Mexico Landsat images collected from 2009–2011. The mean, standard deviation (SD) and maximum area (km^2) of SPDC are provided for each Landsat scene.

Landsat scene index	Mean	SD	Maximum
p16r42	1.18	2.98	19.28
p16r43	5.59	11.11	62.40
p17r40	6.34	13.18	90.84
p17r41	2.08	5.06	32.70
p17r42	1.75	3.65	24.09
p17r43	4.65	10.06	72.29
p18r39	5.92	10.1	48.53
p18r40	2.01	3.34	18.50
p18r41	0.15	0.25	0.74
p18r42	0.02	0.07	0.22
p19r39	0.58	1.64	12.94
p19r40	0.93	1.62	4.90
p19r41	0.11	0.15	0.44
p19r42	0.16	0.16	0.40
p20r39	0.29	1.04	6.22
p20r40	2.09	3.62	14.11
p20r41	0.61	0.73	2.07
p20r42	0.18	0.39	1.15
p21r39	0.60	1.48	9.65
p21r40	3.19	8.00	44.52
p21r41	1.33	1.84	5.60
p21r42	0.85	1.57	4.54
p22r40	8.76	19.24	80.53
p23r40	9.90	26.58	168.17
p24r40	15.34	40.43	195.92
p24r41	1.17	1.47	3.32
p25r40	25.51	59.83	263.60
p25r41	38.45	82.91	390.10
p26r41	12.72	26.23	100.99
Total (all images)	**5.63**	**22.78**	**390.10**

Figures:

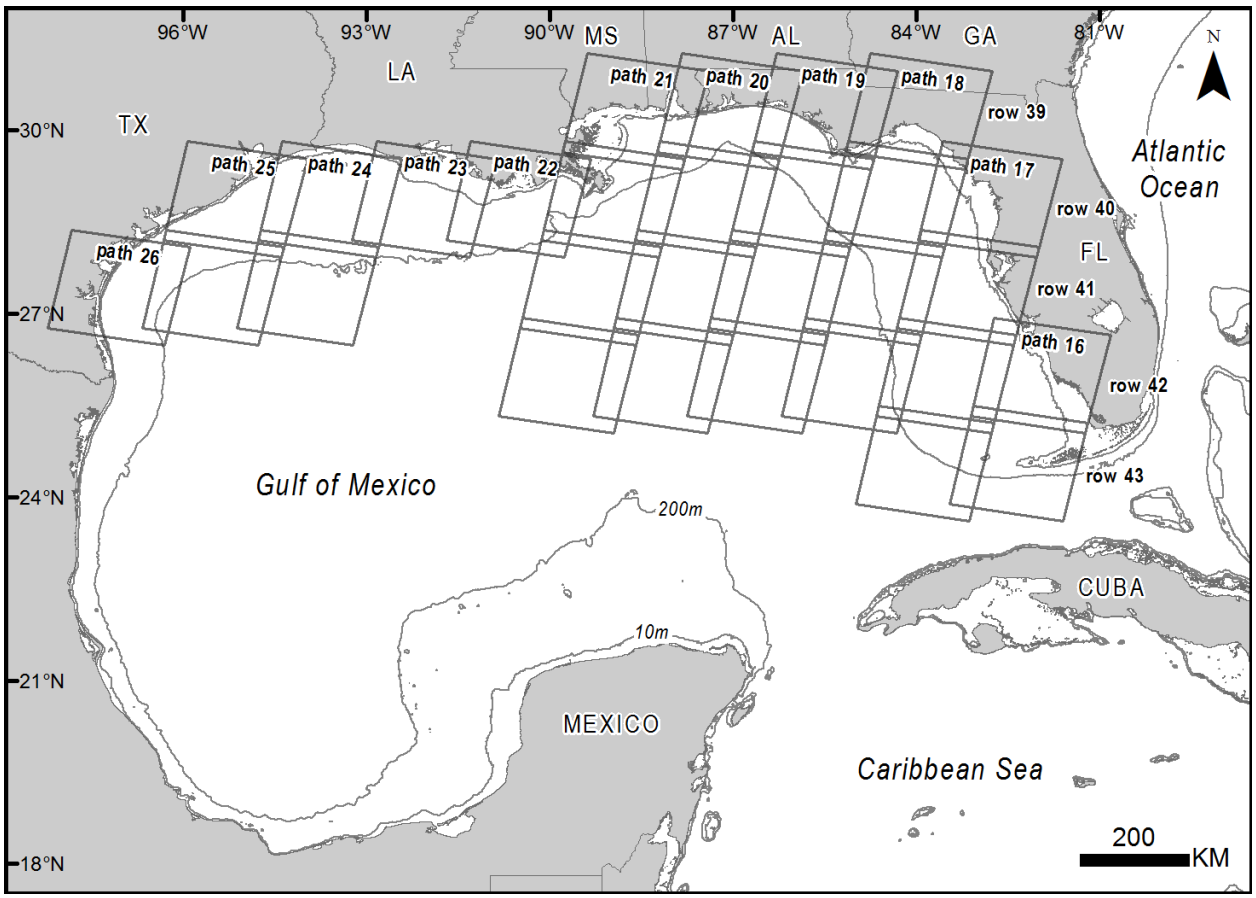

Figure 3.1. The northern Gulf of Mexico study area as defined by the extents of Landsat scenes that were available during 2009–2011. Paths are labeled at the top of each path, and rows are labeled along the right side of each row.

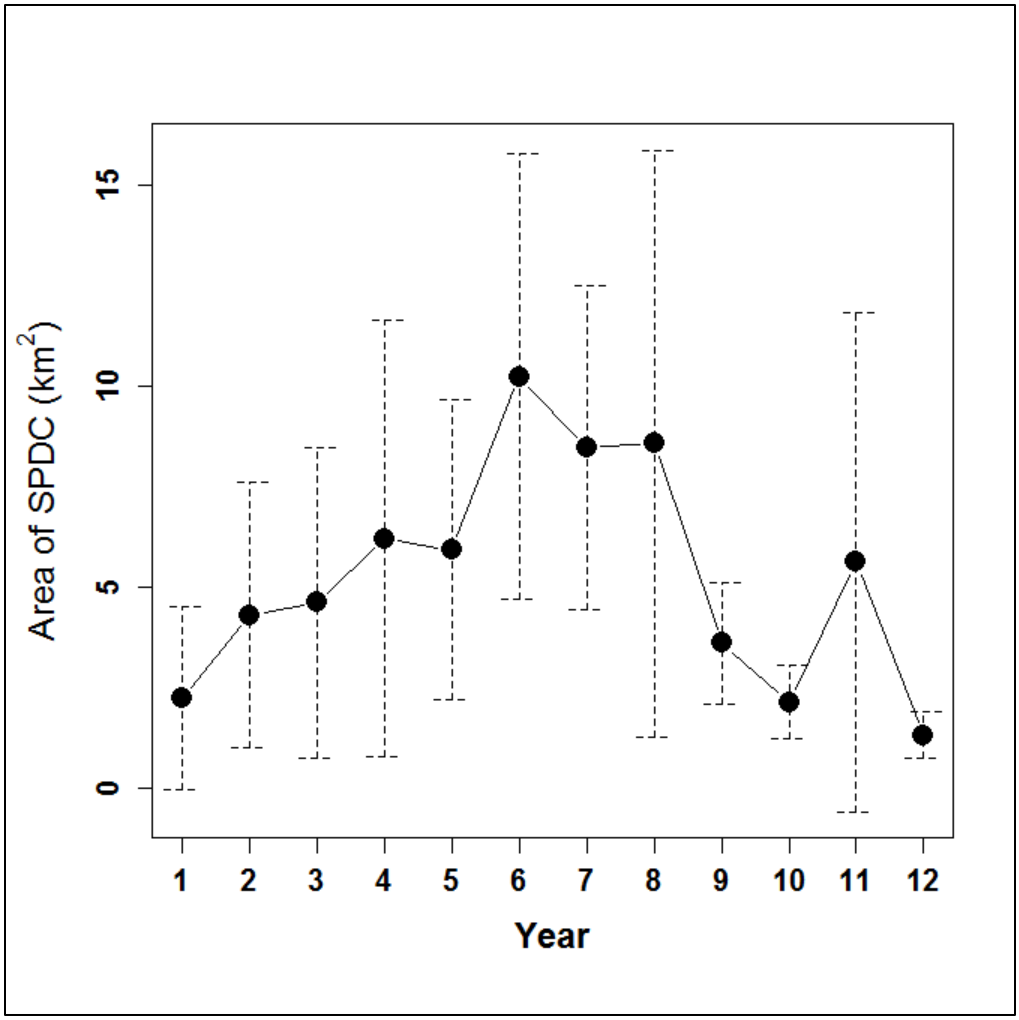

Figure 3.2. The mean area (km^2) of surface-pelagic drift communities (SPDC) observed (by month) within the northern Gulf of Mexico, 2009–2011. Error bars represent 95% confidence intervals surrounding the mean values.

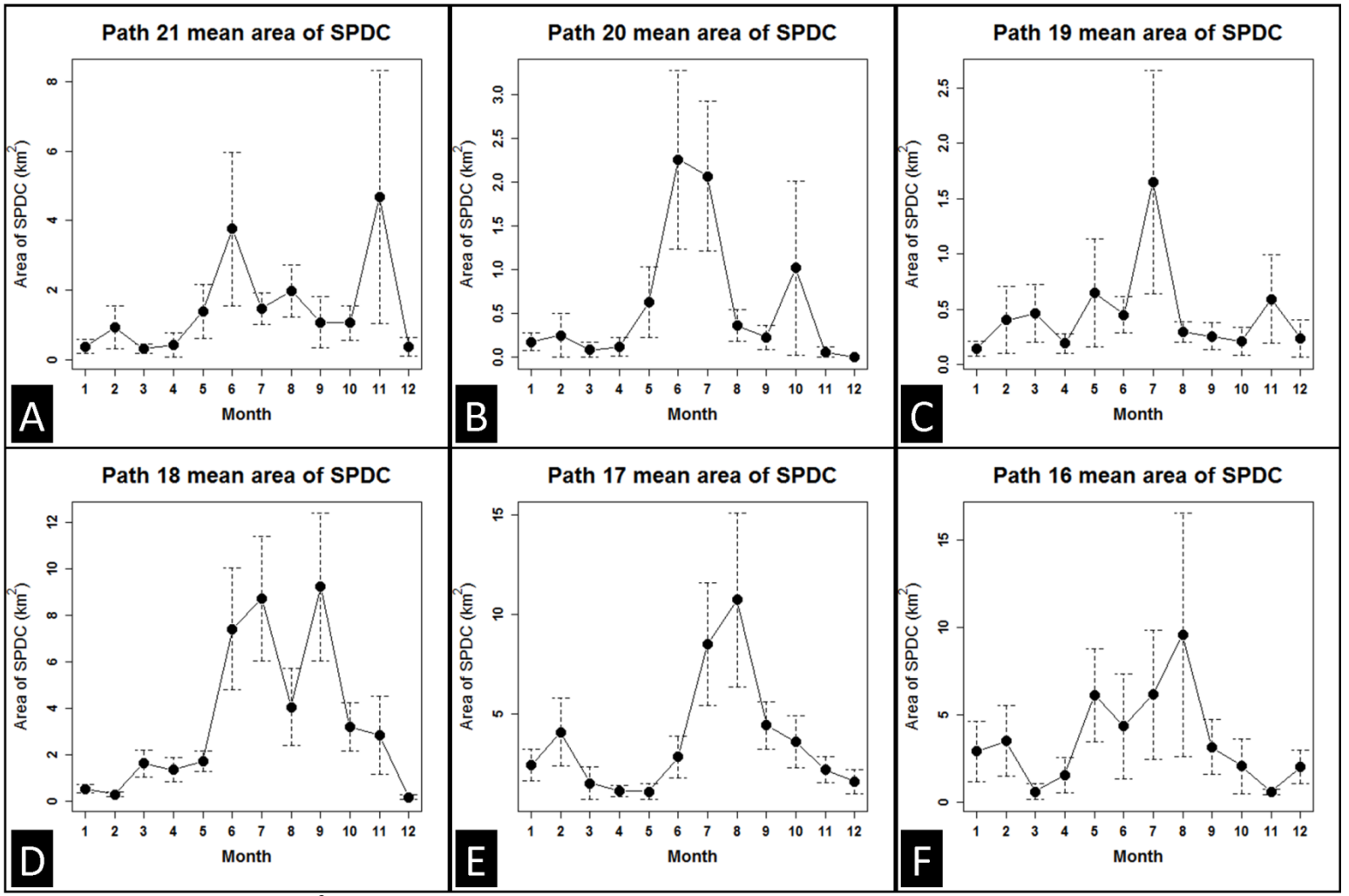

Figure 3.3. The mean area (km^2) of surface-pelagic drift communities (SPDC) per month observed within the eastern Gulf of Mexico, 2009–2011. Each plot represents the monthly mean area of SPDC found within images collected along Landsat paths 16–21. Plots are arranged in their geographic order, from west (path 21; A) to east (path 16; F).

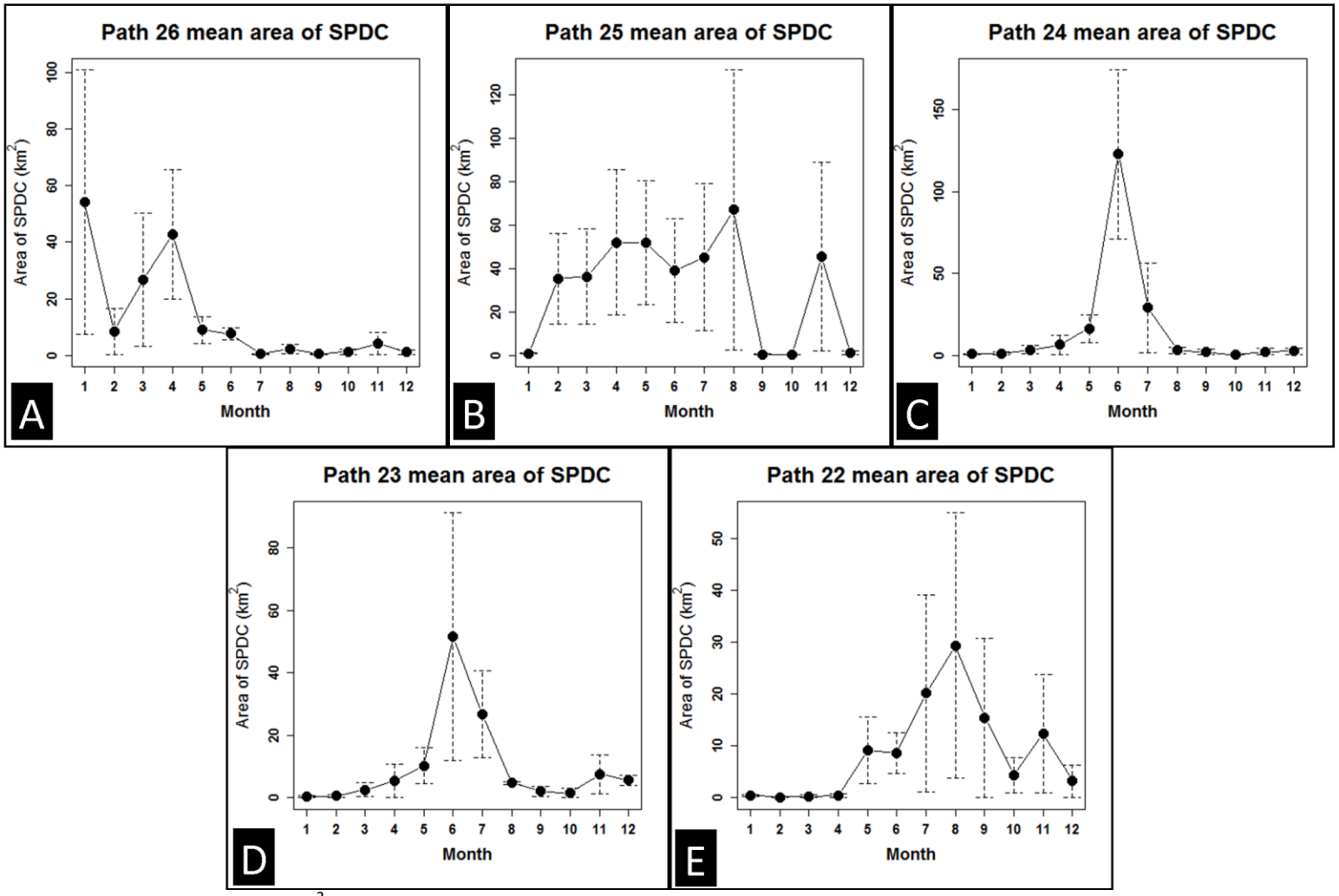

Figure 3.4. The mean area (km^2) of surface-pelagic drift communities (SPDC) per month observed within the western Gulf of Mexico, 2009–2011. Each plot represents the monthly mean area of SPDC found within images collected along Landsat paths 21–26. Plots are arranged in their geographic order, from west (path 26; A) to east (path 22; E).

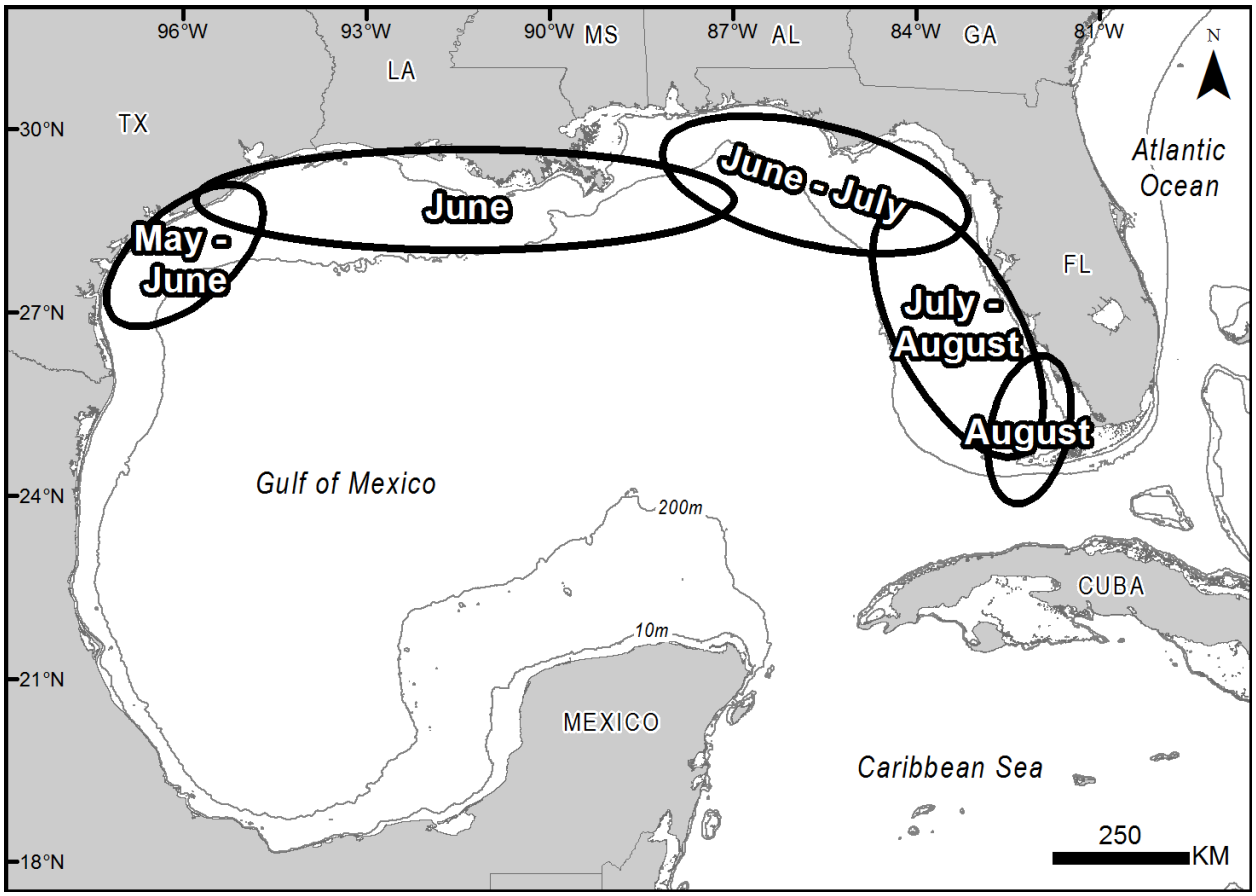

Figure 3.5. Generalized patterns of spring and summer peaks in abundance of surface-pelagic drift communities (SPDC) across the northern and eastern Gulf of Mexico. Localized SPDC abundance peaks occurred outside of these time periods during some years.

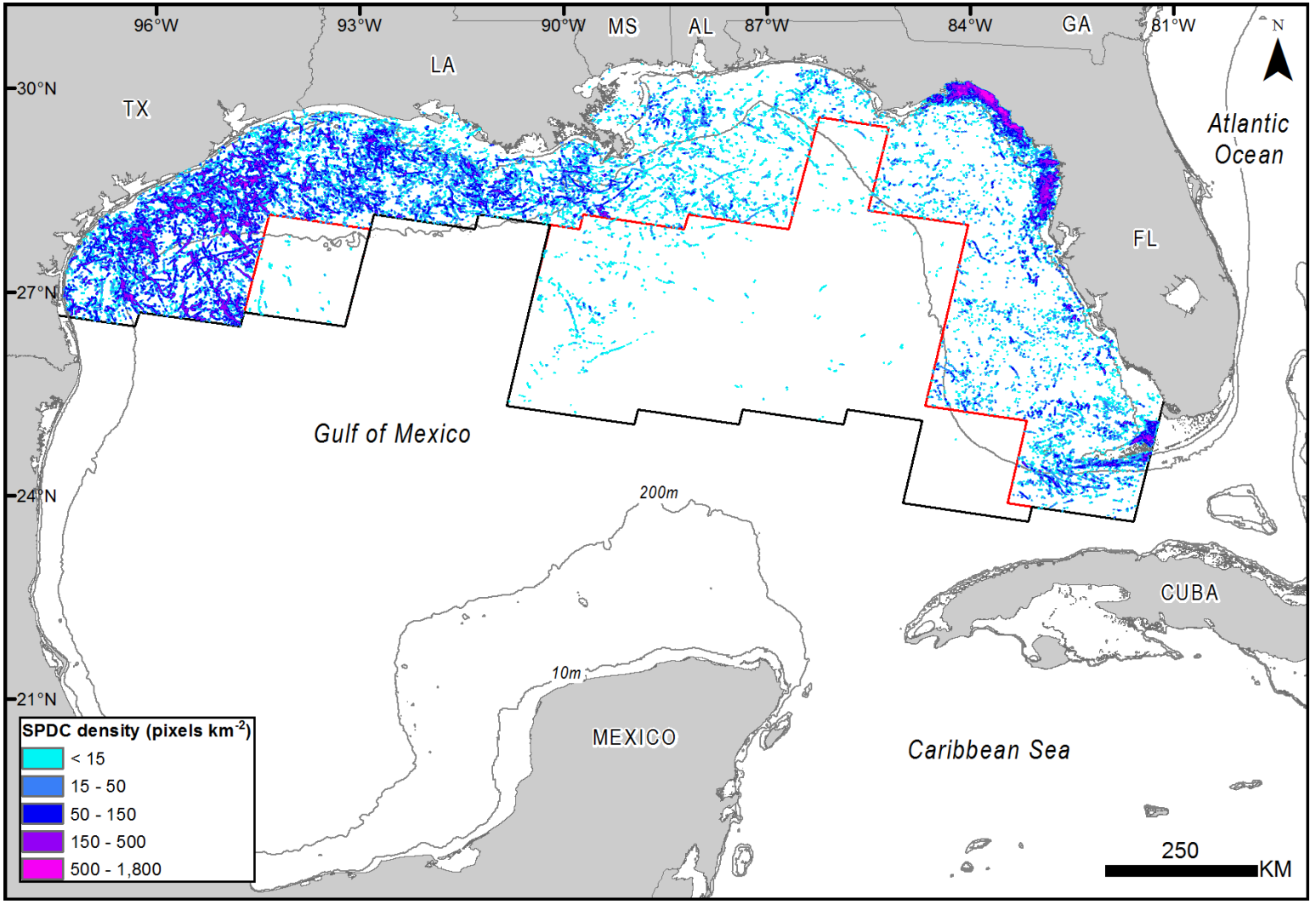

Figure 3.6. The density of surface-pelagic drift communities (SPDC) within the northern and eastern Gulf of Mexico, 2009–2011. The density of SPDC is expressed as the number of SPDC pixels per km^2. The black lines represent the southern extent of the study area. The red lines represent the offshore regions within which the availability of Landsat imagery was limited during the 2009–2011 study period.

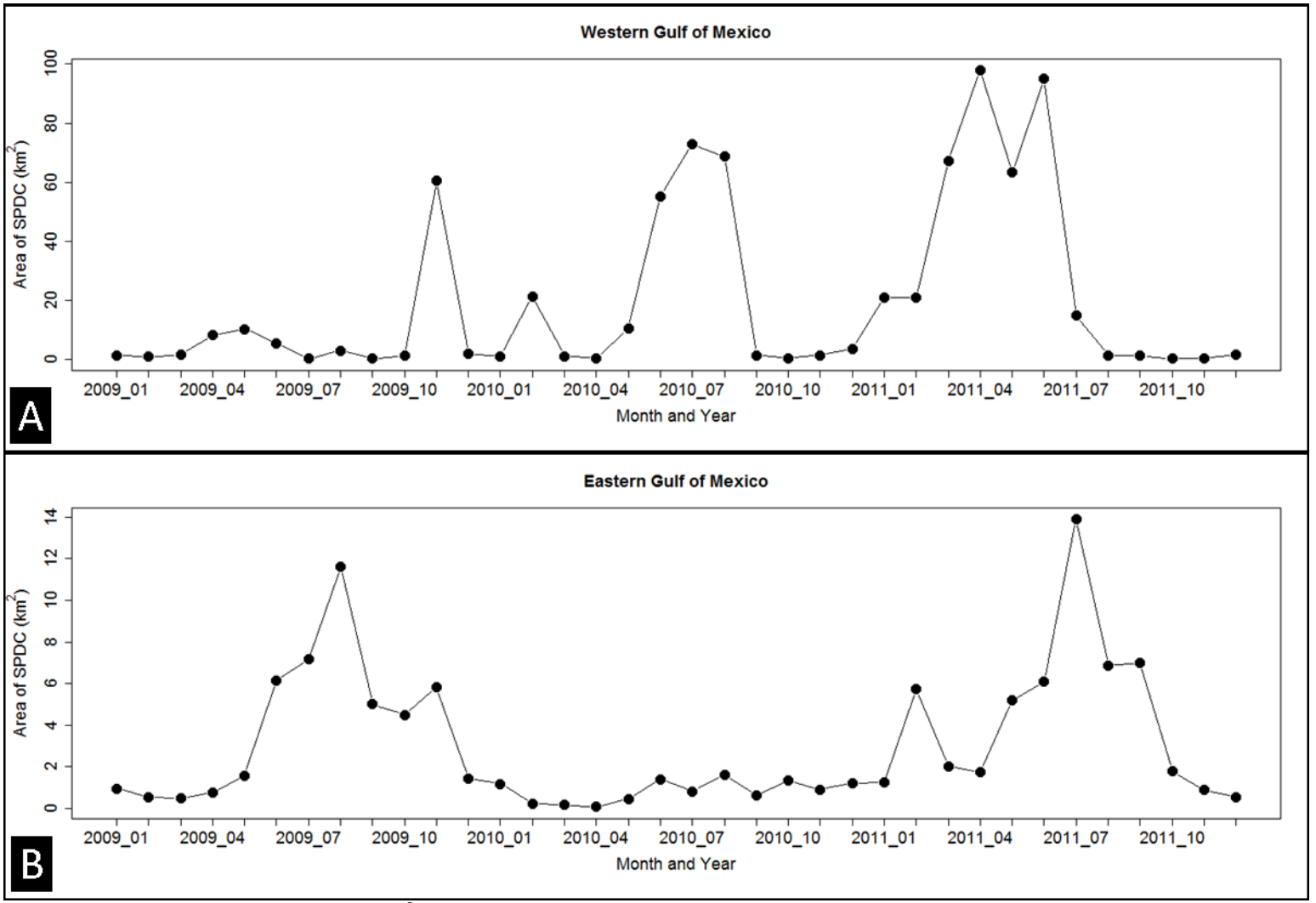

Figure 3.7. The mean monthly area (km^2) of surface-pelagic drift communities (SPDC) within the western (A) and eastern (B) Gulf of Mexico, 2009–2011. The Mississippi River Delta (approximately 90° W) was used to divide the western and eastern regions of the study area. Landsat scenes 22–26 were used to characterize SPDC western Gulf of Mexico. Landsat paths 16–21 were used to characterize SPDC within the eastern Gulf of Mexico.

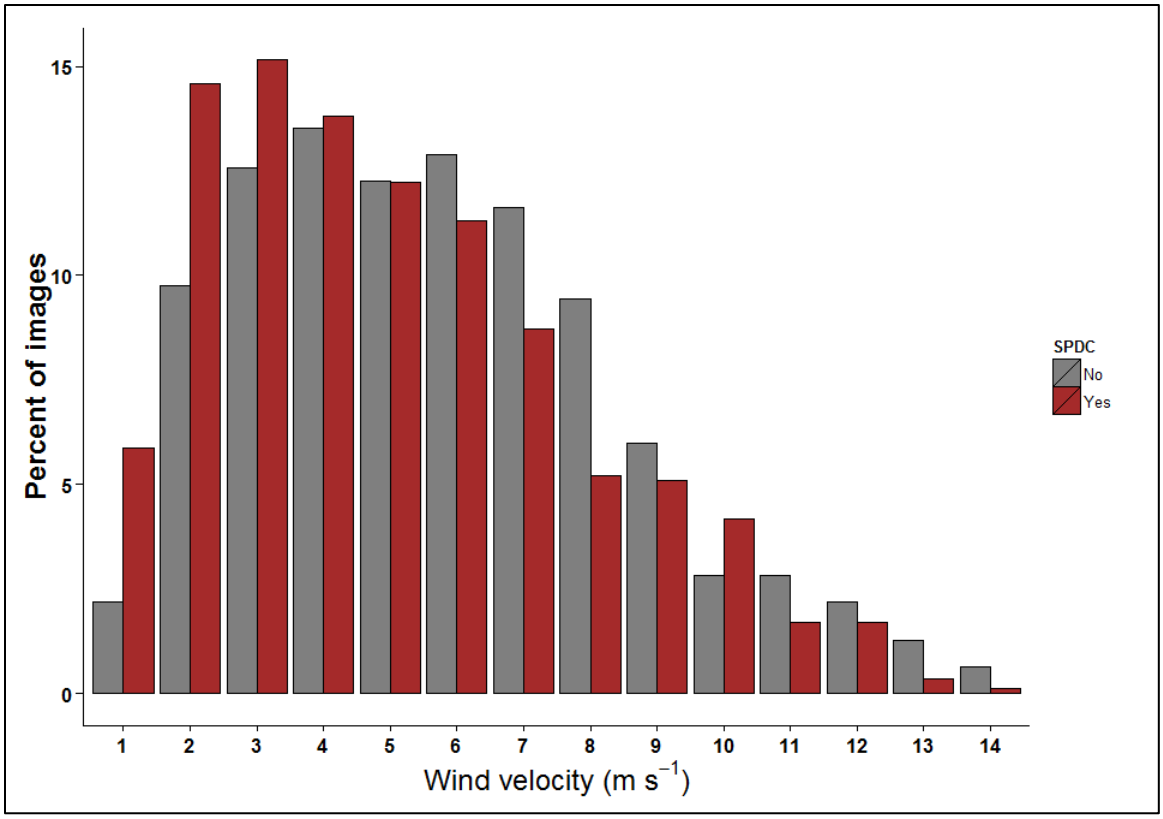

Figure 3.8. Wind velocity and the frequency of occurrence of surface-pelagic drift communities (SPDC) within northern Gulf of Mexico Landsat images. Bars represent the percentage of images within which SPDC was (Yes) or was not (No) detected.

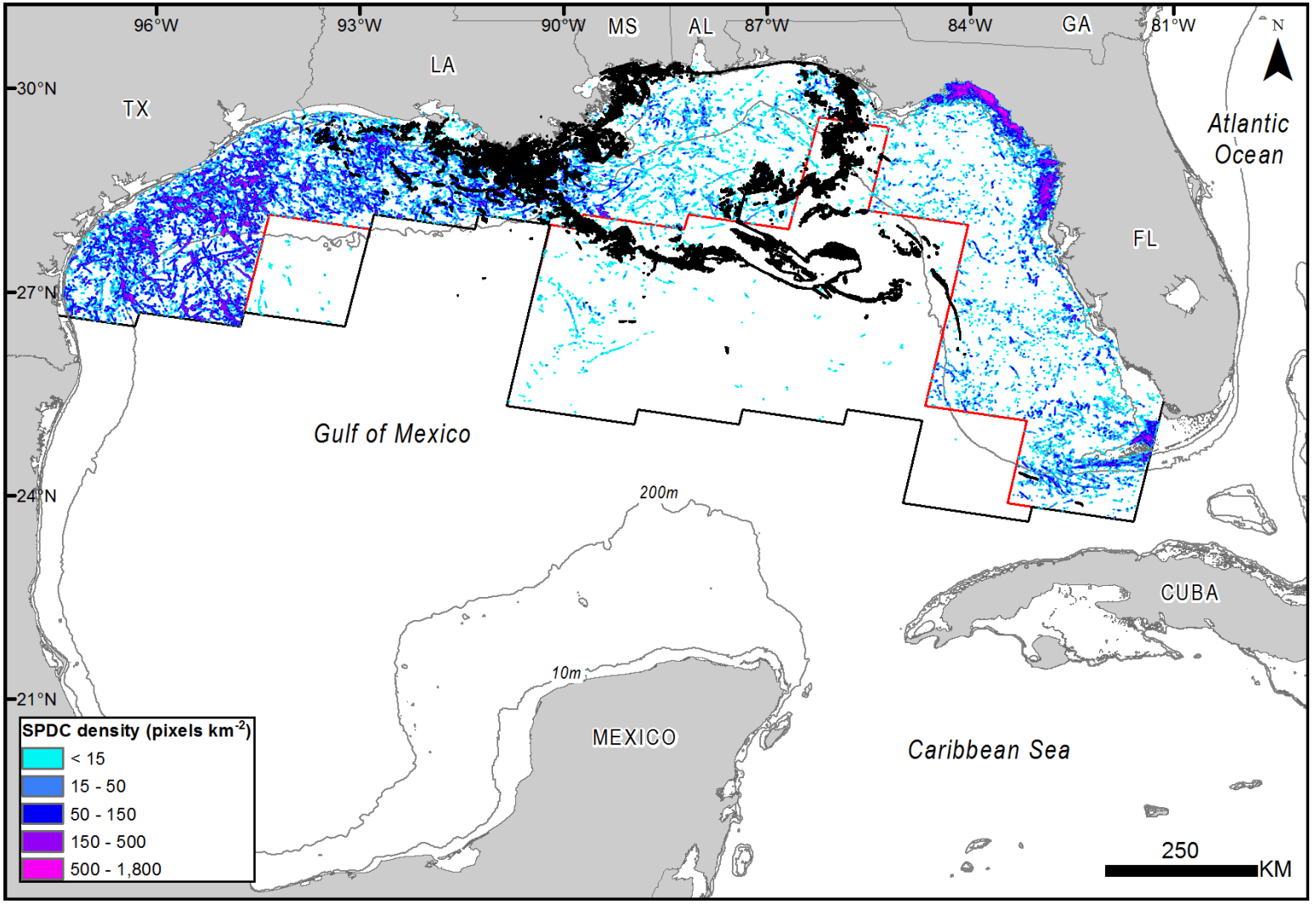

Figure 3.9. The extent of the surface oil from the Deepwater Horizon oil spill (April–August 2010) and the density of surface-pelagic drift communities (SPDC) within the northern and eastern Gulf of Mexico (2009–2011). The black polygon within the north-central Gulf of Mexico represents the cumulative extent of surface oiling based on an analysis of Synthetic Aperture Radar data (Environmental Response Management Application; http://gomex.erma.noaa.gov). The black lines represent the southern extent of the study area.

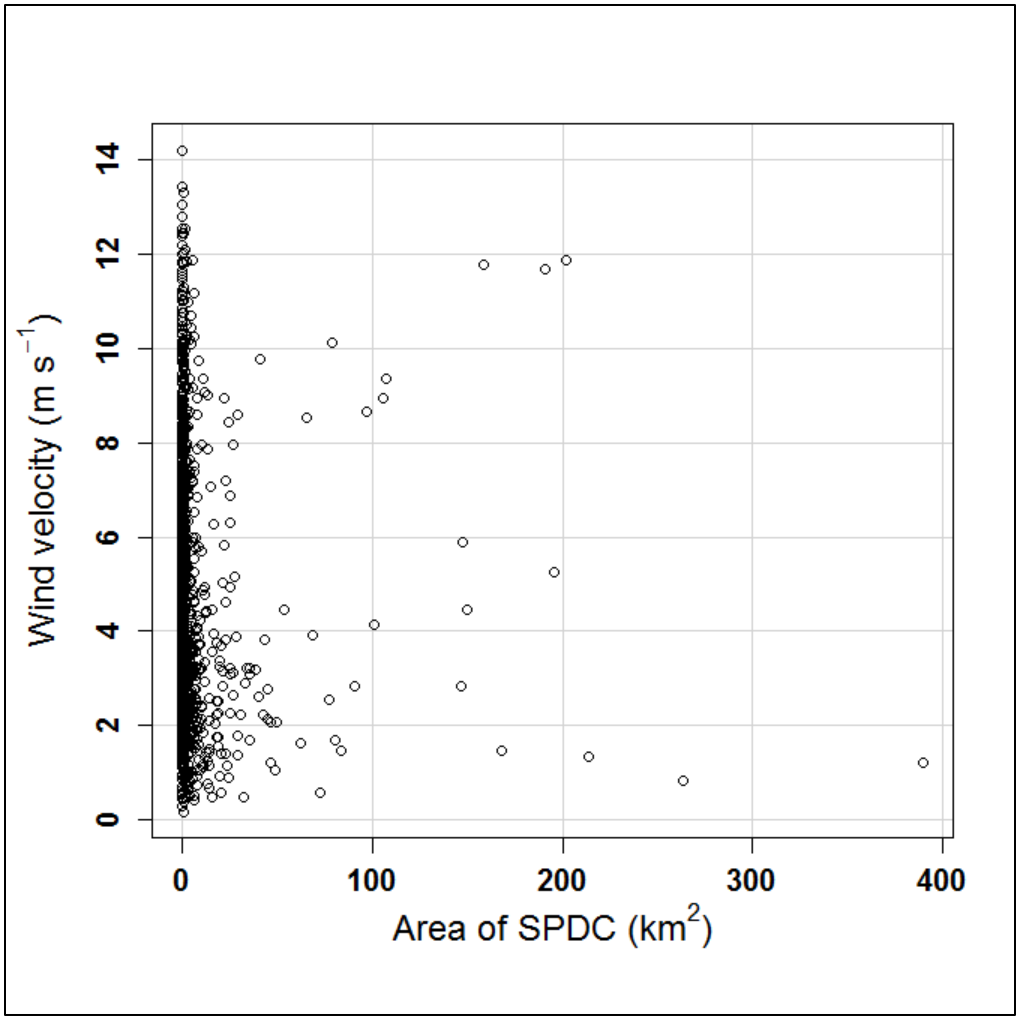

Figure 3.10. Scatterplot of wind velocity (1 m s^{-1}) and the area (km^2) of surface-pelagic drift communities (SPDC) observed within northern Gulf of Mexico Landsat images.